Level set methods for simulating multiphase displacements on the pore scale

Johan Olav Helland

PhD Course Pore-Network Modelling 2015

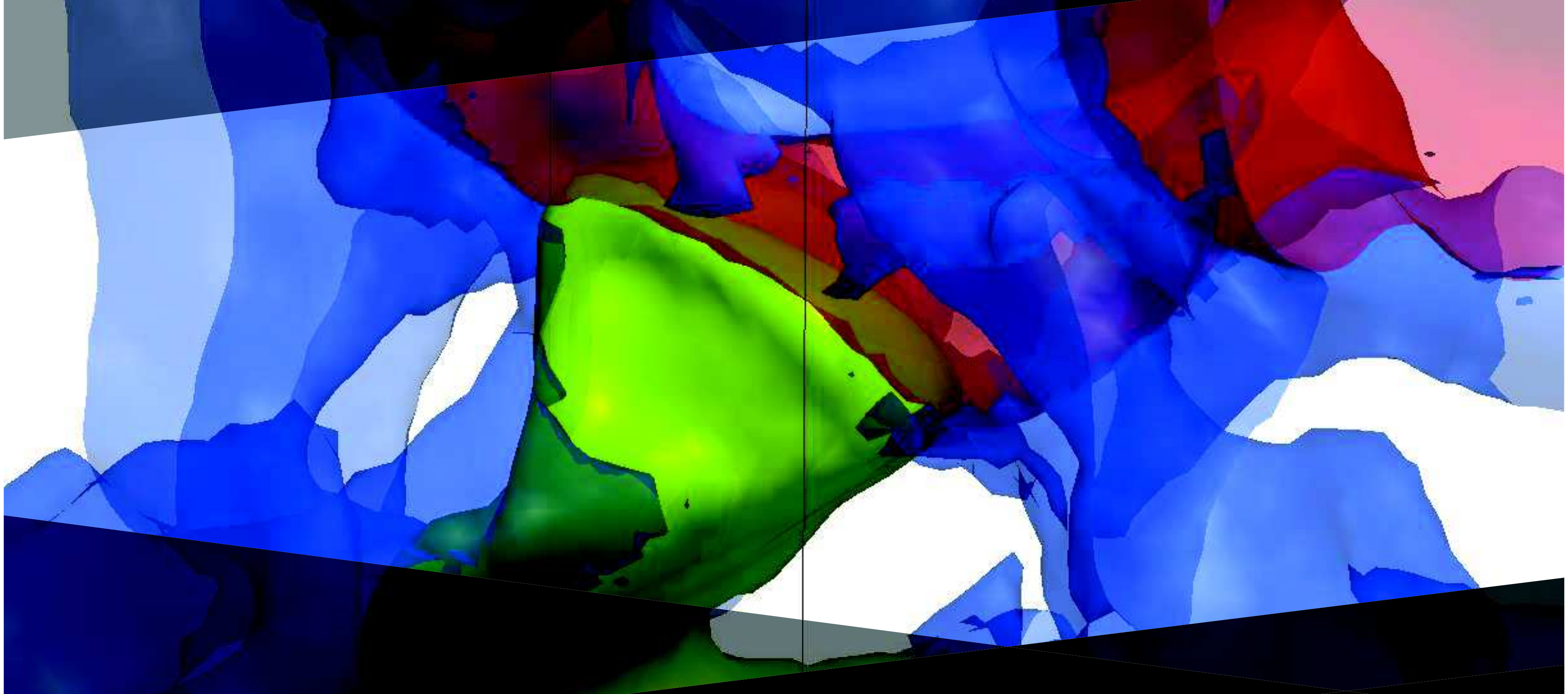

Level Set Methods

› **Reference textbooks:**

- Osher, S. and Fedkiw, R.: «Level set methods and dynamic implicit surfaces», Springer Verlag, 2003.
- Sethian, J.: «Level set methods and fast marching methods», Cambridge University Press, 1999.

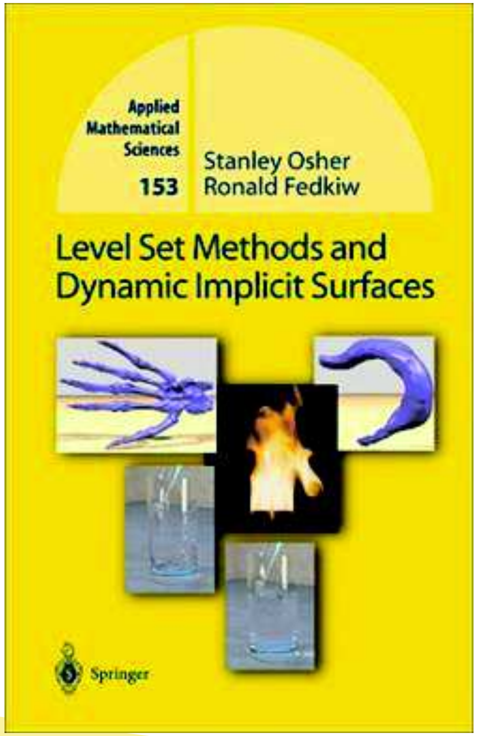

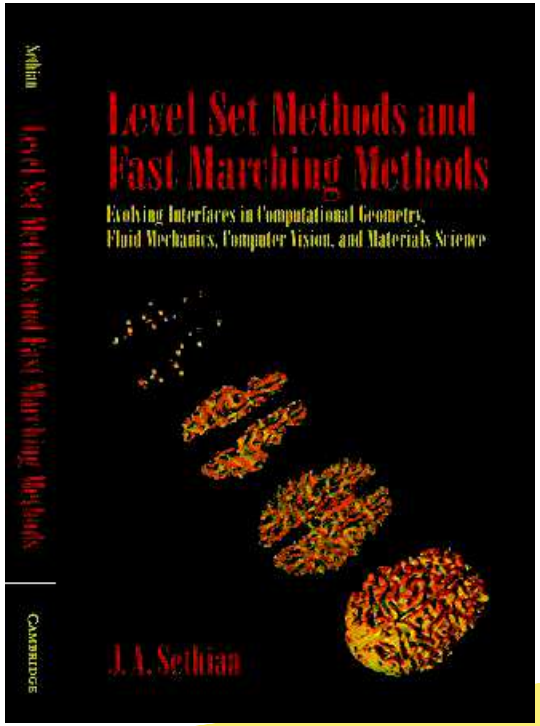

Level set method

› A method to describe evolution of interfaces between fluids (or materials) that may change shape and topology (e.g., merge, split, deform)

› Some applications:

- Computational fluid dynamics
- Fracture mechanics
- Crystal growth, grain rearrangement
- Visualization
- Image analysis (e.g., for medical use)
  - Segmentation, Noise removal, Extraction of objects etc..

Some interesting links…

› Ron Fedkiw: http://physbam.stanford.edu/~fedkiw/
  - 2 times Oscar winner for developing techniques for better visual effects in movies (Harry Potter, Star Wars, Terminator, Pirates of the Carribean, etc…), Examples: simulation of hair, water splash, fire, wind, cloth, destruction etc…

› James Sethian: https://math.berkeley.edu/~sethian/
  - Award-winning soap bubble animation using VIIM (Saye & Sethian JCP 2012, Science 2013):

http://crd.lbl.gov/news-and-publications/news/2013/math-of-popping-bubbles-in-a-foam/

Contents

› Level set methods and related techniques

- Reinitialization (Sussman et al., JCP 1994, Peng et al., 1999)
- Extension velocities (Peng et al., 1999; Adalsteinsson and Sethian, 1999)

› Application example within «Digital Rock Physics» :

- Level set methods for simulating capillary-controlled multiphase displacements on the pore scale:
  – Capillary pressure
  – Hysteresis
  – Trapping and remobilization

Level Set Methods

› An interface tracking method where the interface is given as the zero contour of an implicit function ϕ: $\phi(\vec{x},t) = 0$

› The LS function ϕ is one dimension higher than the interface.

› Regions inside/outside of the interface are defined through the sign of ϕ:

$\Omega^+ = \{\vec{x}: \phi(\vec{x},t) > 0\}$

$\Omega^- = \{\vec{x}: \phi(\vec{x},t) < 0\}$

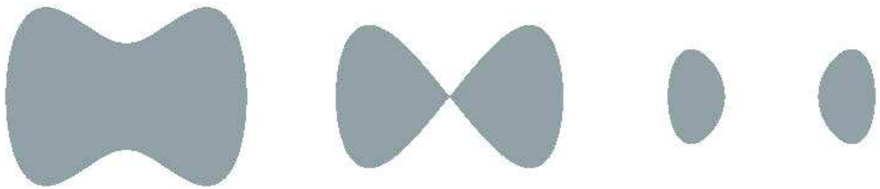

› Normally ϕ is given by the signed distance function (SDF):

$\phi(\vec{x},t) = \pm|\vec{x} - \vec{x}_0|$, where $\vec{x}_0$ is located on the interface.

› SDF has the property $|\nabla\phi| = 1$ which ensures numerical stability.

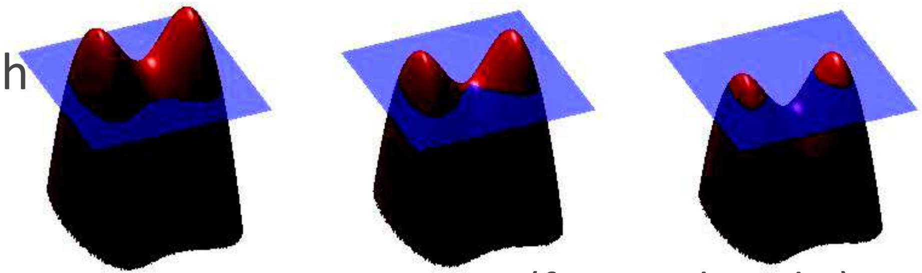

(from Wikipedia)

Level Set Method (LSM)

(Sethian & Osher, 1988)

- Interfaces are described by $\phi(\vec{x}(t), t) = 0$:

  => $\phi_t + \nabla\phi \cdot \frac{d\vec{x}}{dt} = 0$, $\vec{V} = \frac{d\vec{x}}{dt}$ (velocity).

  Assume $\vec{V} = V_n \vec{N} + V_T\vec{T}$, $\vec{T}$ = tangential vector.

  $\vec{N} \cdot \nabla\phi = |\nabla\phi|$ and $\vec{T} \cdot \nabla\phi = 0.$

  => $\phi_t + V_N|\nabla\phi| = 0$

- The method handles topological changes, such as interface merging and splitting, in a natural manner.
- Surface normal $\vec{N}$ and curvature $\kappa = \nabla \cdot \vec{N}$ are directly related to ϕ
- The surface evolves by specifying a surface velocity which could include a normal and advective component:

$$\phi_t + V_N|\nabla\phi| + \vec{V}_{adv} \cdot \nabla\phi = 0$$

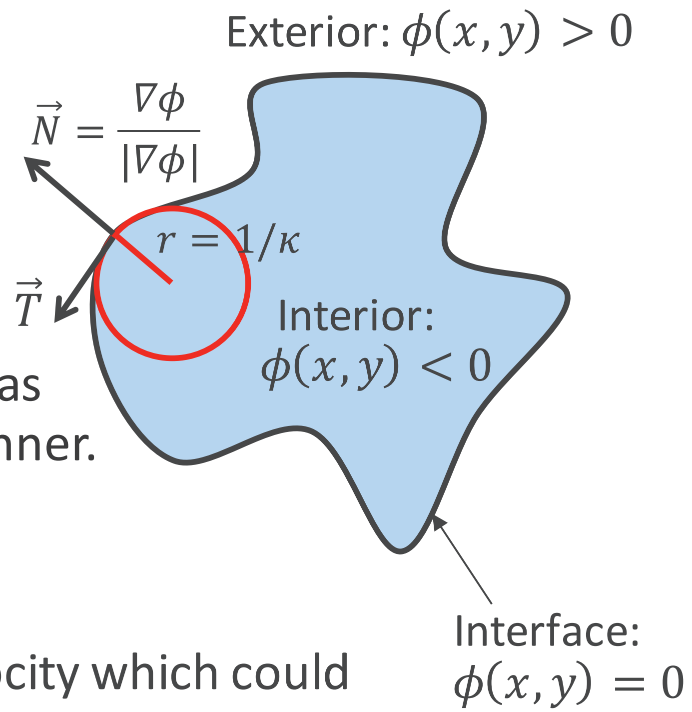

Reinitialization

› During iterations with the evolution equation, steep gradients $\nabla\phi$ may develop and ϕ will loose its SDF property ($|\nabla\phi| = 1$)

› Therefore, to maintain numerical stability, the LS function ϕ must be reinitialized to SDF occasionally. This is done by solving

$$\phi_t + S(\phi)(|\nabla\phi| - 1) = 0, \quad S(\phi) = \text{sign function}$$

› An example of void/solid SDF calculation:

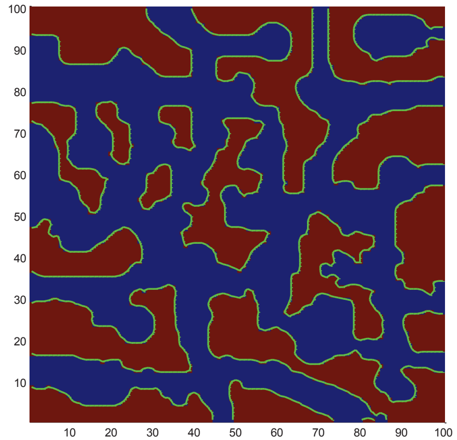

— $\psi = 0$ (void/solid LS function)

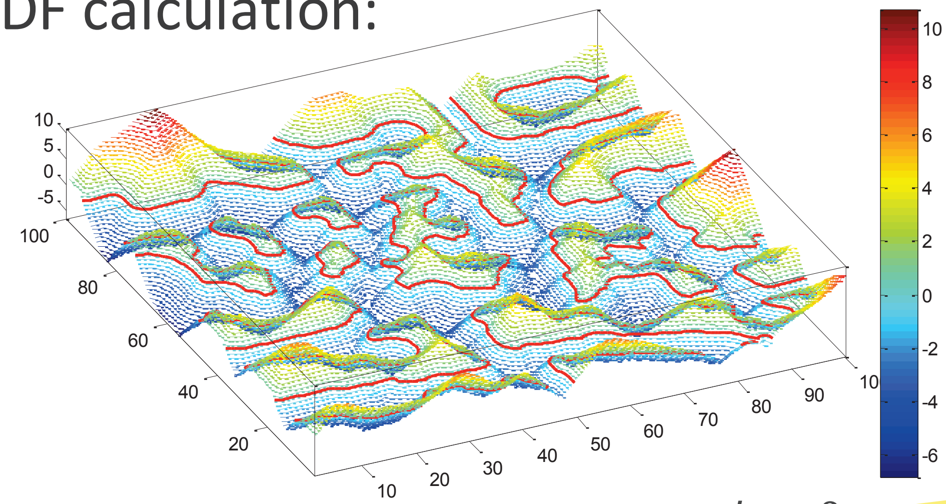

— $\psi = 0$

Simulation Procedure

IRIS

1. Initialize LS-function ϕ to a signed distance function by solving:

$$\phi_t + S(\phi)(|\nabla\phi| - 1) = 0 \qquad (*)$$

2. Iterate ϕ forward in time with LS evolution equation

$$\phi_t + v_N|\nabla\phi| + \vec{v}_{adv} \cdot \nabla\phi = 0, \qquad (**)$$

ϕ_t:
Time iteration with Runge-Kutta Methods (e.g., 3rd order)

$v_N|\nabla\phi|$:
WENO & upwinding schemes.
Central differences for curvature ($\kappa = \nabla\phi/|\nabla\phi|$)

$\vec{v}_{adv} \cdot \nabla\phi$:
WENO & advective upwinding scheme

WENO = Weighted Essentially Non-Oscillatory

[1st order RK: Forward Euler step: $\phi^{n+1} = \phi^n - \Delta t(v_N^n|\nabla\phi^n| + \vec{v}_{adv}^n \cdot \nabla\phi^n)$]

3. Repeat from step 1.

4. Reinitialize ϕ by solving (*) after specified time iterations. Similar techniques are used for solving (*) and (**).

Extension Velocity

- WHAT: Velocity (given on the interface) extended (extrapolated) in the normal direction OFF the interface such that:

$$\nabla v_{ext} \cdot \nabla \phi = 0$$

- WHY: Extension velocity provides a meaningful velocity for problems it is not known away from the interface regions
- Advantages:
  - Extension velocity preserves ϕ as an SDF ($|\nabla \phi| = 1$), allowing less frequent reinitializations in numerical implementations
  - Allows for larger time steps (based on CFL conditions)
- HOW: Construct extension velocity by solving PDE:

$$v_t + S(\phi)\vec{N} \cdot \nabla v = 0, \quad v = \text{velocity component}$$

$$\vec{N} = \frac{\nabla \phi}{|\nabla \phi|}$$

Extension Velocity

› We shall show that, for an LS evolution equation,

$$\phi_t + v_N|\nabla\phi| + \vec{v}_{adv}\cdot\nabla\phi = 0, \quad \vec{v}_{adv} = (v_1, v_2, v_3),$$

we can construct extension velocities satisfying

$$\nabla v_N \cdot \nabla\phi = 0$$
$$\nabla v_1 \cdot \nabla\phi = 0$$
$$\nabla v_2 \cdot \nabla\phi = 0$$
$$\nabla v_3 \cdot \nabla\phi = 0,$$

such that $|\nabla\phi| = 1$ for all time (in theory).

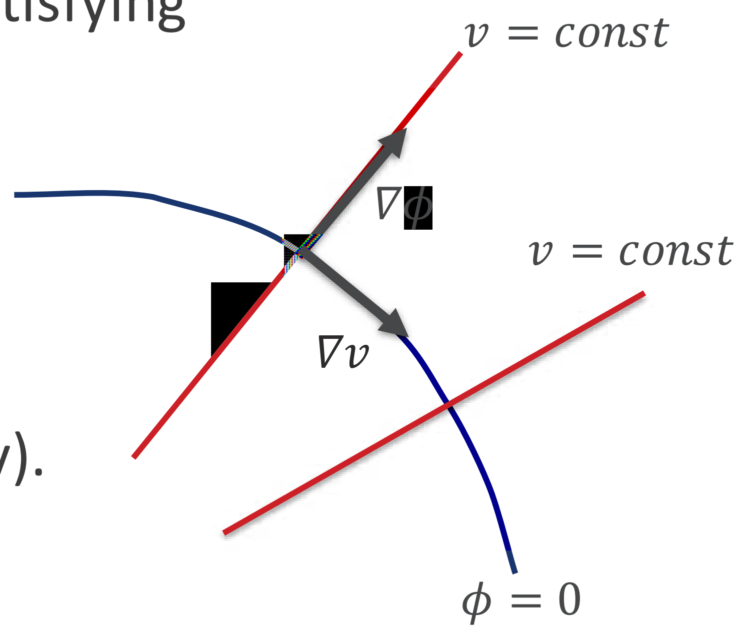

Extension Velocity (Proof)

1. Normal velocity, v_N:

$$\phi_t + v_N|\nabla\phi| = 0$$

$$\Rightarrow \nabla\phi_t = -\nabla(v_n|\nabla\phi|)$$

$$\begin{aligned}\frac{d}{dt}|\nabla\phi|^2 &= 2\nabla\phi \frac{d}{dt}\nabla\phi \\ &= -2\nabla\phi\cdot\nabla(v_n|\nabla\phi|) \\ &= -2\underbrace{\nabla\phi\cdot\nabla v_n}_{=0}|\nabla\phi| - 2\nabla\phi\cdot v_n\underbrace{\nabla|\nabla\phi|}_{=0} \\ &= 0.\end{aligned}$$

2. Advective velocity components, v_i:

$$\phi_t + v_1\phi_x = 0$$

$$\Rightarrow \nabla\phi_t = -\nabla(v_1\phi_x)$$

$$\begin{aligned}\frac{d}{dt}|\nabla\phi|^2 &= 2\nabla\phi \frac{d}{dt}\nabla\phi \\ &= -2\nabla\phi\cdot\nabla(v_1\phi_x) \\ &= -2\underbrace{(\nabla\phi\cdot\nabla v_1)}_{=0}\phi_x - 2v_1\underbrace{\nabla\phi\cdot\nabla\phi_x}_{=\frac{1}{2}\frac{\partial}{\partial x}|\nabla\phi|^2 = 0} \\ &= 0.\end{aligned}$$

› Similar for y- and z-components.

Extension Velocity

› Simulation procedure:

1. Construct extension velocities by solving

   $v_t + S(\phi)\vec{N} \cdot \nabla v = 0,$ for each velocity component v.

2. Iterate ϕ one time step forward with LS evolution equation

   $\phi_t + v_N|\nabla\phi| + \vec{v}_{adv} \cdot \nabla\phi = 0,$

   using extension velocities from step 1.

3. Repeat from step 1.
4. Perform reinitialization periodically.

Applications - Objective

IRIS

› Develop pore-scale models for simulating capillary-controlled motion of two & three fluids directly on 3D rock geometries

› At equilibrium:

- Young-Laplace equation satisfied in pore space:

$$P_{cij} = \sigma_{ij} C_{ij},\ ij = go, ow, gw\ .$$

- Young's equation satisfied on pore walls:

$$\sigma_{ij} \cos\theta_{ij} = \sigma_{is} - \sigma_{js},\ ij = go, ow, gw.$$

This yields a constraint on σ_{ij} and θ_{ij}:

$$\sigma_{gw}\cos\theta_{gw} = \sigma_{go}\cos\theta_{go} + \sigma_{ow}\cos\theta_{ow}$$ (Bartell-Osterhof Eq.).

C_{ij} = Interface curvature
σ_{ij} = Interfacial tension
θ_{ij} = Contact angle

› Two fluids: Level set method

› Three fluids: Variational (or Multiple) level set method

Rock imaging: Micro-CT at LBNL

› Reconstructed and segmented Bentheim sandstone sample

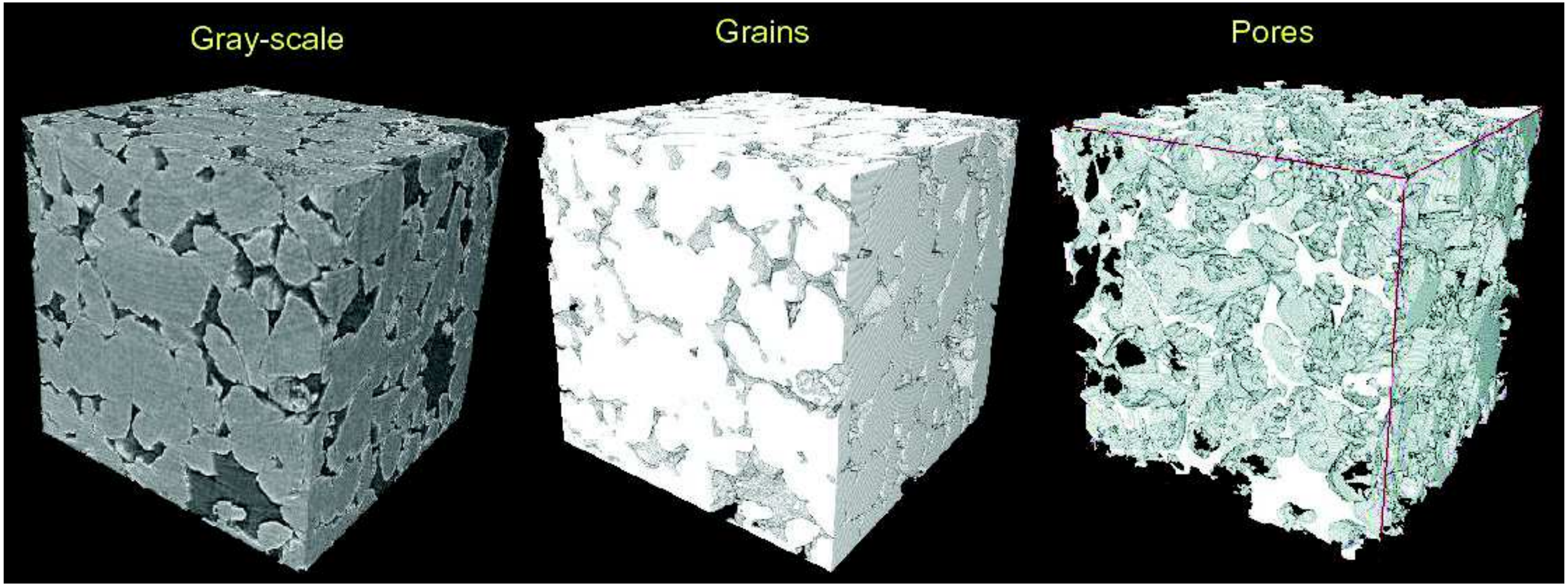

- Size of subset: 750x750x750 voxels
- Resolution 4.5 microns
- Total sample size 5x5x5 mm^3

Synchrotrons

Advanced Light Source (ALS)
at LBNL, Berkeley:

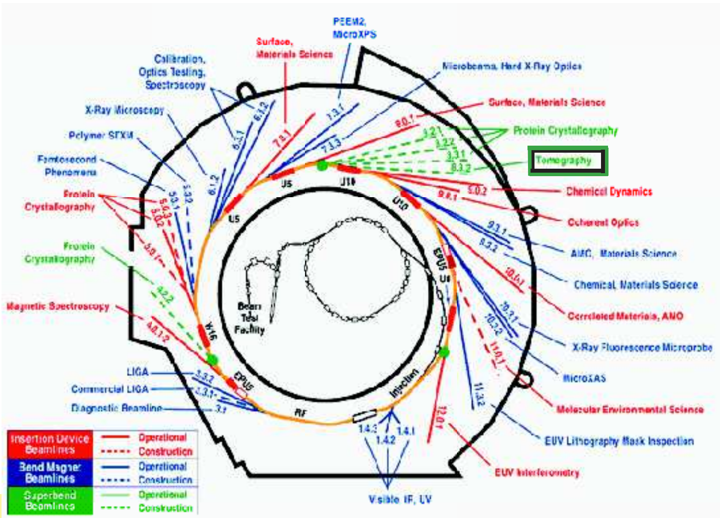

Advanced Photon Source (APS)
in Argonne, Illinois (used by
Oregon State University):

LSM: Capillary Displacements at the Pore Scale IRIS

(Prodanović & Bryant, JCIS 2006)

- For each capillary pressure, evolve ϕ until equilibrium using

$$\phi_t + (C - \kappa)|\nabla\phi| = 0,$$

where $V_n = C - \kappa$ and $C = P_c/\sigma =$ Input interface curvature.

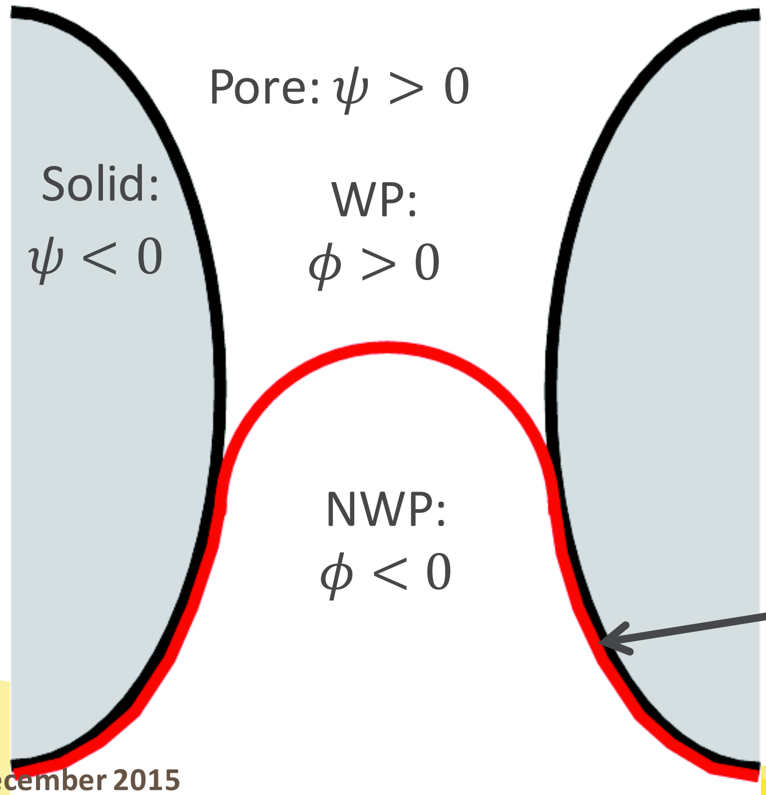

The solution $V_N = 0$ yields surfaces of constant mean curvature.

$\psi =$ Static pore/solid LS function

$\psi = 0$ (black line)

$\phi = 0$ (red line)

A constraint prevents $\phi = 0$ from invading solid ($\theta = 0°$).

3D Simulation: Castlegate Sandstone

- Void-solid surface described by $\psi = 0$:

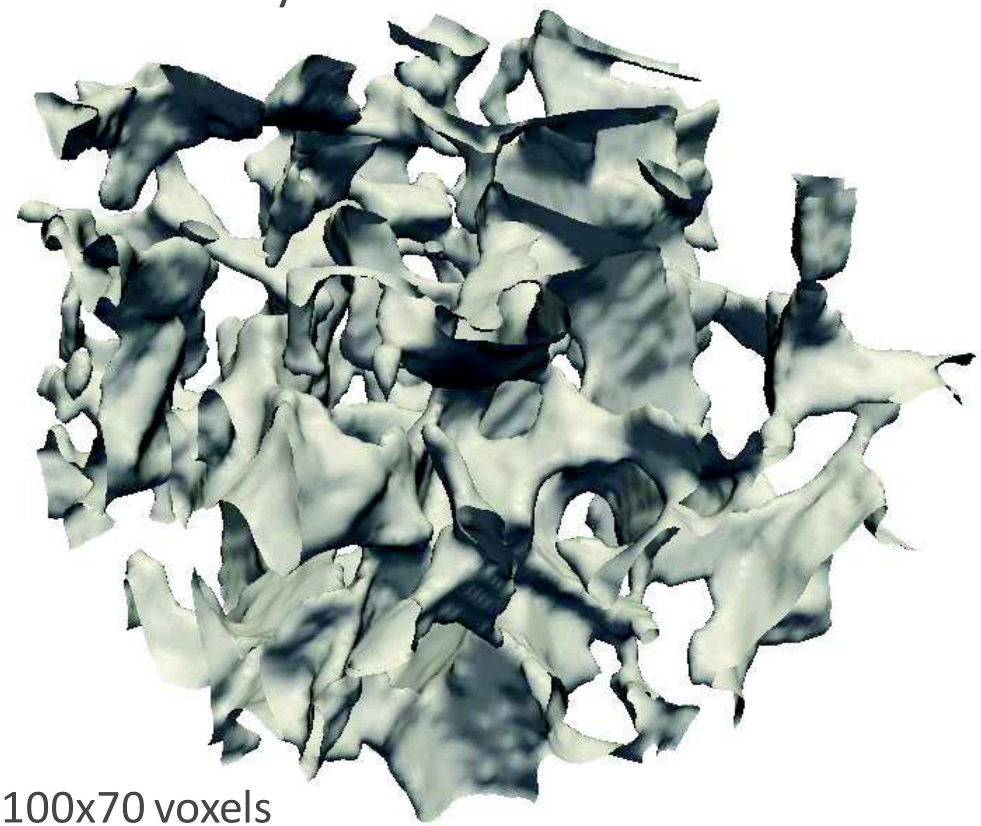

- Porosity 20.6 %
- Voxel size 5.6 μm
- Small subset 100x100x70 voxels

Data set available on the internet (Network Generation Comparison Forum): http://xct.anu.edu.au/network_comparison/

Castlegate Sandstone

$C = 0.30$

= Non-wetting phase ($\phi_{nw} < 0$)

Castlegate Sandstone

$C = 0.50$

= Non-wetting phase

Castlegate Sandstone

$C = 0.60$

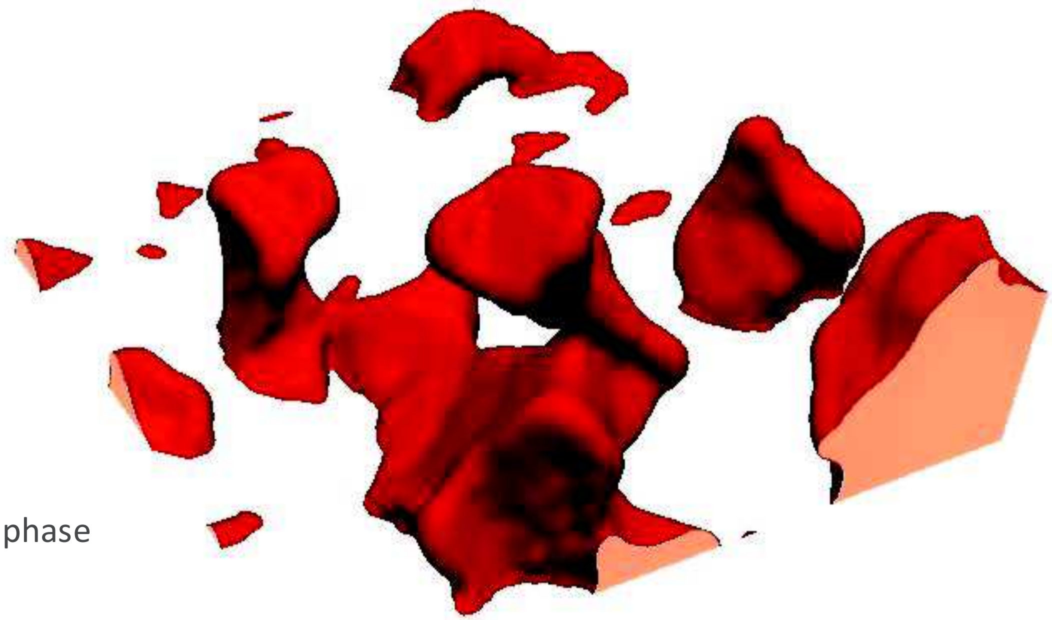

= Non-wetting phase

Castlegate Sandstone

$C = 0.75$

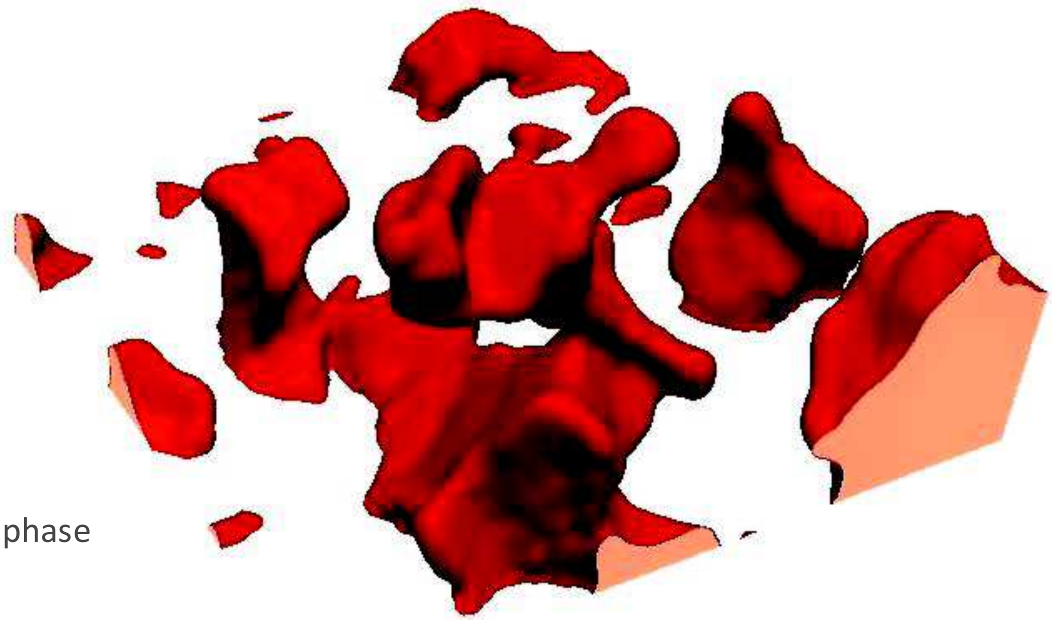

= Non-wetting phase

Castlegate Sandstone

$C = 0.80$

= Non-wetting phase

Castlegate Sandstone

$C = 0.85$

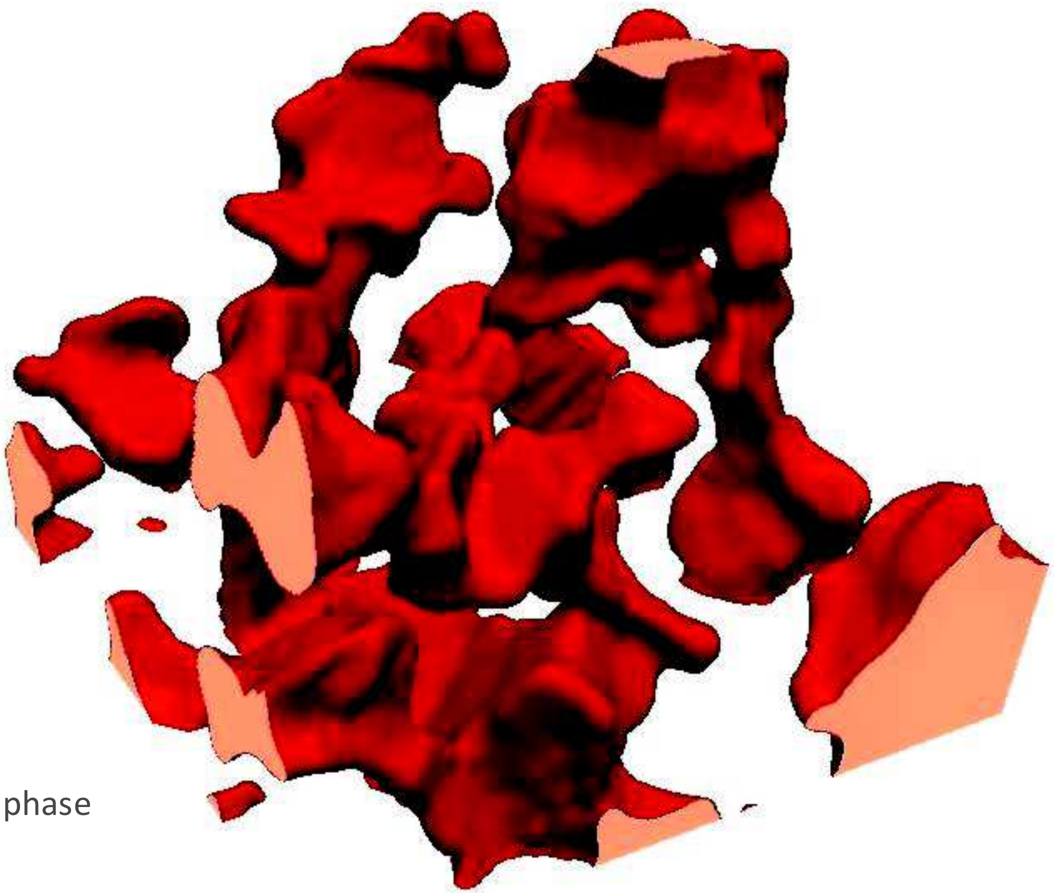

= Non-wetting phase

Castlegate Sandstone

$C = 0.95$

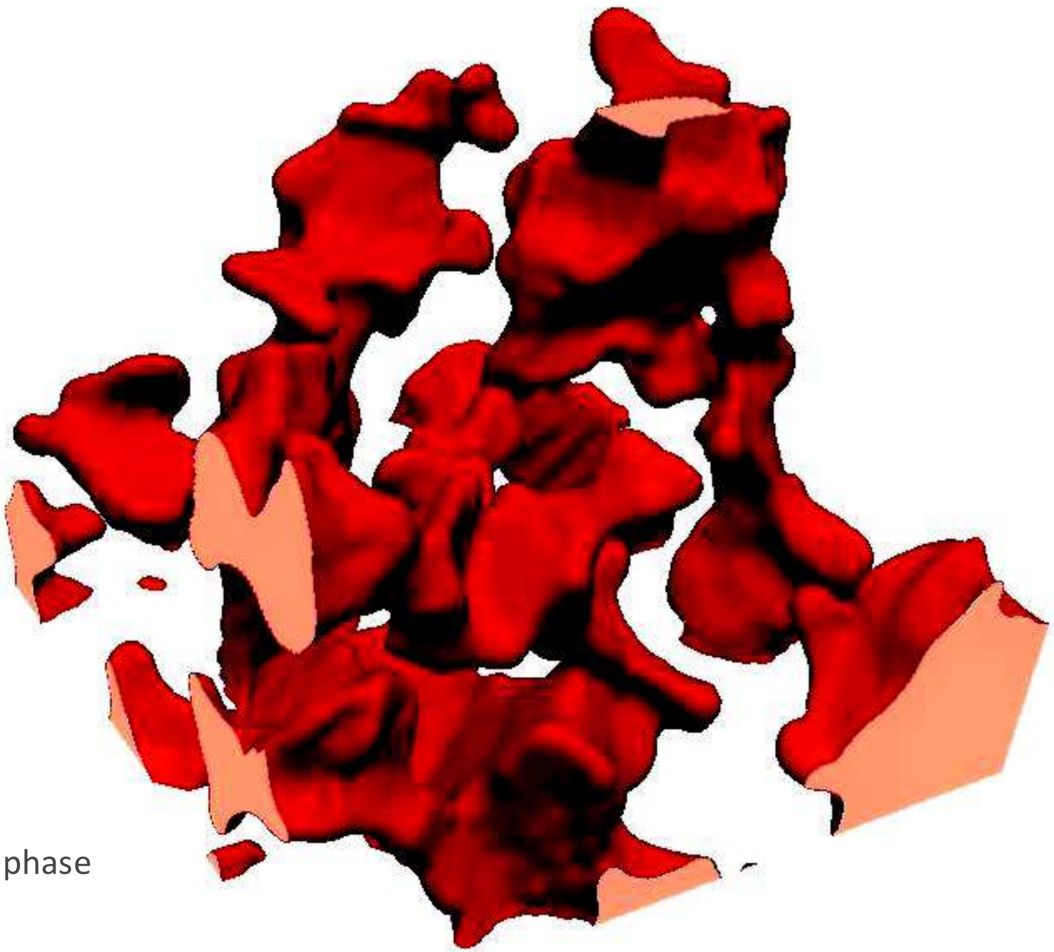

= Non-wetting phase

Castlegate Sandstone

$C = 1.05$

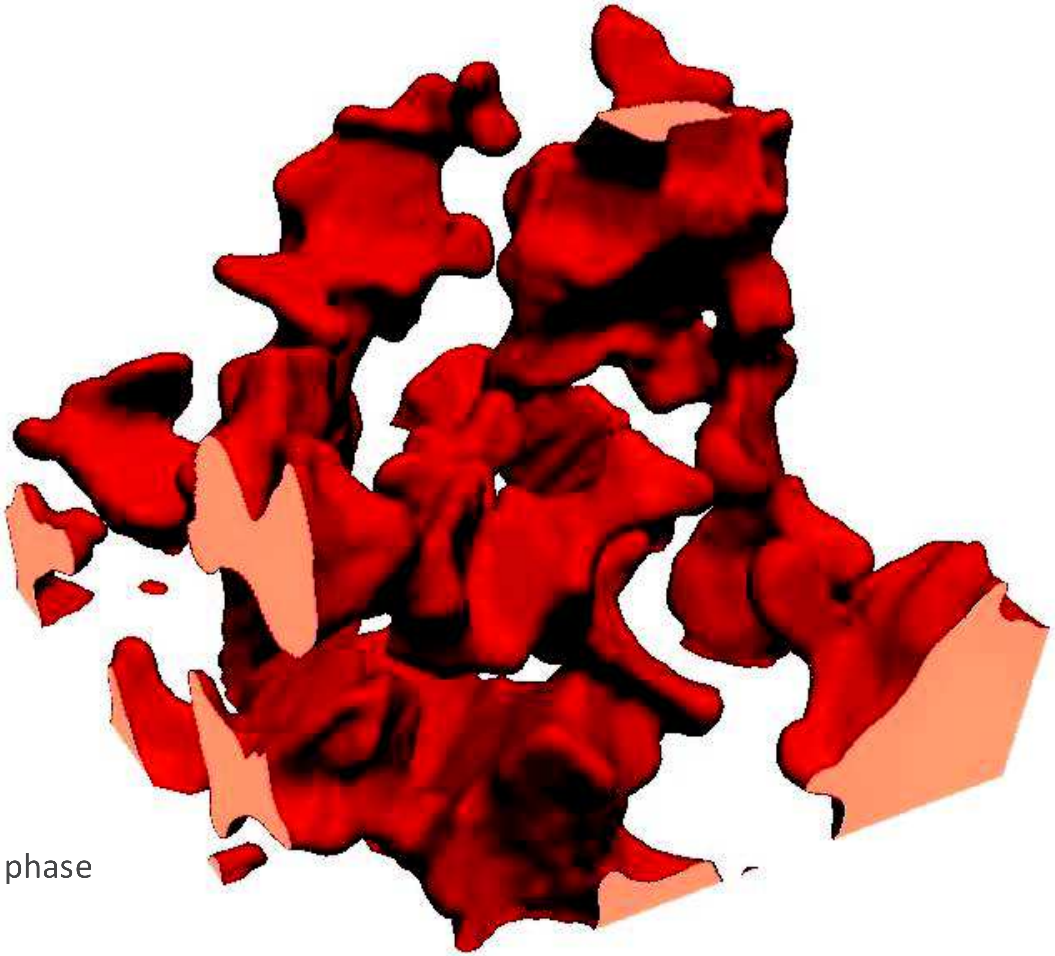

= Non-wetting phase

Castlegate Sandstone

$C = 1.15$

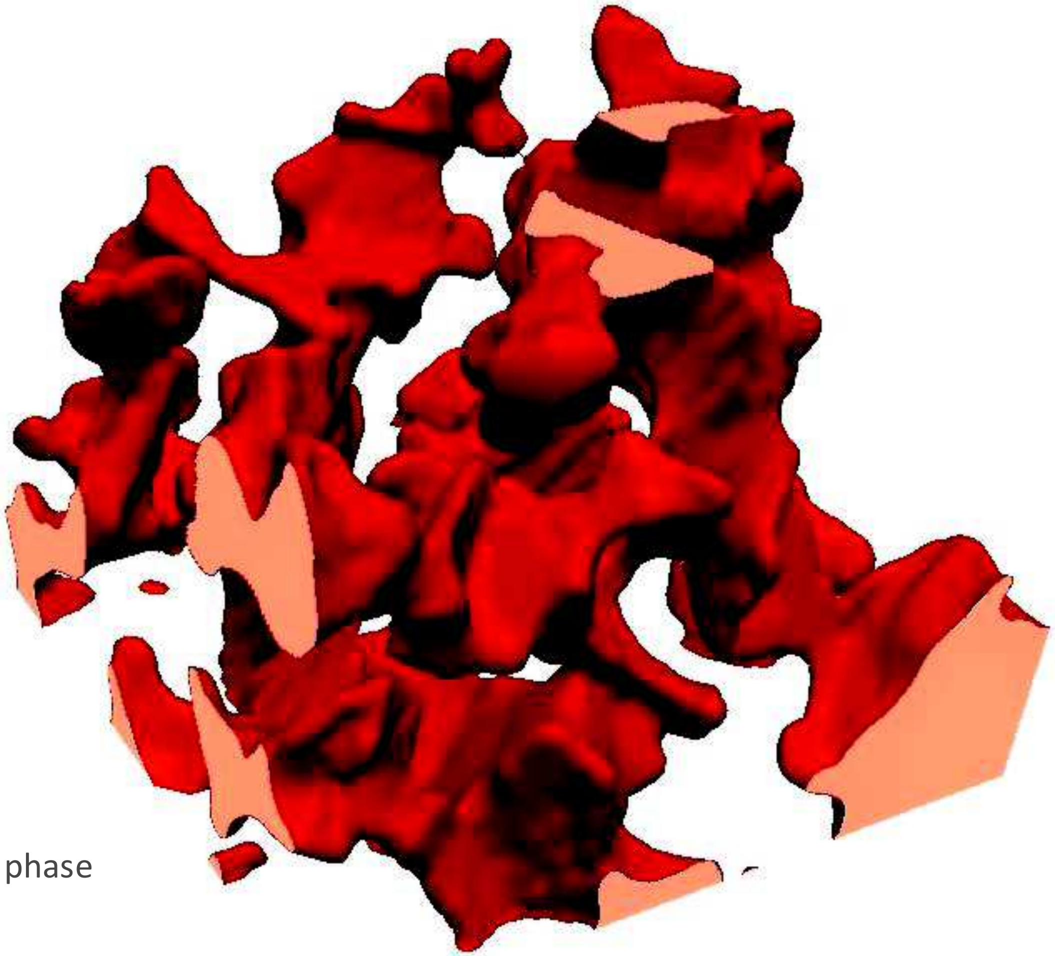

= Non-wetting phase

Castlegate Sandstone

$C = 1.35$

= Non-wetting phase

Castlegate Sandstone

$C = 1.5$

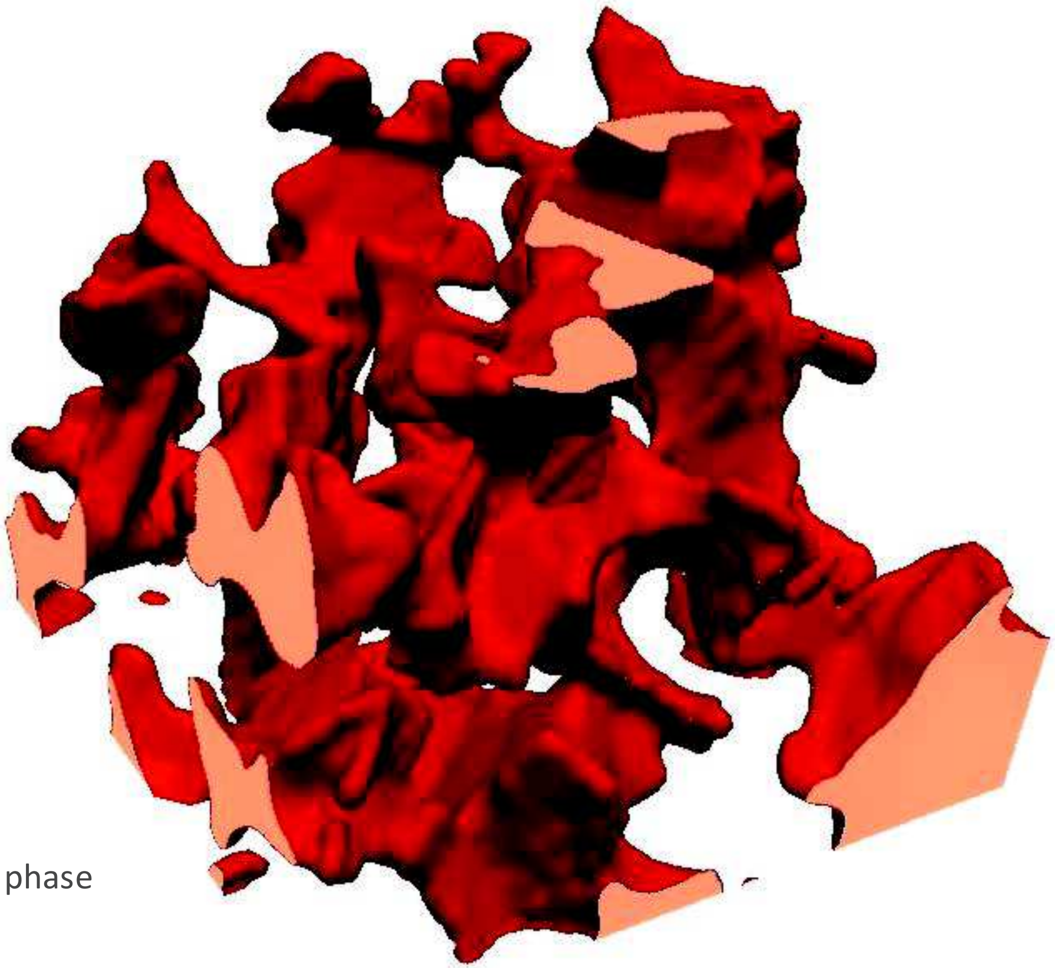

= Non-wetting phase

3D LSM simulation: Castlegate sandstone

$C = 1.6$

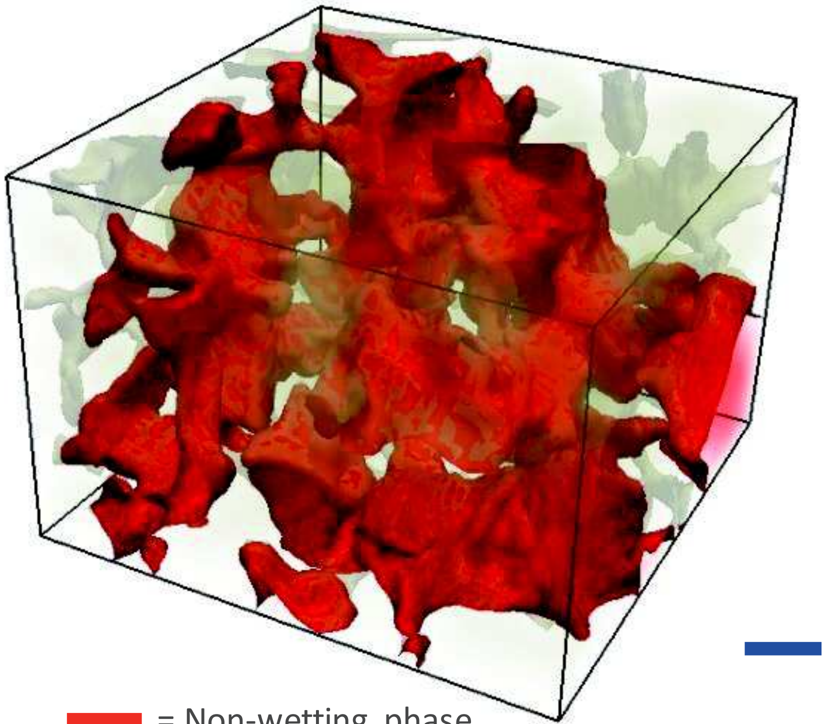

= Non-wetting phase

Structure of the wetting phase:

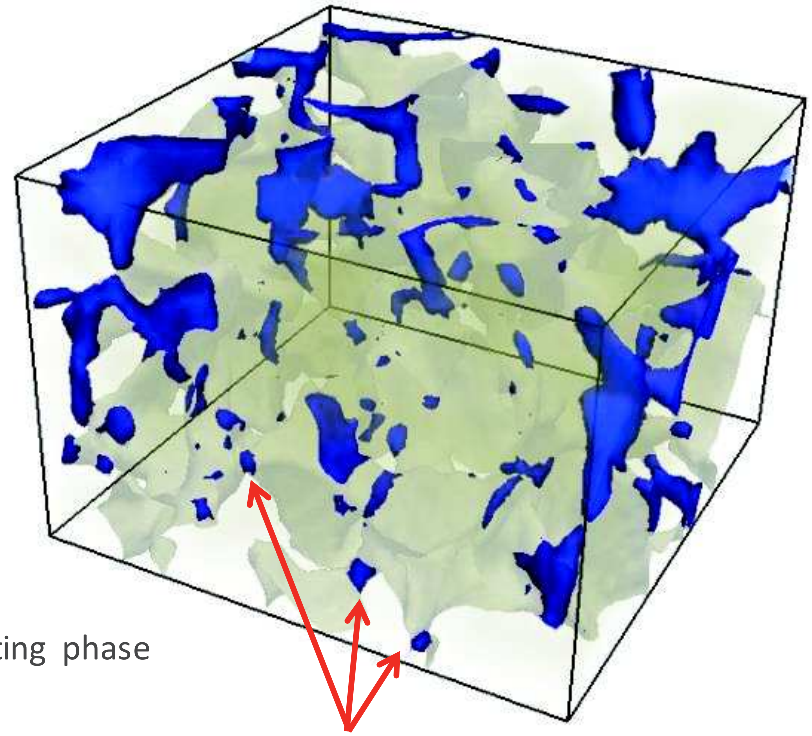

= Wetting phase

Isolated wetting phase is located in narrow pore throats and constrictions

Castlegate sandstone

Capillary pressure curve:

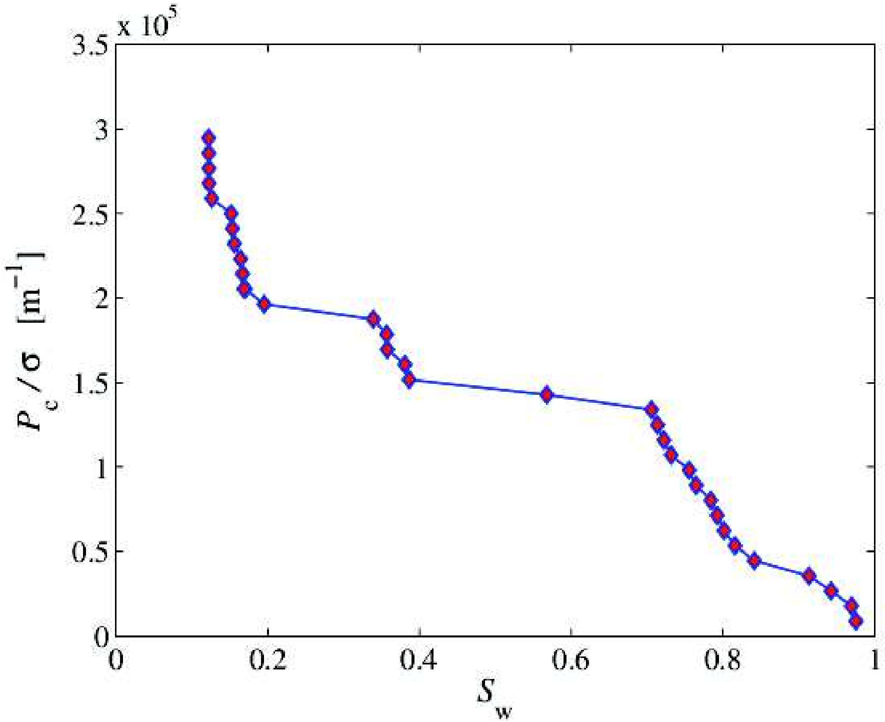

Simulation in fractured rock

IRIS

- Computer-generated fractured sample from LBNL
- The non-wetting phase invades the diagonal micro-fracture and some of the large pores first

$$C = 0.25$$

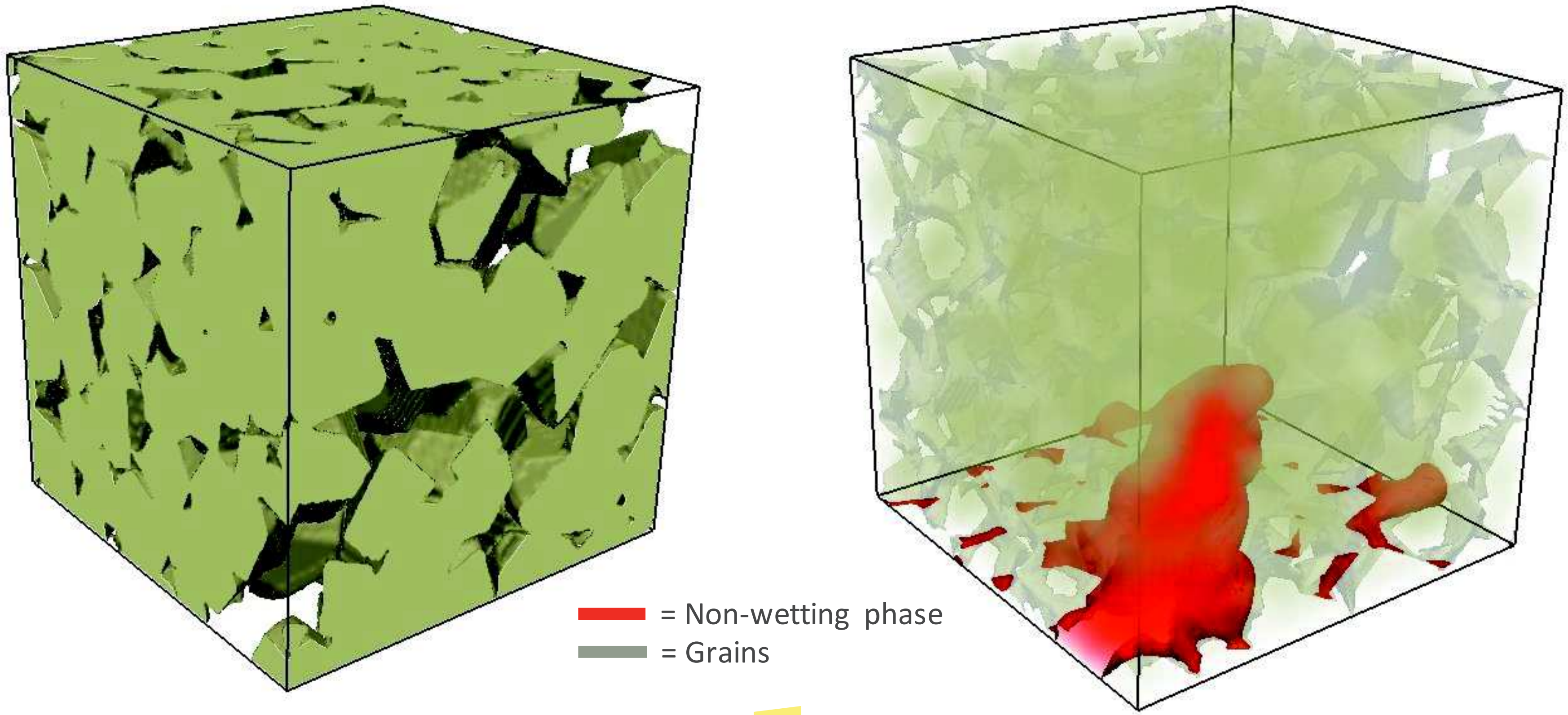

Simulation in fractured rock

- Computer-generated fractured sample from LBNL
- The non-wetting phase invades the diagonal micro-fracture and some of the large pores first

$C = 0.55$

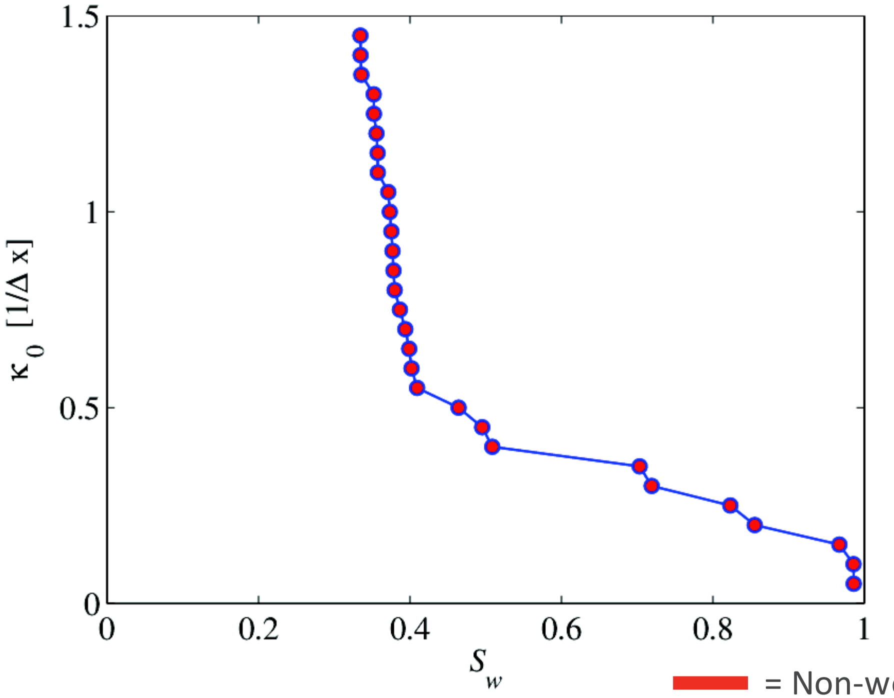

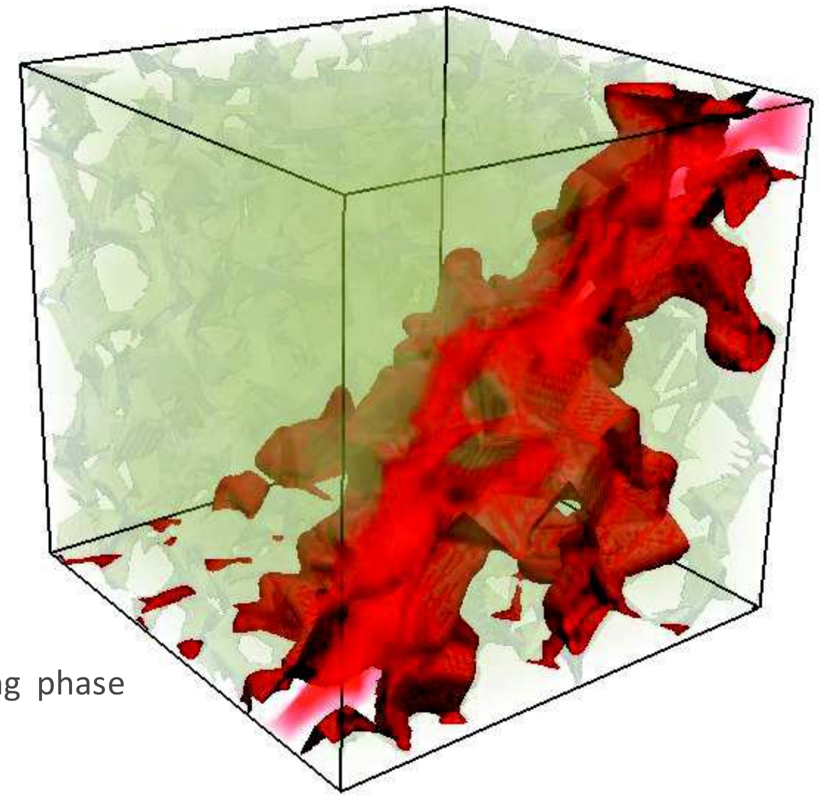

= Non-wetting phase
= Grains

LS Method with Contact Angle (CA-LSM)

(Jettestuen, et al., WRR 2013)

› Formation of the contact angle in the solid at steady state:

$$\cos\beta = \vec{n}_{\psi} \cdot \vec{n}_{\phi} = \frac{\nabla\psi}{|\nabla\psi|} \cdot \frac{\nabla\phi}{|\nabla\phi|} = -\cos\theta$$

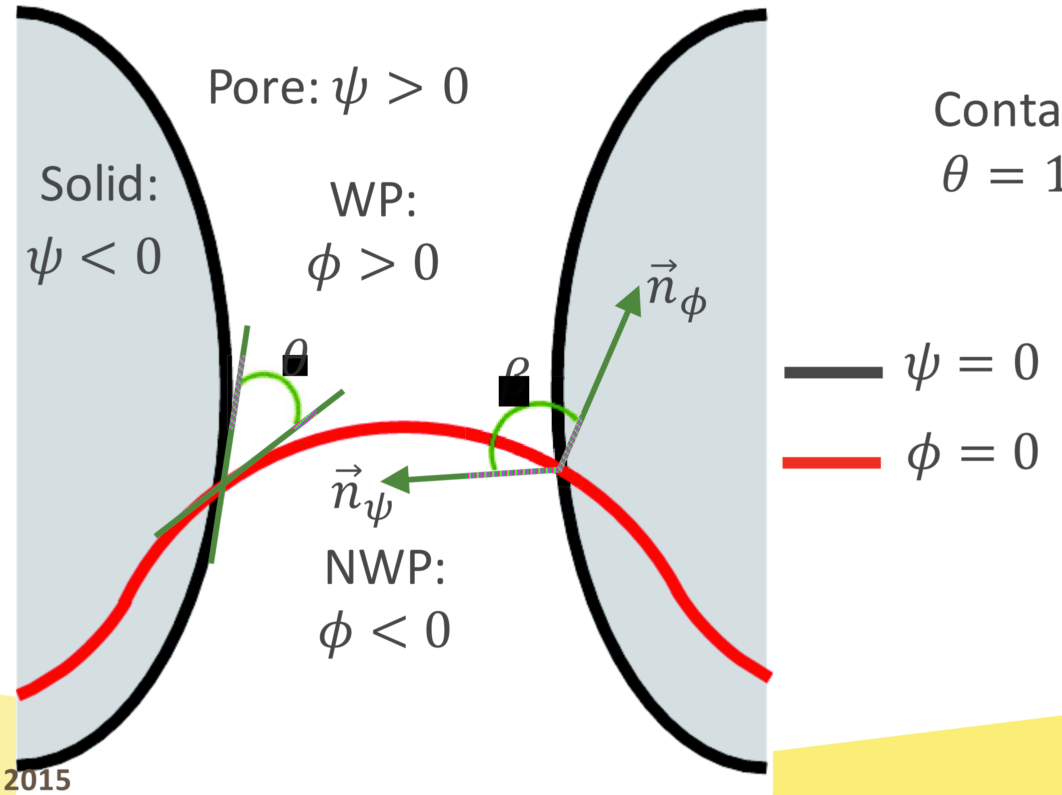

Contact angle:
$\theta = 180° - \beta$

LS Method with Contact Angle (CA-LSM)

› Formation of the contact angle in the solid at steady state:

$$\nabla\psi \cdot \nabla\phi - \cos\beta\,|\nabla\psi||\nabla\phi| = 0$$

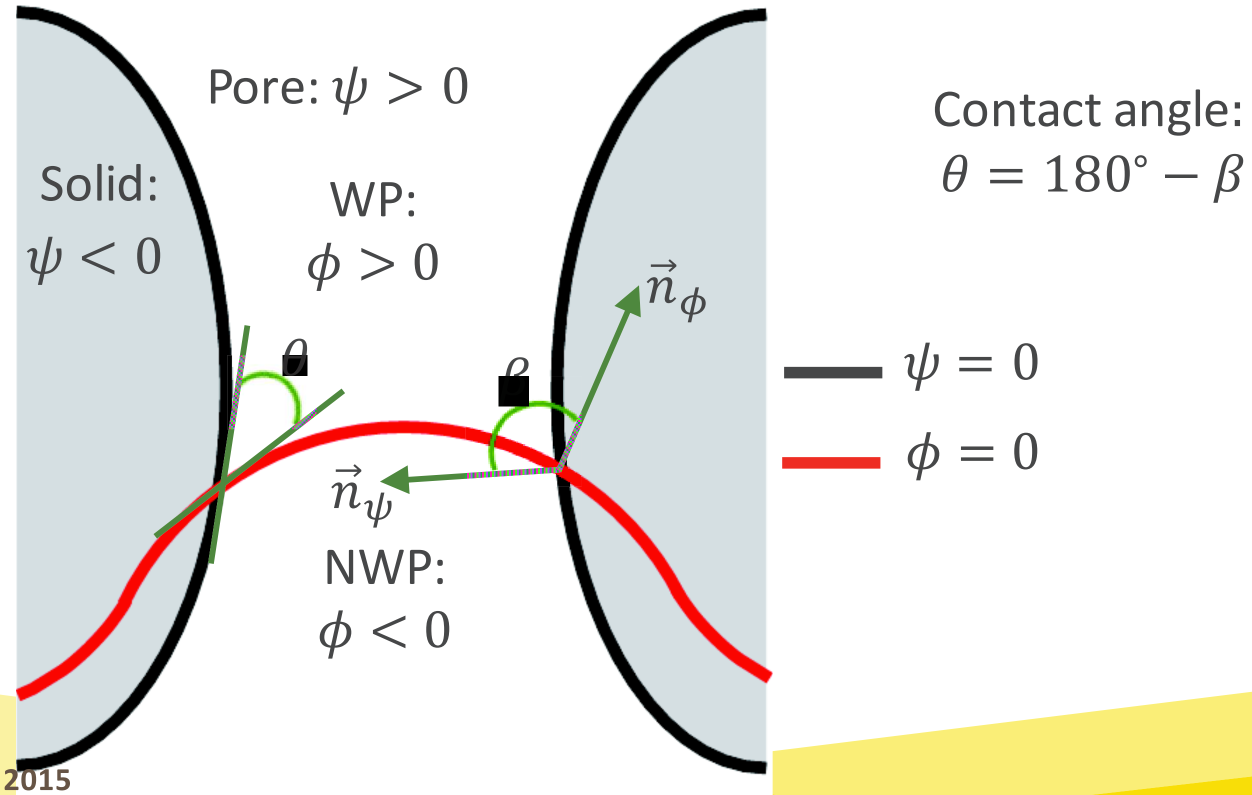

LS Method with Contact Angle (CA-LSM)

› Resulting evolution equation:

$$\phi_t + H(\psi)(C-\kappa)|\nabla\phi| + H(-\psi)S(\psi)B(\nabla\psi\cdot\nabla\phi - \cos\beta|\nabla\psi||\nabla\phi|) = 0$$

Pore space: $\psi > 0$ — Balance between capillary and interfacial forces in the pore space

Solid phase: $\psi < 0$ — Formation of the contact angle in the solid phase

$B = O(1/\Delta x)$ constant
$\theta = 180° - \beta =$ Contact angle
$\psi =$ LS function describing the pore walls
$H =$ Heaviside step function
$S =$ Sign function

(Jettestuen, et al., WRR 2013)

Heaviside $H(\phi)$ and delta $\delta(\phi)$ functions facilitates phase volume and interfacial area calculation.

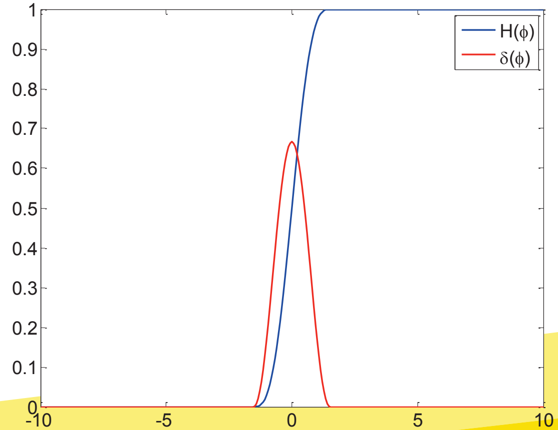

Castlegate sandstone - Drainage

$\theta = 0°$ (standard level set model)

$\theta = 20°$

$\theta = 40°$

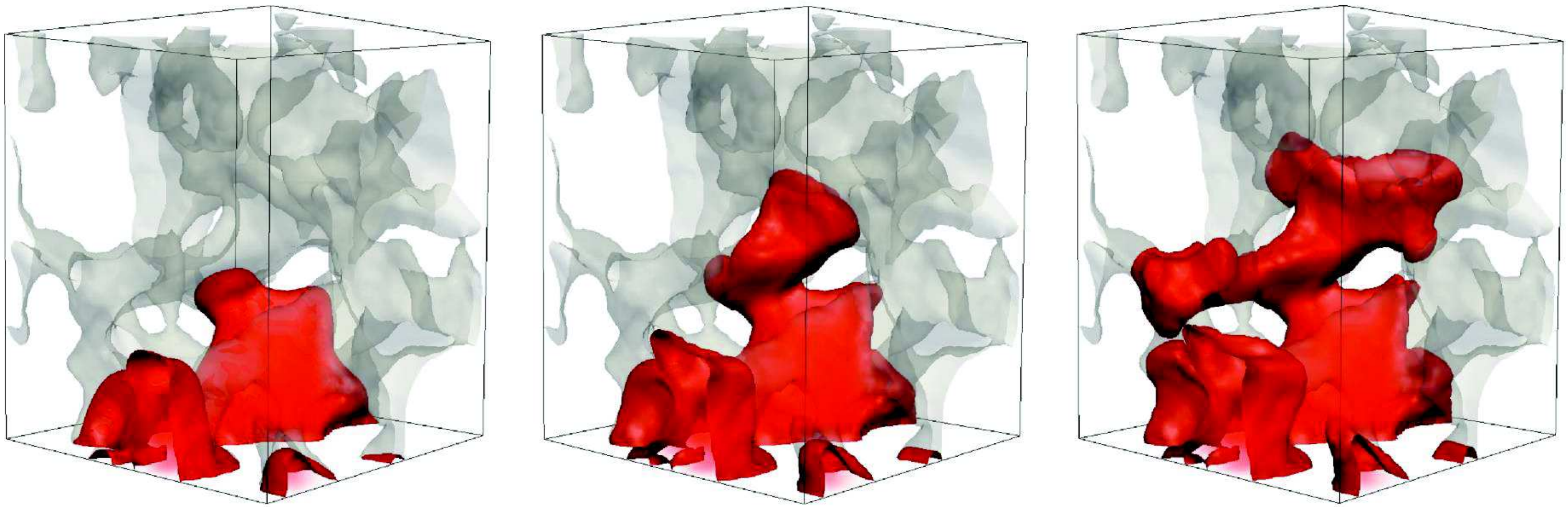

$C = 0.50$

= Non-wetting phase

= Grains

Castlegate sandstone - Drainage

$\theta = 0°$
(standard level set model)

$\theta = 20°$

$\theta = 40°$

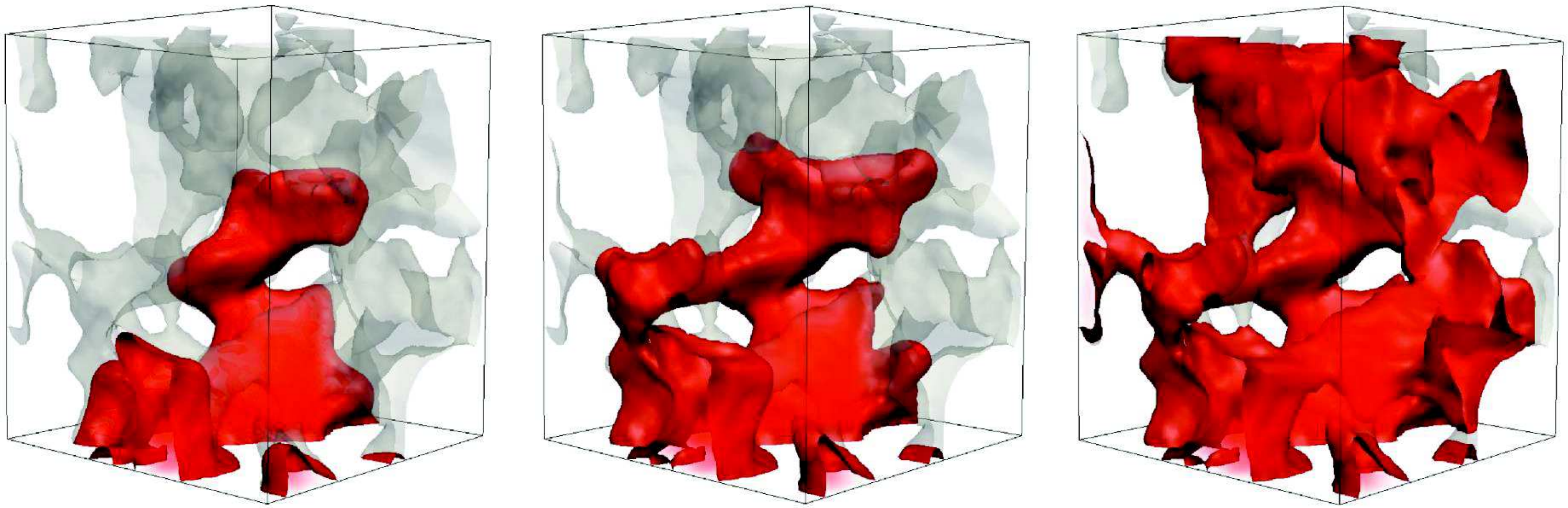

$C = 0.60$

= Non-wetting phase
= Grains

Castlegate sandstone - Drainage

$\theta = 0°$ (standard level set model)

$\theta = 20°$

$\theta = 40°$

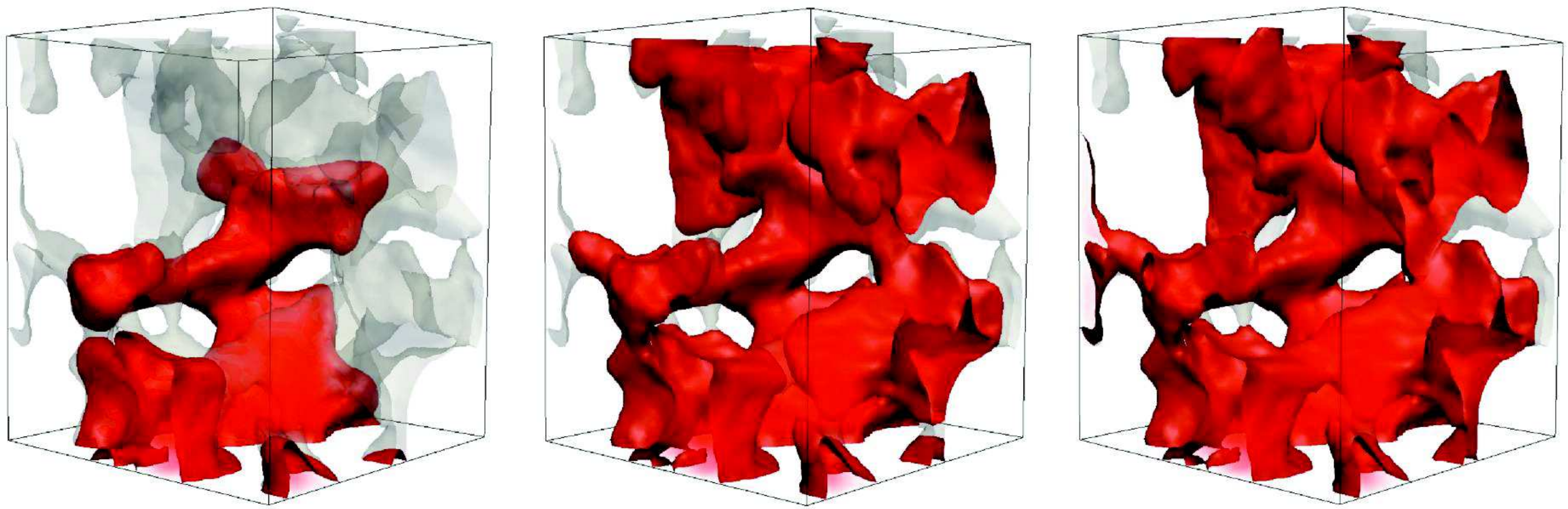

$C = 0.70$

= Non-wetting phase

= Grains

Castlegate sandstone - Drainage

$\theta = 0°$ (standard level set model)	$\theta = 20°$	$\theta = 40°$

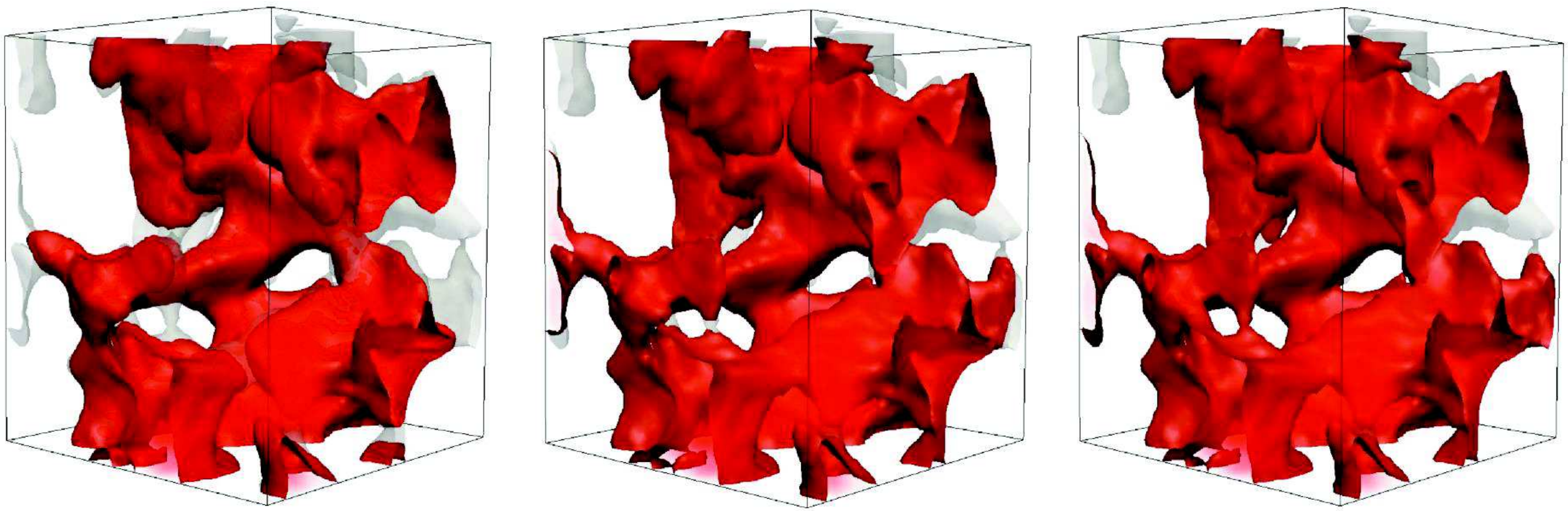

$C = 1.0$

= Non-wetting phase
= Grains

Castlegate sandstone - Imbibition

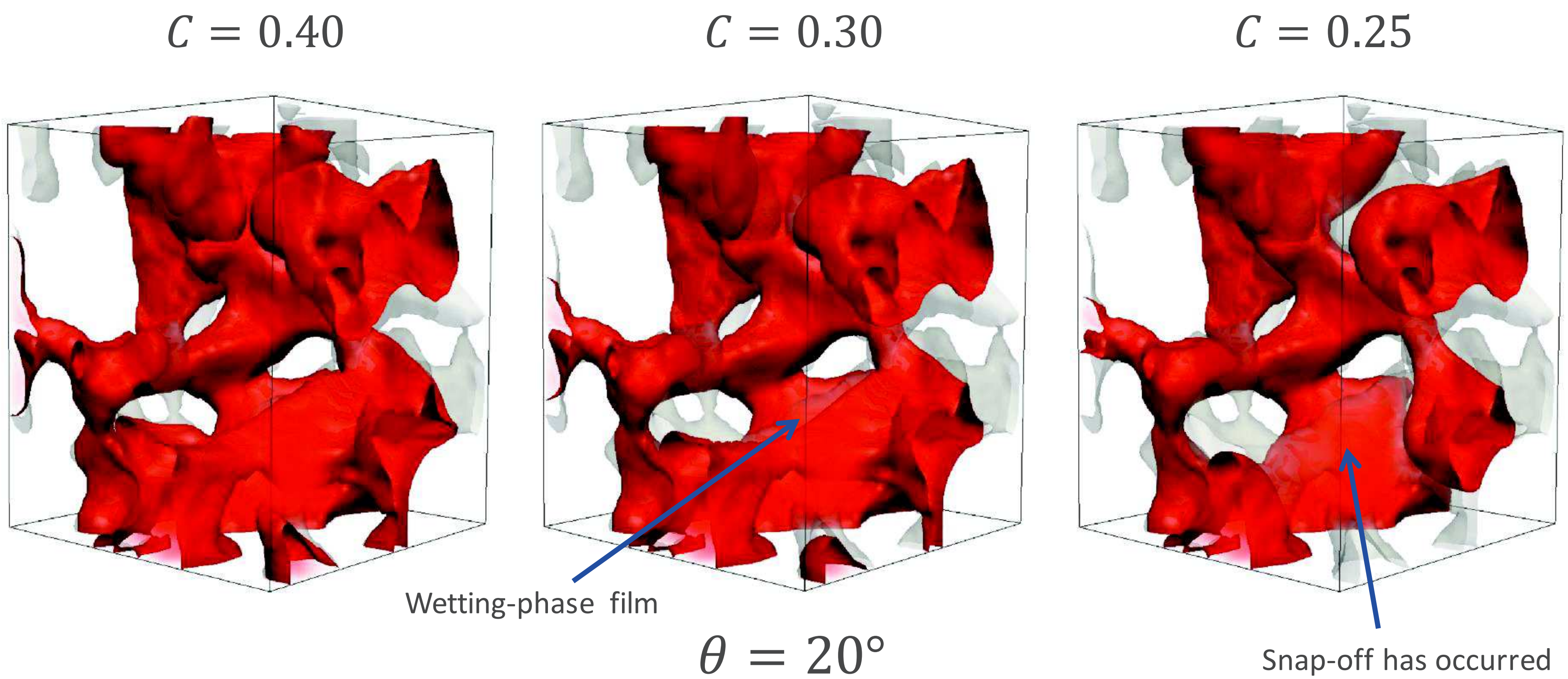

$\theta = 20°$

- Non-wetting phase retracts to larger pore openings after growth of wetting-phase films has led to snap-off in pore-throat constrictions

Castlegate sandstone – Capillary pressure curves

Drainage:

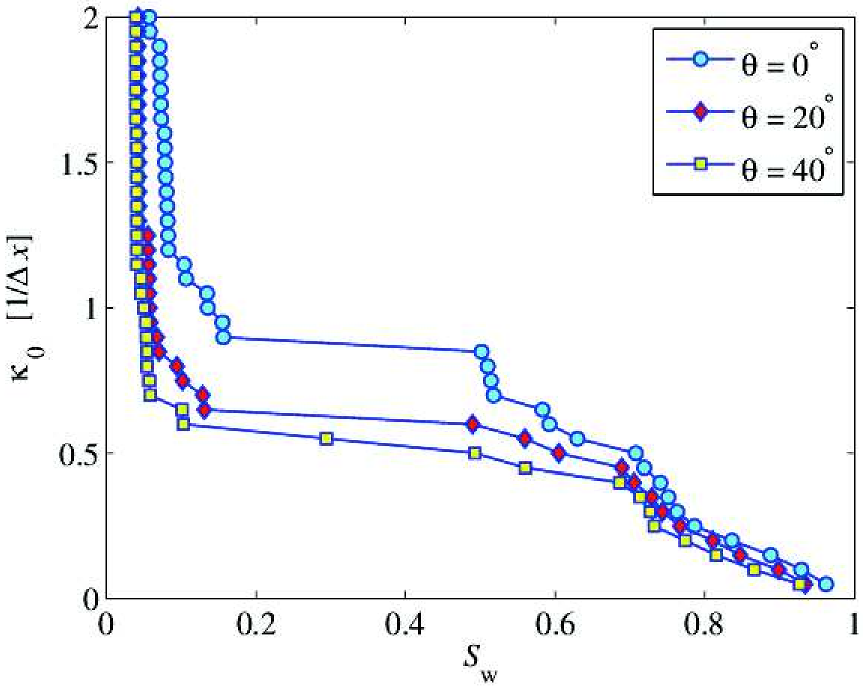

Drainage & imbibition ($\theta = 20°$):

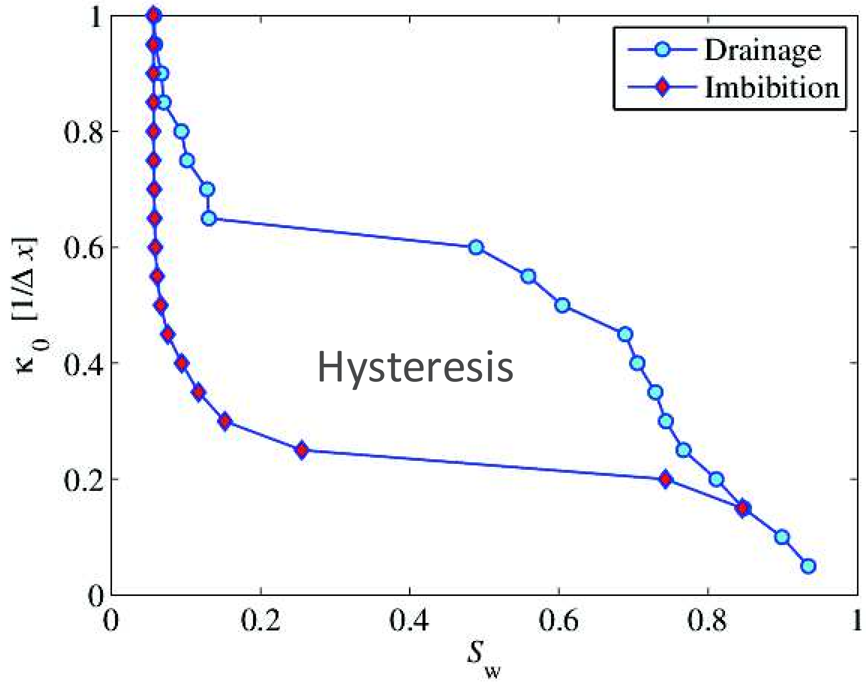

Summary

A 3D level set based pore-scale model has been developed to simulate capillary-controlled displacements in rock images.

› A method to include arbitrary contact angles has been developed and implemented.

› Simulations in 3D pore geometries demonstrate that the model accounts for well-known pore-scale mechanisms:

- Piston-like invasion
- Haines jumps (drainage)
- Wetting-phase film growth and snap-off (imbibition)
- Interface coalescence and retraction
- Hysteresis occurs between drainage and imbibition due to different displacement mechanisms

Variational Level Set (VLS) Method

(Zhao et al, J Comput Phys 127, 1996; Helland & Jettestuen, SCA 2014)

- Developed for motion of triple junctions
- We add solid phase and contact angle to existing method

For each fluid:

ϕ_i (LS function)

p_i (phase pressure)

γ_i (surface tension)

β_i (solid/pore intersection angle)

$\gamma_s - \gamma_i \cos\beta_i$ (solid/fluid interfacial tension)

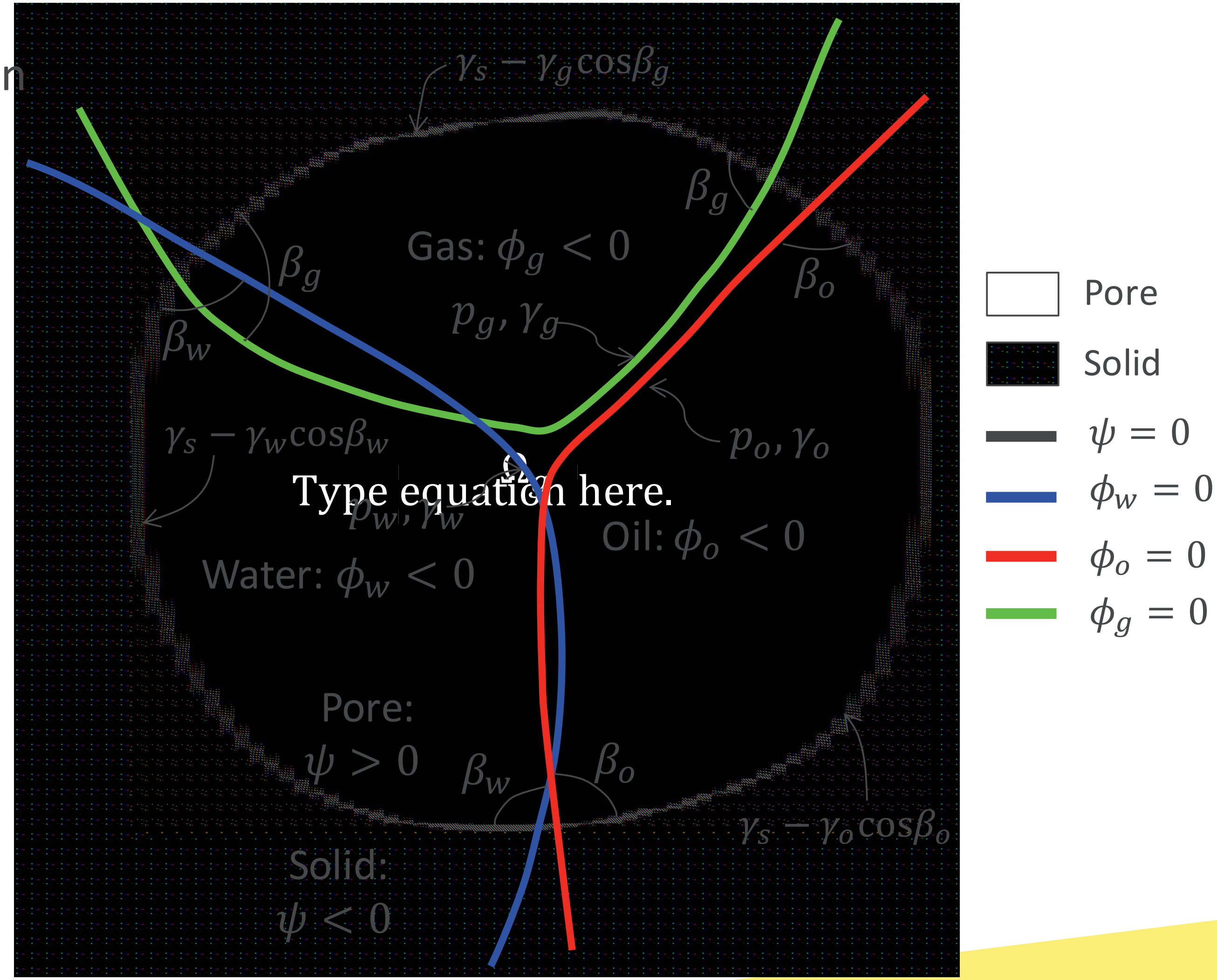

Variational Level Set Method

Total energy:

$$E = E_1 + E_2 + E_3$$

Bulk energy:

$$E_1 = \sum_{i=g,o,w} p_i \int_{\Omega} H(-\phi_i) H(\psi)\, dV$$

Fluid/fluid interfacial energy:

$$E_2 = \sum_{i=g,o,w} \gamma_i \int_{\Omega} \delta(\phi_i) |\nabla \phi_i| H(\psi)\, dV$$

Solid/fluid interfacial energy:

$$E_3 = \sum_{i=g,o,w} (\gamma_s - \gamma_i \cos \beta_i) \times \int_{\Omega} H(-\phi_i) \delta(\psi) |\nabla \psi|\, dV$$

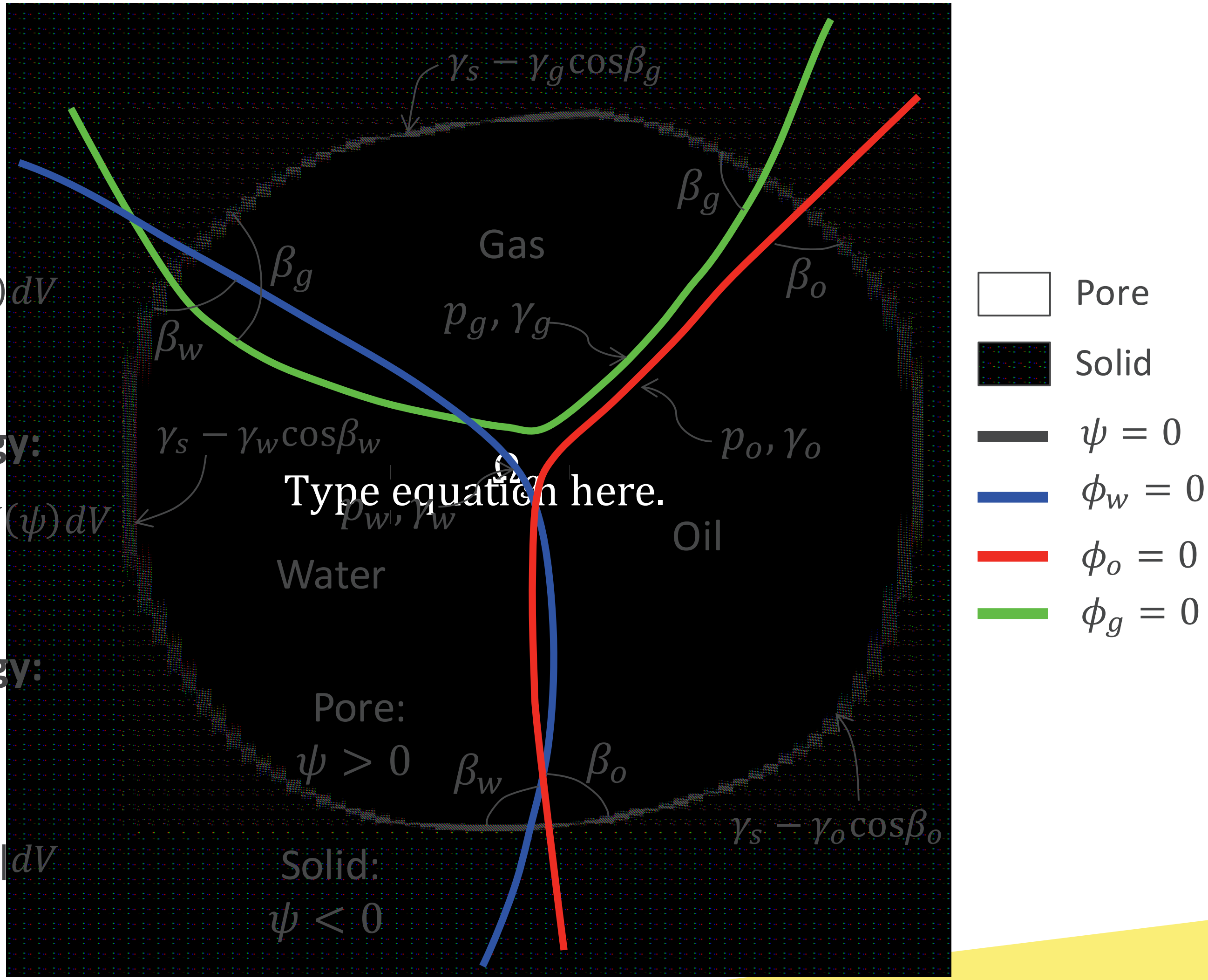

Variational Level Set Method

Overlap/vacuum regions occur if ϕ_i moves with independent velocities.

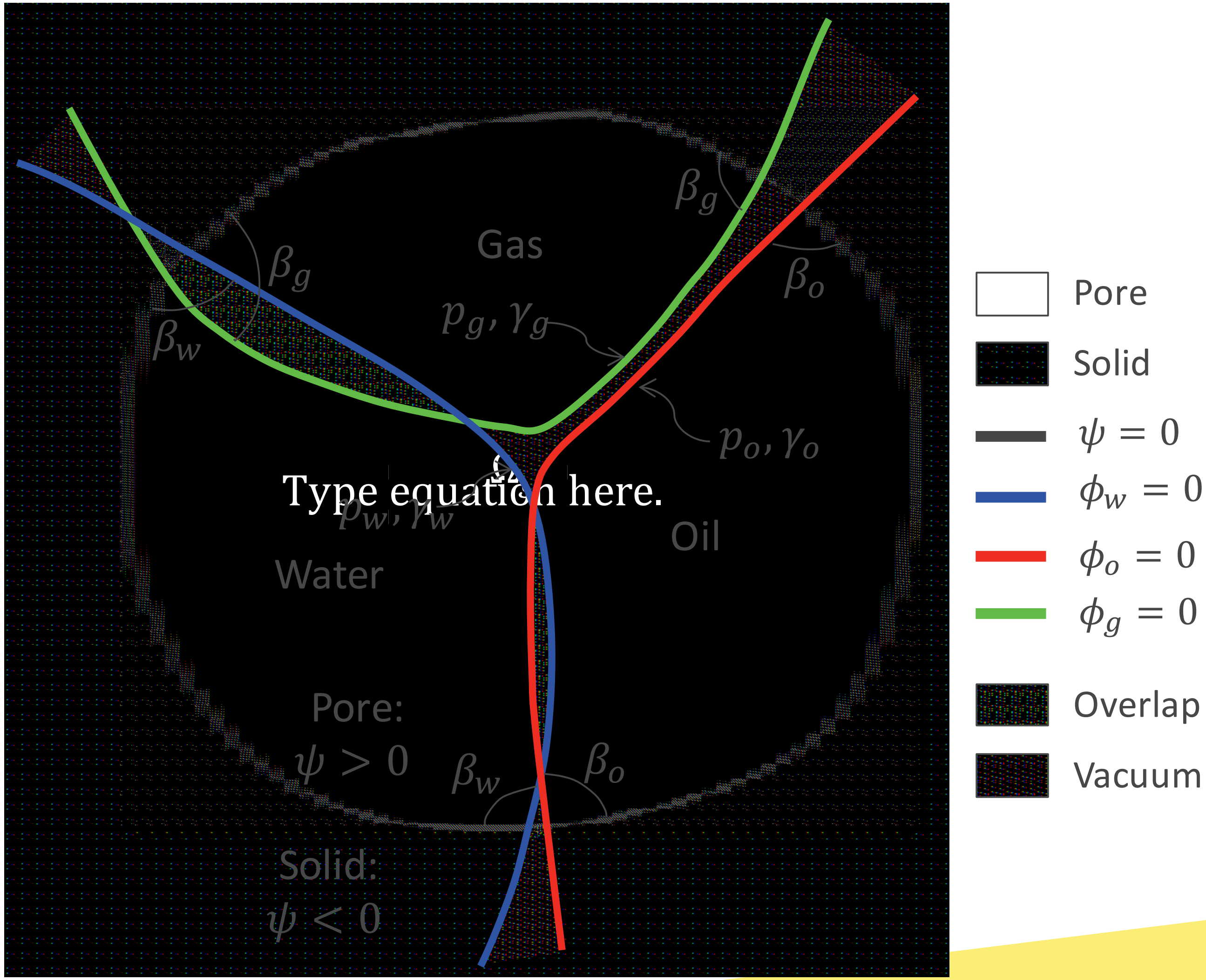

Variational Level Set Method

Constraint prevents overlap/vacuum regions:

$$\frac{1}{2}\int_{\Omega}\left(\sum_{i=g,o,w} H(-\phi_i) - 1\right)^2 dV = 0$$

$$\Downarrow$$

Interfacial tensions (σ_{ij}), capillary pressures (P_{cij}) and contact angles (θ_{ij}) are defined at the interfaces.

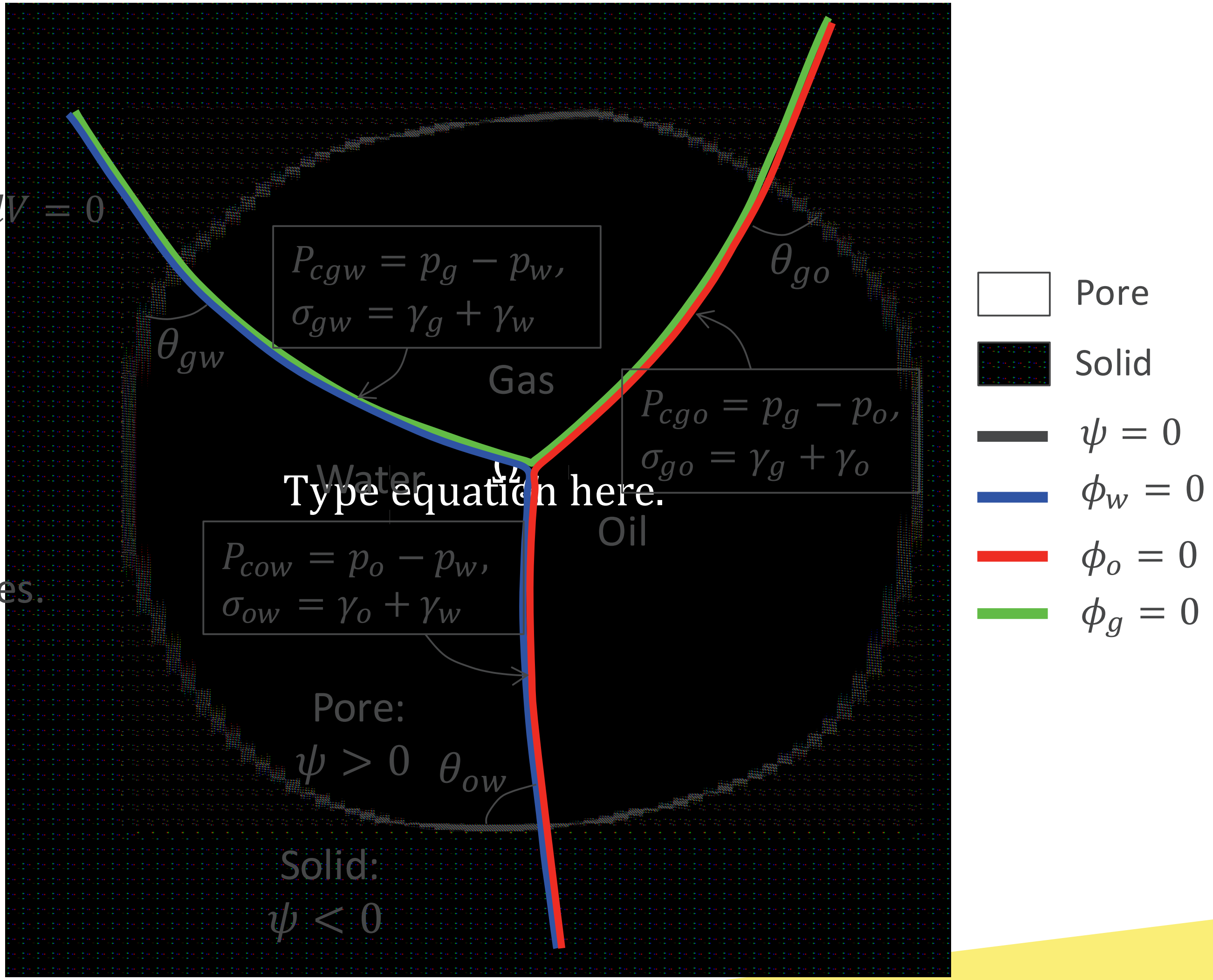

Variational Level Set Method

Stable interface configurations:

Pore space:

$$P_{cij} = (\gamma_i + \gamma_j)\kappa_i$$

(Young-Laplace Equation)

Pore walls (& solid):

$$\cos\theta_{ij} = \frac{\gamma_j \cos\beta_j - \gamma_i \cos\beta_i}{\gamma_i + \gamma_j}$$

(Young Equation)

⇕

$$\sigma_{gw}\cos\theta_{gw} = \sigma_{go}\cos\theta_{go} + \sigma_{ow}\cos\theta_{ow}$$

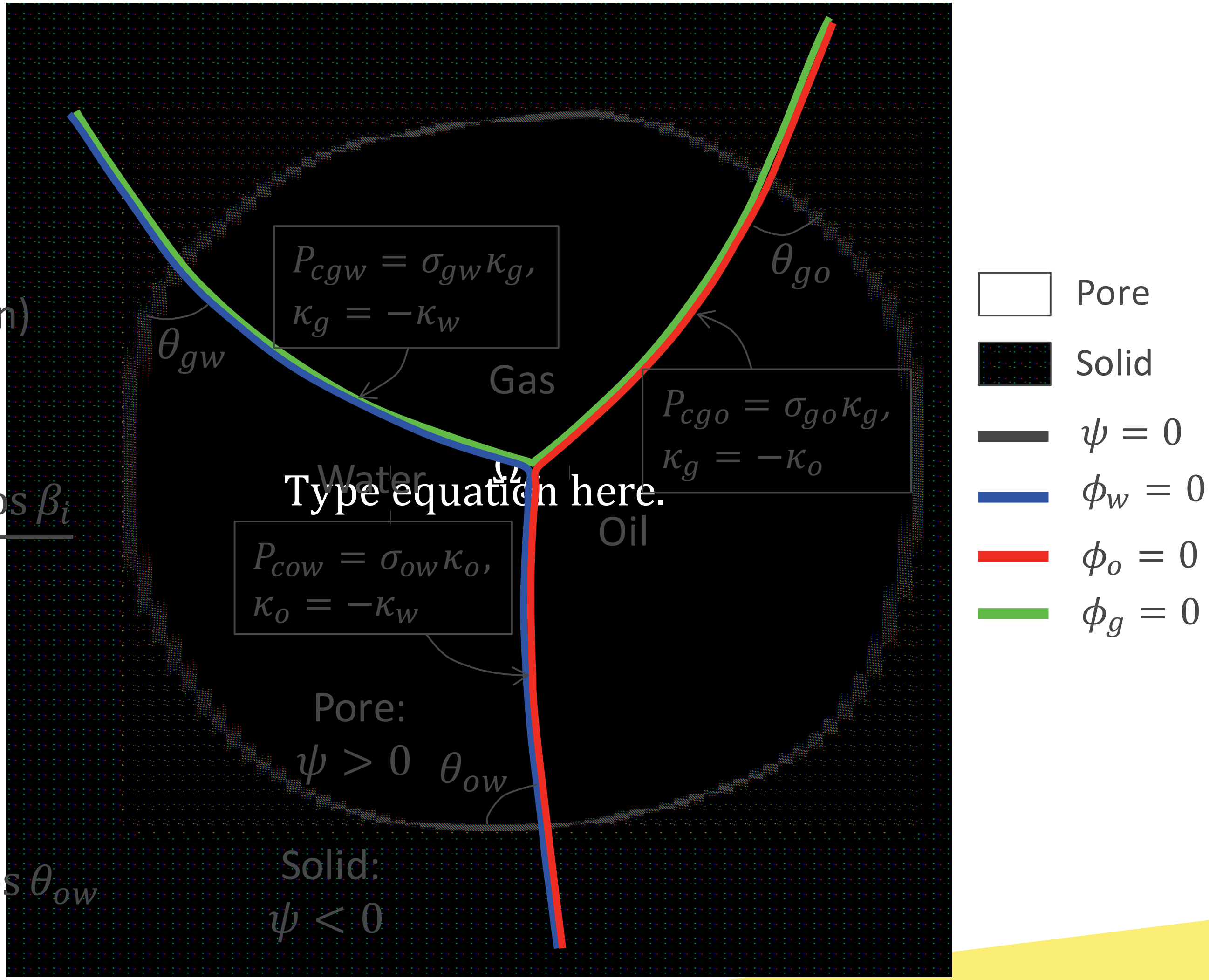

Variational Level Set Method

› Putting it all together:

$$
\begin{aligned}
f(\phi_g, \phi_o, \phi_w) &= \int_\Omega \Bigg(\sum_{i=g,o,w} p_i H(-\phi_i) H(\psi) + \sum_{i=g,o,w} \gamma_i \delta(\phi_i) |\nabla \phi_i| H(\psi) \\
&+ \frac{\lambda}{2} \left(\sum_{i=g,o,w} H(-\phi_i) - 1 \right)^2 \\
&- \sum_{i=g,o,w} \gamma_i \left(\frac{\nabla \phi_i}{|\nabla \phi_i|} \cdot \frac{\nabla \psi}{|\nabla \psi|} - \cos \beta_i \right) \delta(\psi) |\nabla \psi| H(-\phi_i) \Bigg) dV
\end{aligned}
$$

(Young-Laplace in pore space)

(No overlap/vacuum constraint)

(Formation of contact angle on pore/solid surface)

λ = Lagrange multiplier

Variational Level Set Method

› Minimizing f with respect to $\phi_i, i = g, o, w$ gives three evolution equations:

$$(\phi_i)_t + \lambda\left(\sum_{j=g,o,w} H(-\phi_j) - 1\right)|\nabla\phi_i| + H(\psi)(p_i - \gamma_i\kappa_i)|\nabla\phi_i| + \frac{H(-\psi)}{\Delta x} S(\psi)\gamma_i(\nabla\phi_i \cdot \nabla\psi - \cos\beta_i\,|\nabla\phi_i||\nabla\psi|) = 0, \qquad i = g, o, w$$

› $H(-\psi)/\Delta x$ has replaced $\delta(\psi)$ to extend contact angle into solid, which is more accurate numerically.

› The solution ϕ_i must satisfy the constraint at at all times:

$$\frac{d}{dt}\frac{1}{2}\int_\Omega \left(\sum_{i=g,o,w} H(-\phi_i) - 1\right)^2 dV = -\sum_{i=g,o,w}\int_\Omega \left(\sum_{j=g,o,w} H(-\phi_j) - 1\right)\delta(\phi_i)(\phi_i)_t dV = 0$$

› This gives an expression for the Lagrange multiplier λ.

Relation between β, γ and θ

- At equilibrium, the zero contours of ϕ in solid satisfy:

$$\gamma_i(\nabla\psi \cdot \nabla\phi_i - \cos\beta_i |\nabla\psi||\nabla\phi_i|) = \gamma_j(\nabla\psi \cdot \nabla\phi_j - \cos\beta_j |\nabla\psi||\nabla\phi_j|)$$

- The intersection angles between the zero contours of ψ and ϕ form the contact angles at the interfaces:

$$\cos\theta_{ij} = \vec{n}_\psi \cdot \vec{n}_{\phi_j} = \frac{\nabla\psi}{|\nabla\psi|} \cdot \frac{\nabla\phi_j}{|\nabla\phi_j|} \qquad (\nabla\phi_j = -\nabla\phi_i)$$

- This yields the following contact angle expressions:

$$\cos\theta_{ij} = \frac{\gamma_j \cos\beta_j - \gamma_i \cos\beta_i}{\gamma_j + \gamma_i}, \ ij = go, ow, gw.$$

- These relations satisfy the Bartell-Osterhof equation:

$$\sigma_{gw}\cos\theta_{gw} = \sigma_{go}\cos\theta_{go} + \sigma_{ow}\cos\theta_{ow}$$

Alternative Approach: Multiphase Level Set Method with «Projection Step»

- Alternative technique for removing overlap/vacuum regions
- Uncoupled evolution equations:

$$(\phi_i)_t + H(\psi)(p_i - \gamma_i \kappa_i)|\nabla\phi_i| + \frac{H(-\psi)}{\Delta x} S(\psi)\gamma_i(\nabla\phi_i \cdot \nabla\psi - \cos\beta_i\,|\nabla\phi_i||\nabla\psi|) = 0, \qquad i = g, o, w$$

- After each time iteration, perform a projection step:
  - Subtract the average of the two smallest ϕ_i from all ϕ_i in each point
- Example when $\phi_g > \phi_o, \phi_w$:

$$\phi_g = \phi_g - (\phi_o + \phi_w)/2,$$
$$\phi_o = \phi_o - (\phi_o + \phi_w)/2,$$
$$\phi_w = \phi_w - (\phi_o + \phi_w)/2.$$

(Losasso, Fedkiw et al., 2006)

Multiphase Level Set Method – «Projection Step»

- So, what is the role of the «projection step»?
- Illustrating 1D example – Initial configuration:

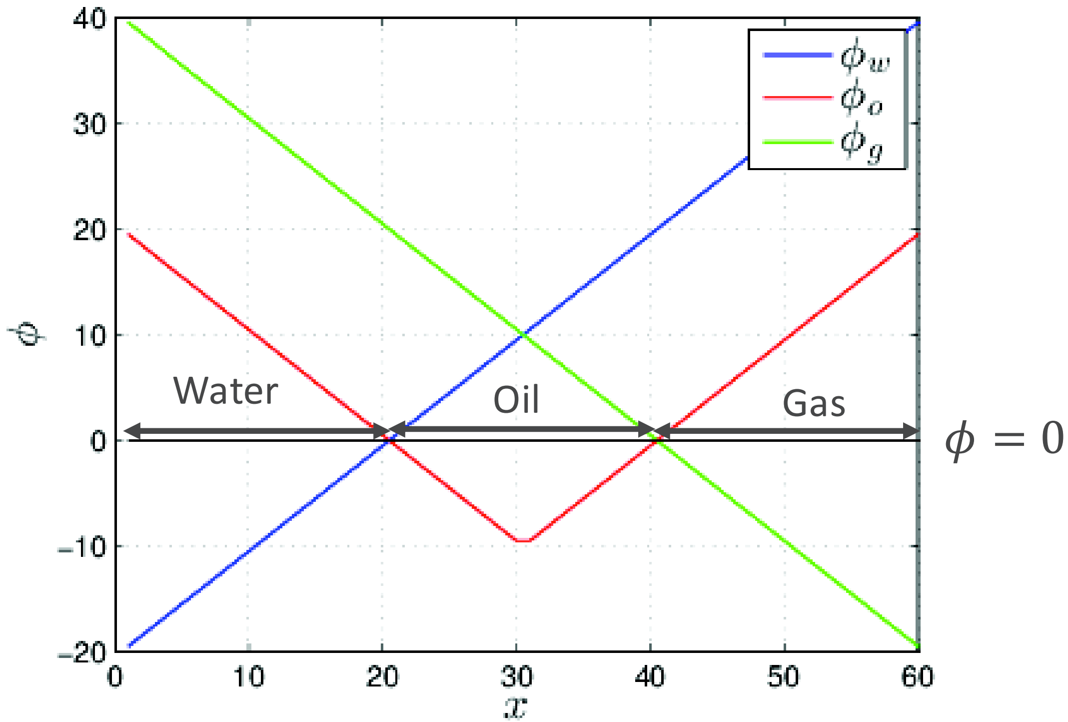

Multiphase Level Set Method – «Projection Step»

- Illustrating 1D example:
- Configuration after some time using uncoupled equations without projection step (dashed curves):

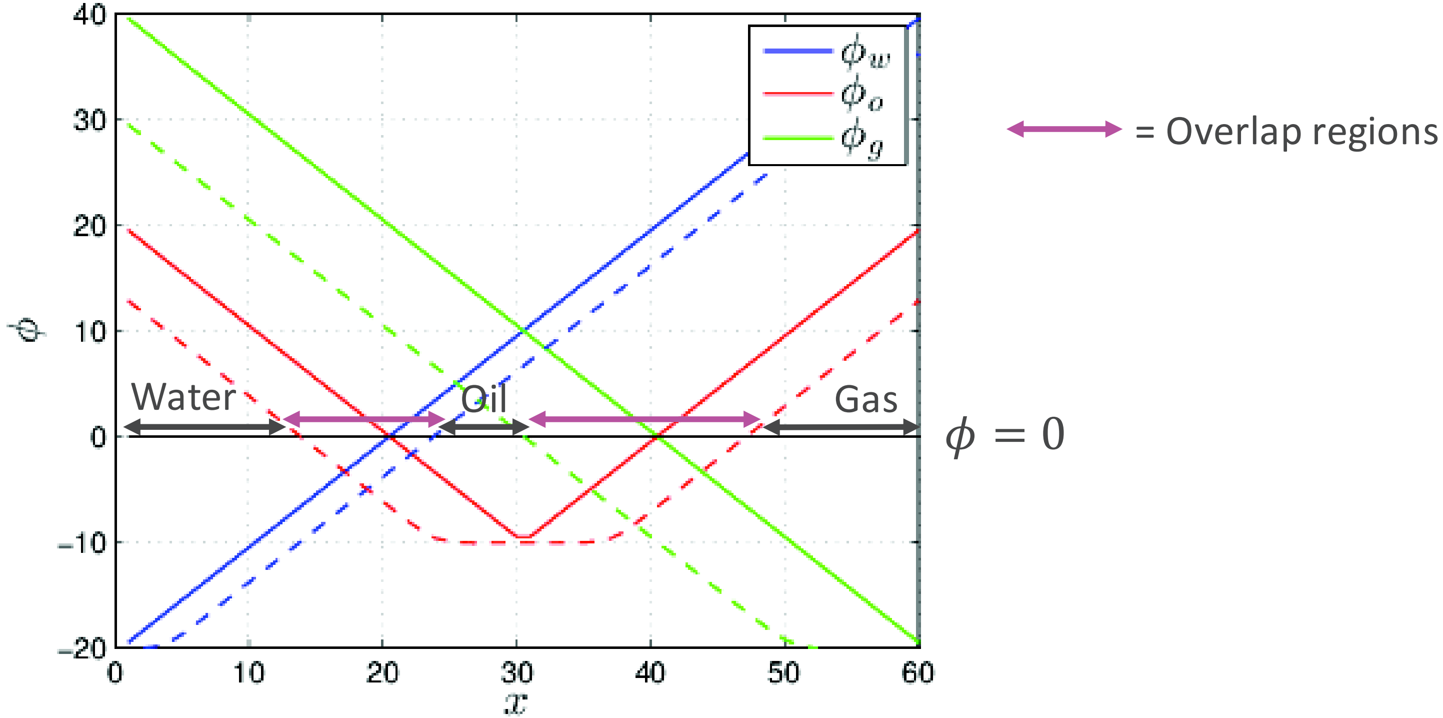

Multiphase Level Set Method – «Projection Step»

› Illustrating 1D example:

› Configuration after projection step:

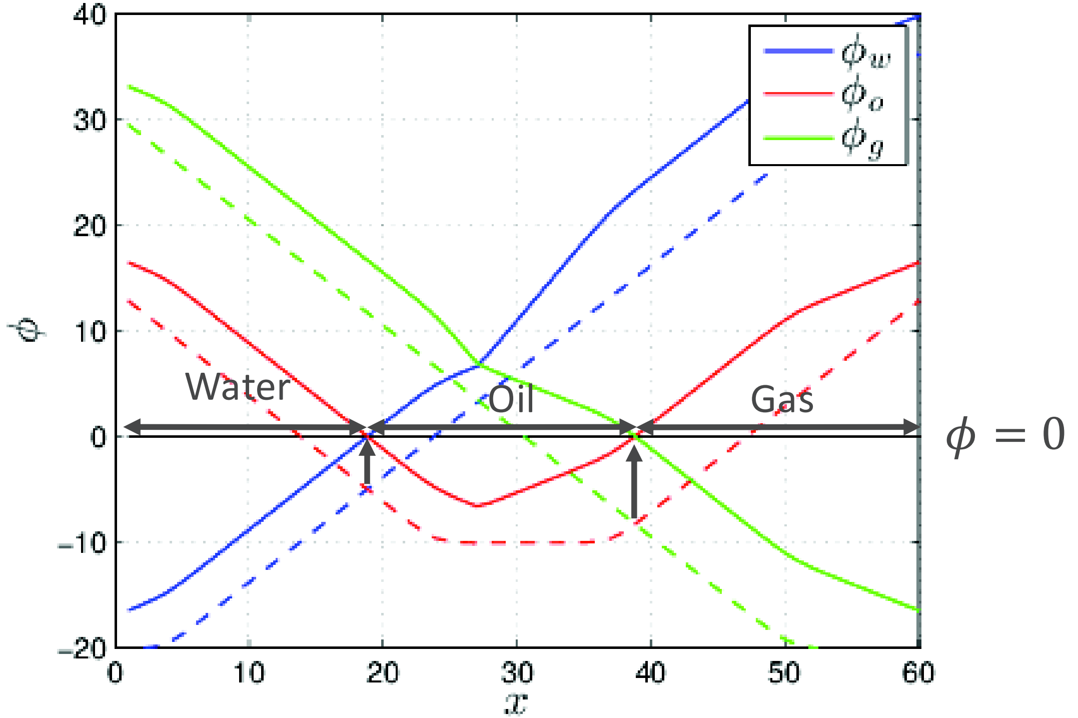

The projection step moves the intersections between ϕ_i to level $\phi = 0$.

Multiphase Level Set Method – «Projection Step»

› Illustrating 1D example:

› Configuration after projection step & reinitialization:

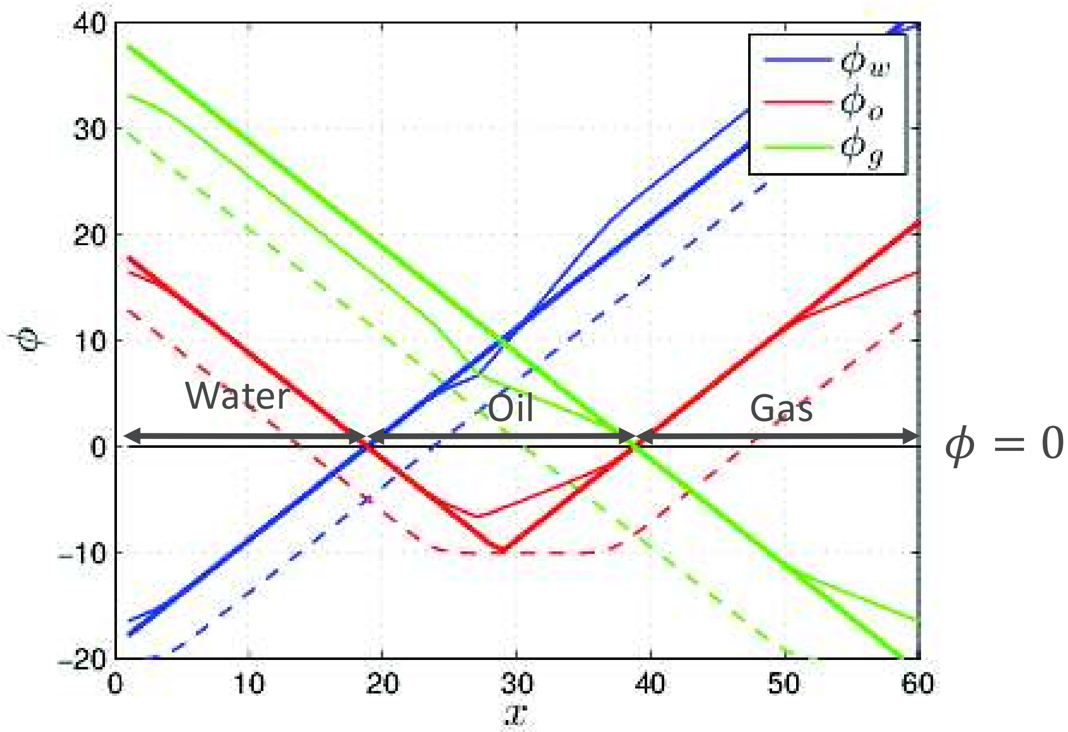

Implementation

- Input parameters: p_i, γ_i and $\beta_i, i = g, o, w$.
- Quasi-static three-phase VLS simulation by changing phase pressures stepwise
- In each pressure step, evolve $\phi_i, i = g, o, w$ until equilibrium is reached (i.e., solve the 3 evolution equations) and calculate fluid saturations
- Standard explicit numerical techniques for LS methods are used
- For invasion of non-wetting phase: Add a layer of pore space with invading phase at the inlet
- For invasion of wetting or intermediate-wetting phase: Add a porous plate wetted and saturated by the invading phase at inlet
- Boundary conditions:
  - Inlet: Linear extrapolation
  - All other boundaries: $\vec{n} \cdot \nabla \phi_i = 0, i = g, o, w$
- We simulate two-phase saturation history with contact-angle LS method (Jettestuen et al., WRR 2013)

Simulation on sandstone: Simultaneous Water-Alternate-Gas (SWAG) invasion

(Helland & Jettestuen, SCA 2014)

Interfacial tensions:
$\sigma_{ow} = 0.02, \sigma_{go} = 0.0101,$
$\sigma_{gw} = 0.03$ N/m

Contact angles:
$\theta_{ow} = 20°, \theta_{go} = 7.9°,$
$\theta_{gw} = 16.3°$

Water cusps at gas/oil/water triple lines

$P_{cow} = 1.25$ kPa
$P_{cgo} = 0.67$ kPa

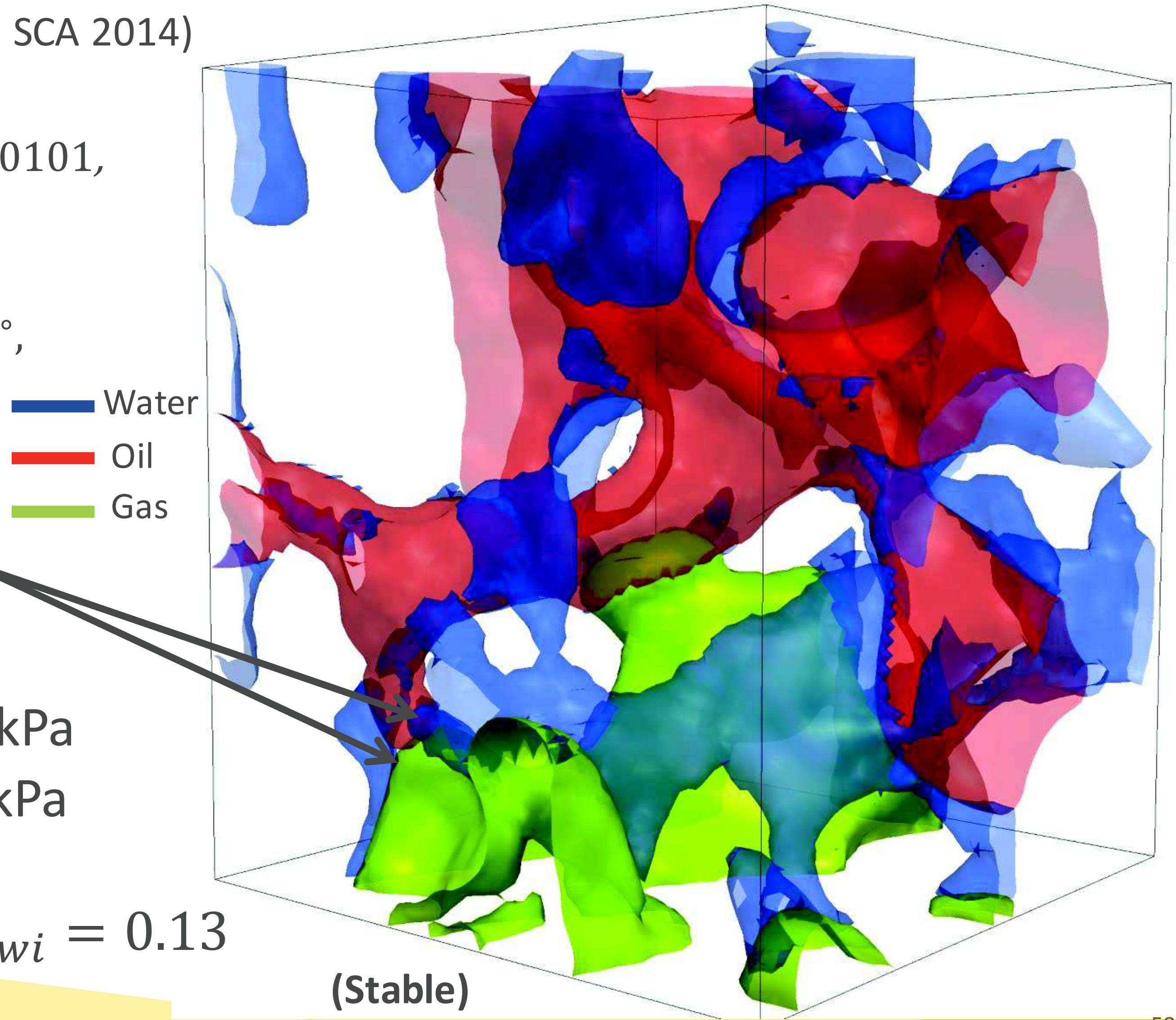

$S_{wi} = 0.13$

(Stable)

SWAG invasion

Water snap-off due to water-cusp growth at gas/oil/solid contact lines

Oil and gas retract to larger Pore openings after water invaded throat

(unstable)

$$P_{cow} = 1.07 \text{ kPa}$$
$$P_{cgo} = 0.76 \text{ kPa}$$

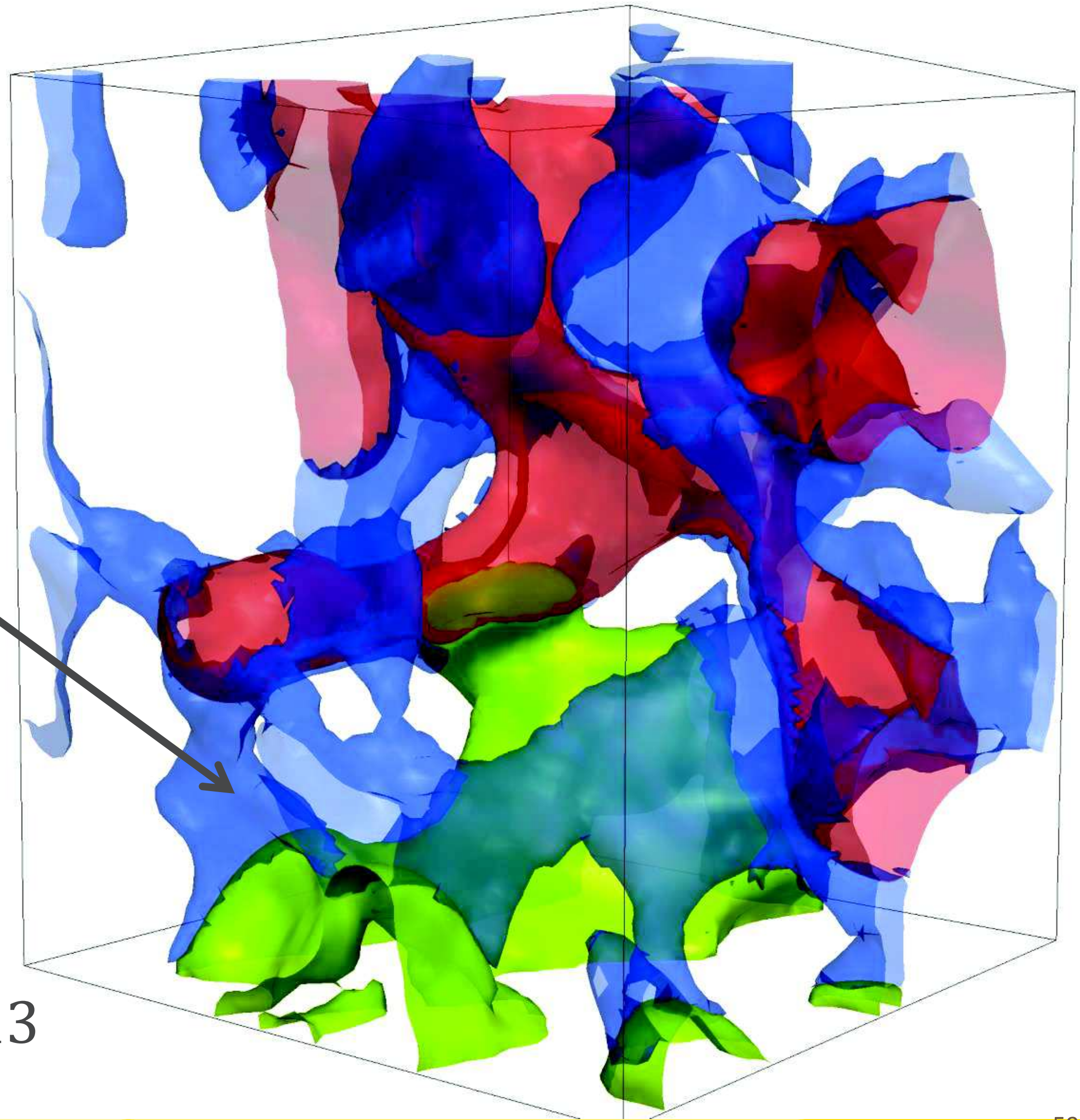

$$S_{wi} = 0.13$$

SWAG invasion

Oil retracts to larger pore openings after water occupied throat due to 2-phase snap-off event

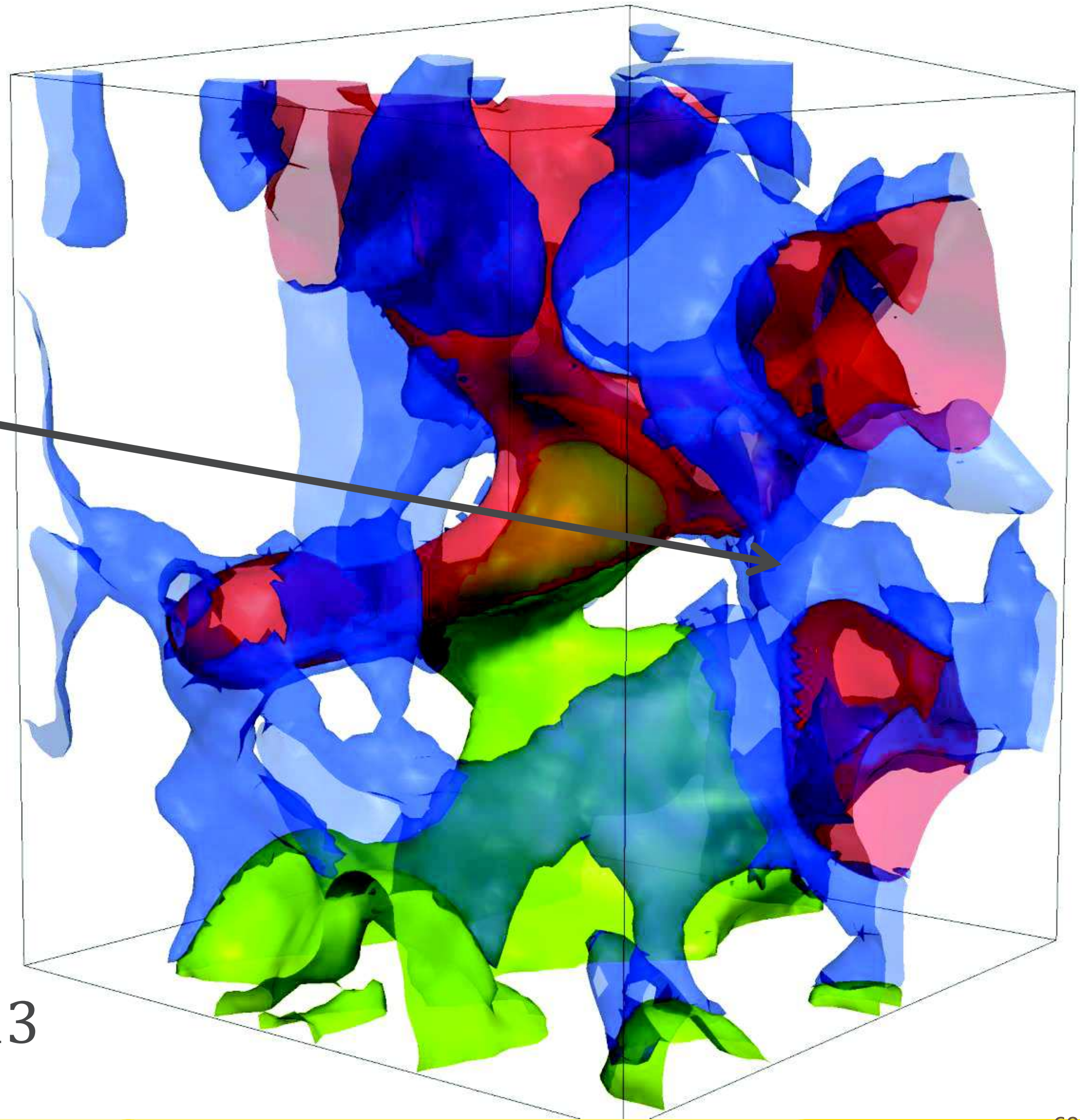

(unstable)

$P_{cow} = 1.07$ kPa
$P_{cgo} = 0.76$ kPa

$S_{wi} = 0.13$

SWAG invasion

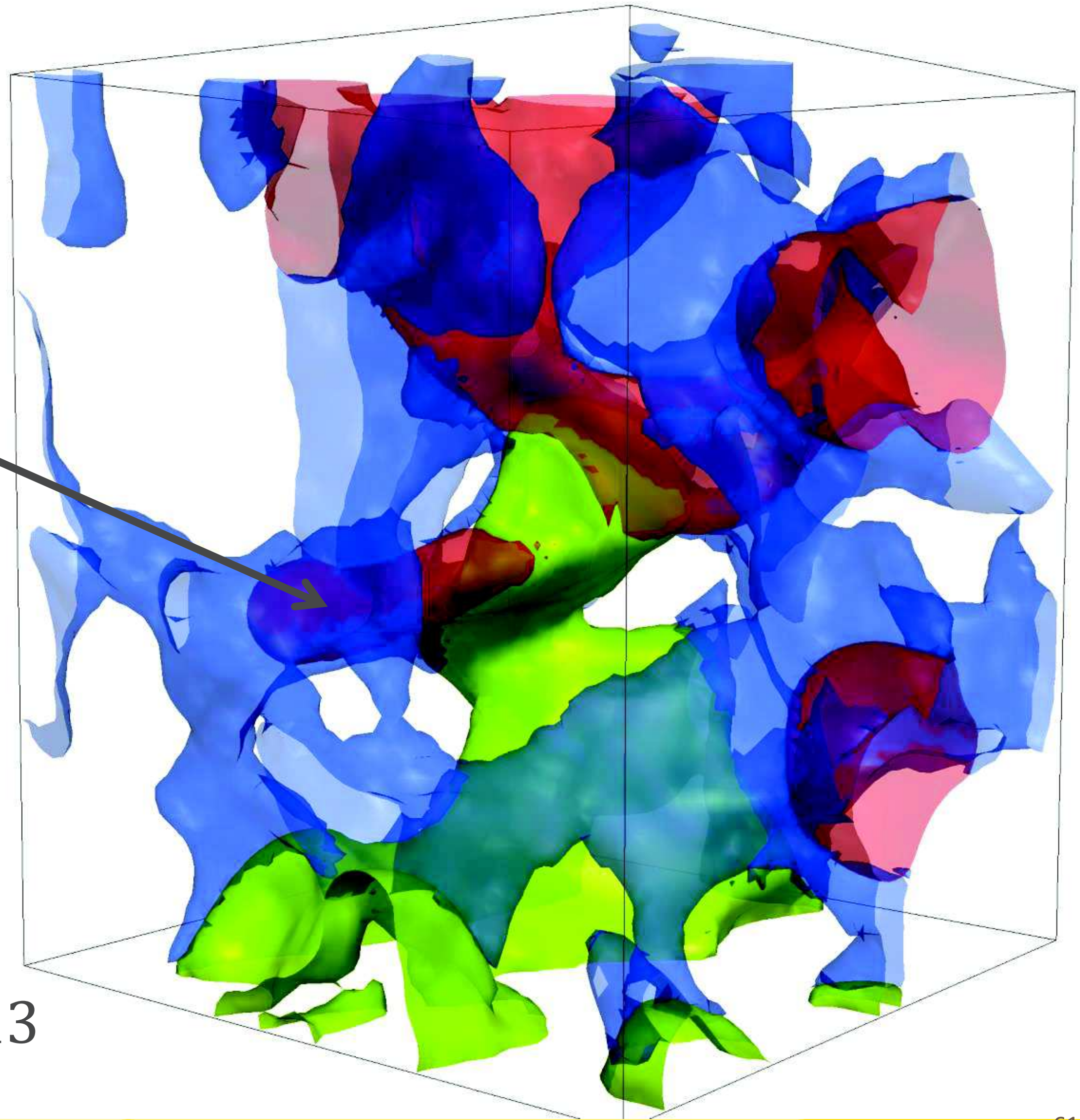

Oil isolated between water and gas

(unstable)

$$P_{cow} = 1.07 \text{ kPa}$$
$$P_{cgo} = 0.76 \text{ kPa}$$

$$S_{wi} = 0.13$$

SWAG invasion

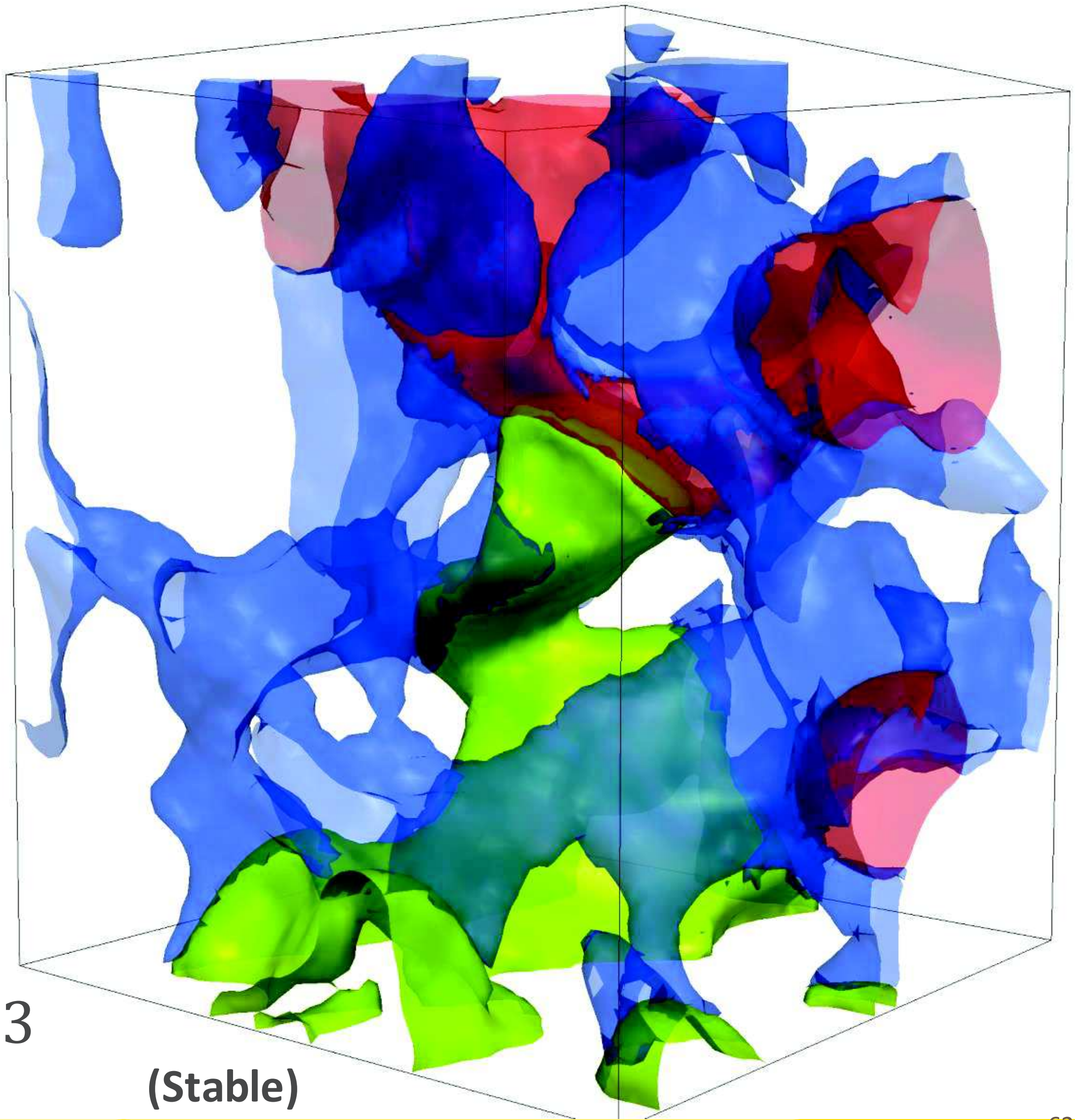

$P_{cow} = 1.07$ kPa
$P_{cgo} = 0.76$ kPa

$S_{wi} = 0.13$

(Stable)

SWAG invasion

Thickness of water layer increases

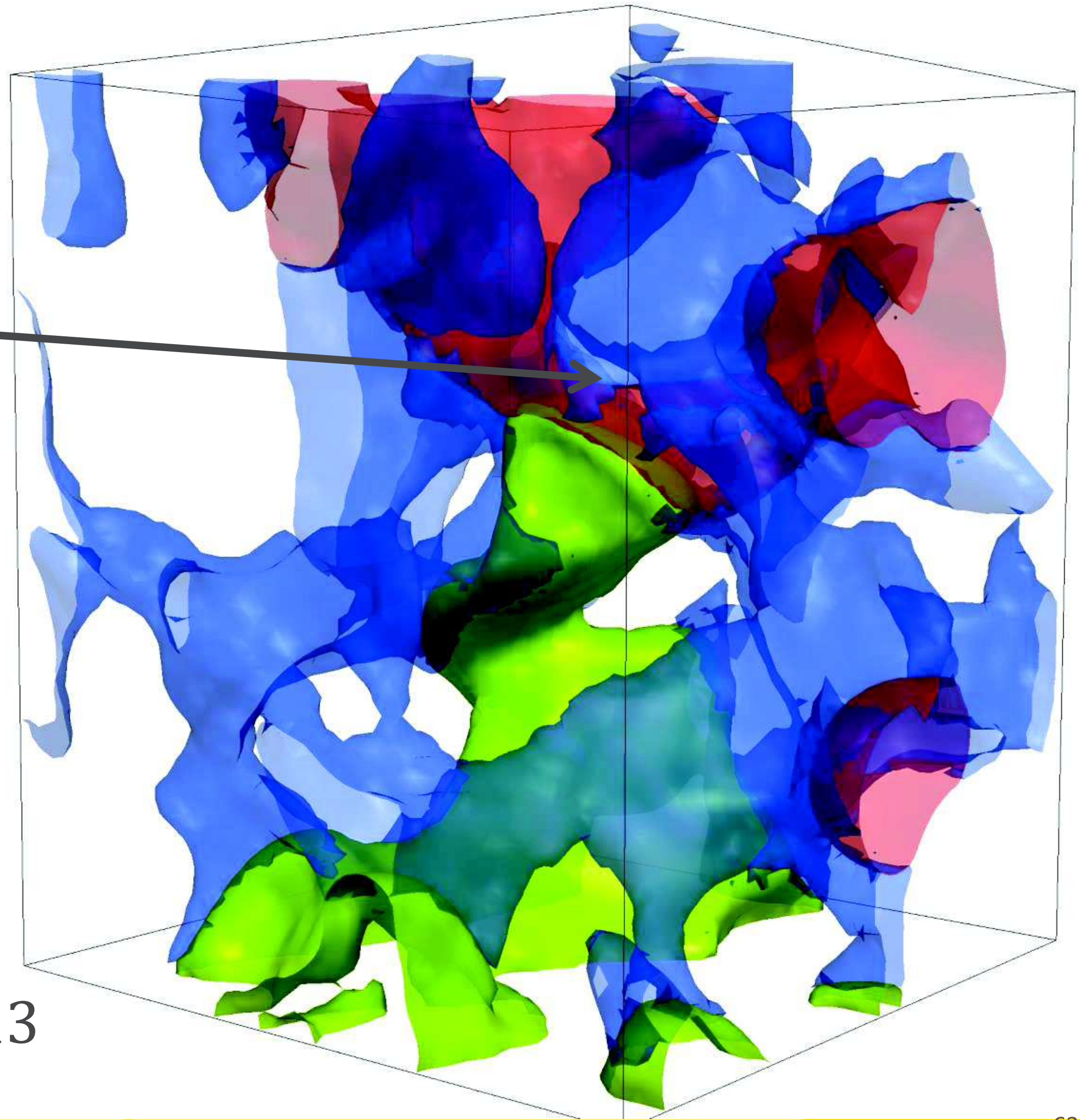

(unstable)

$P_{cow} = 0.89$ kPa

$P_{cgo} = 0.85$ kPa

$S_{wi} = 0.13$

SWAG invasion

Gas/oil/water triple lines form

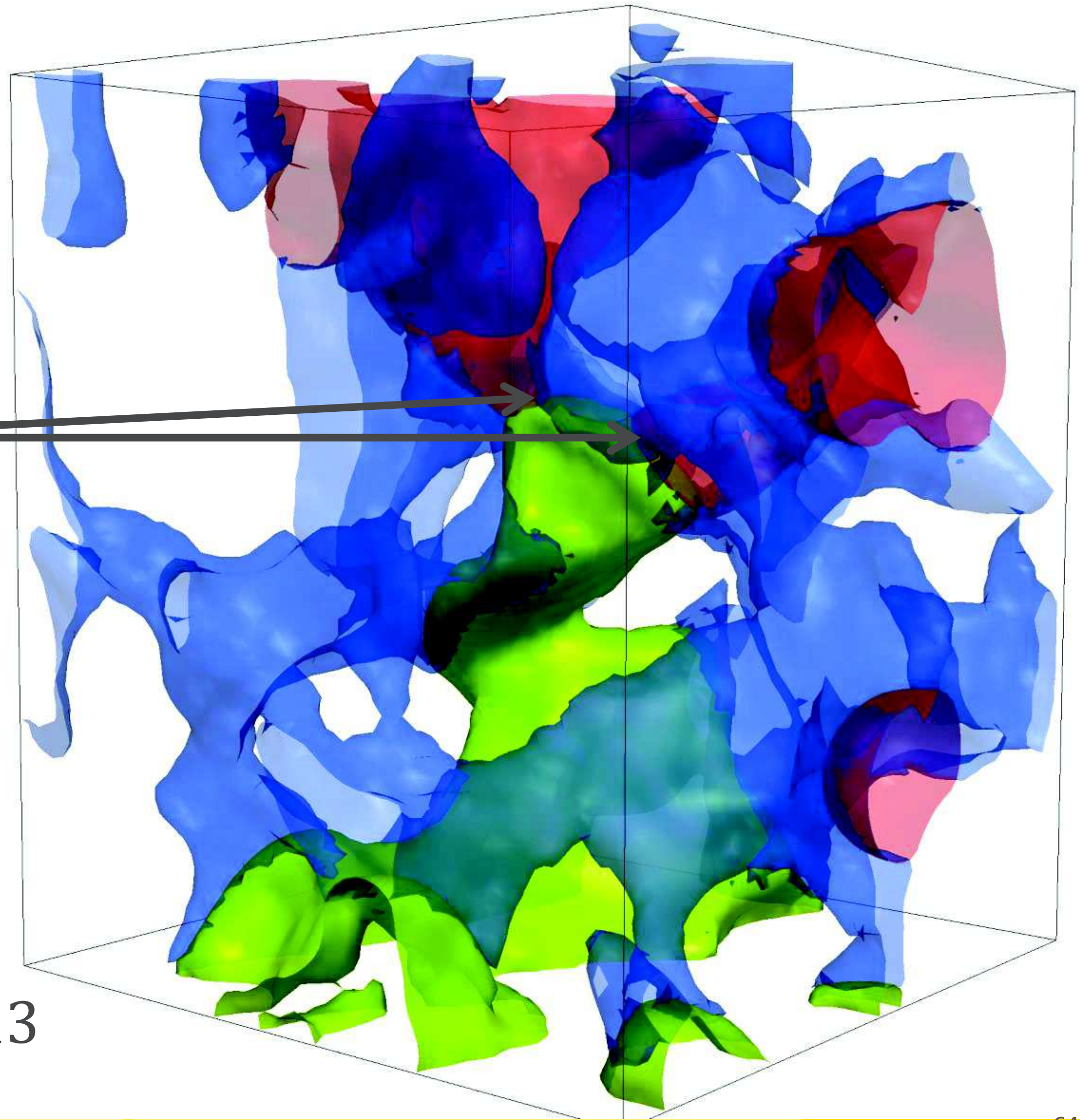

(unstable)

$P_{cow} = 0.89$ kPa
$P_{cgo} = 0.85$ kPa

$S_{wi} = 0.13$

SWAG invasion

«3-phase snap-off» occurs as a result of water-cusp growth at the gas/oil/water triple lines

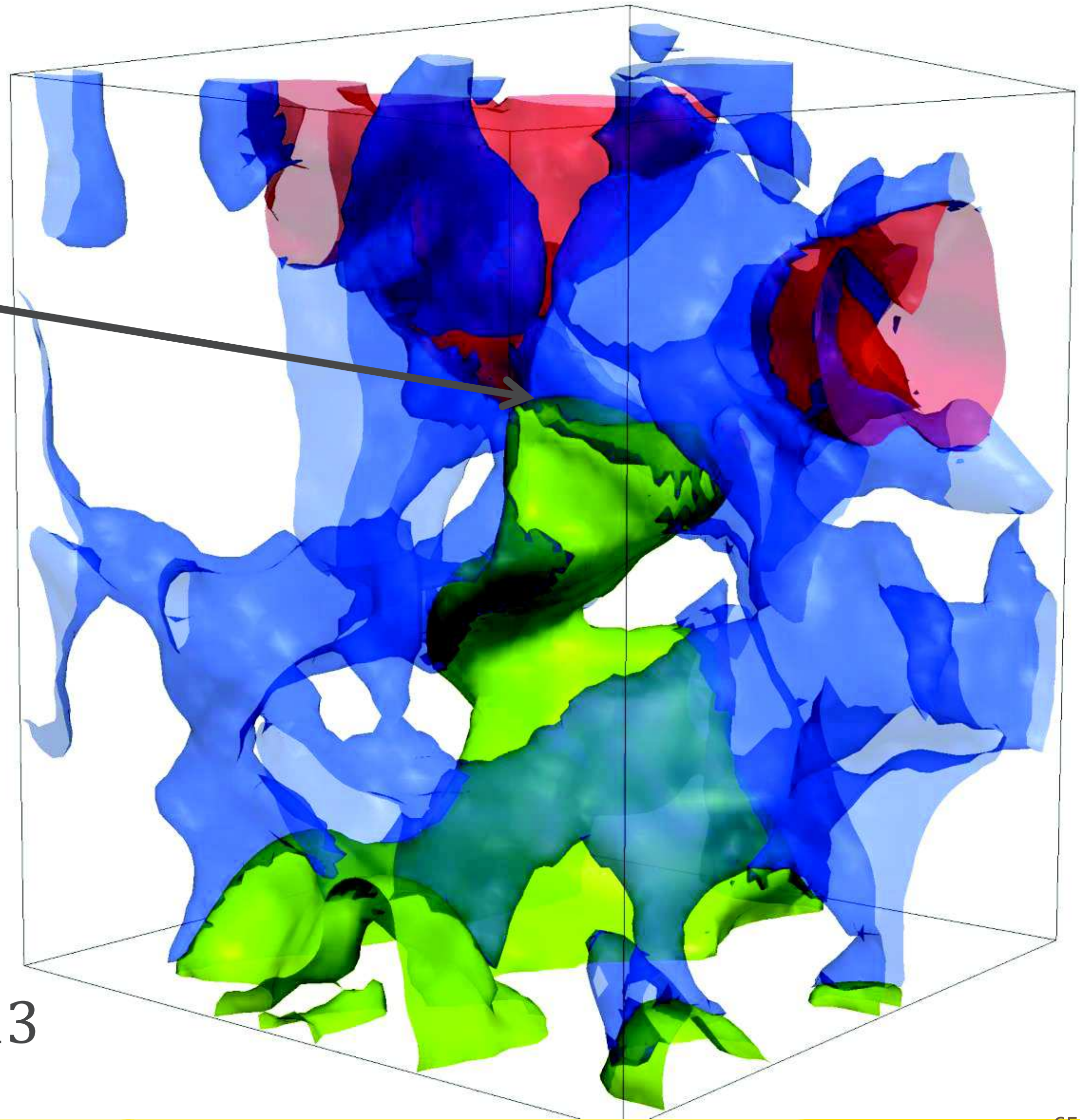

(unstable)

$$P_{cow} = 0.89 \text{ kPa}$$
$$P_{cgo} = 0.85 \text{ kPa}$$

$$S_{wi} = 0.13$$

SWAG invasion

Gas and oil retract to larger pore openings

$$P_{cow} = 0.89 \text{ kPa}$$
$$P_{cgo} = 0.85 \text{ kPa}$$

$$S_{wi} = 0.13$$

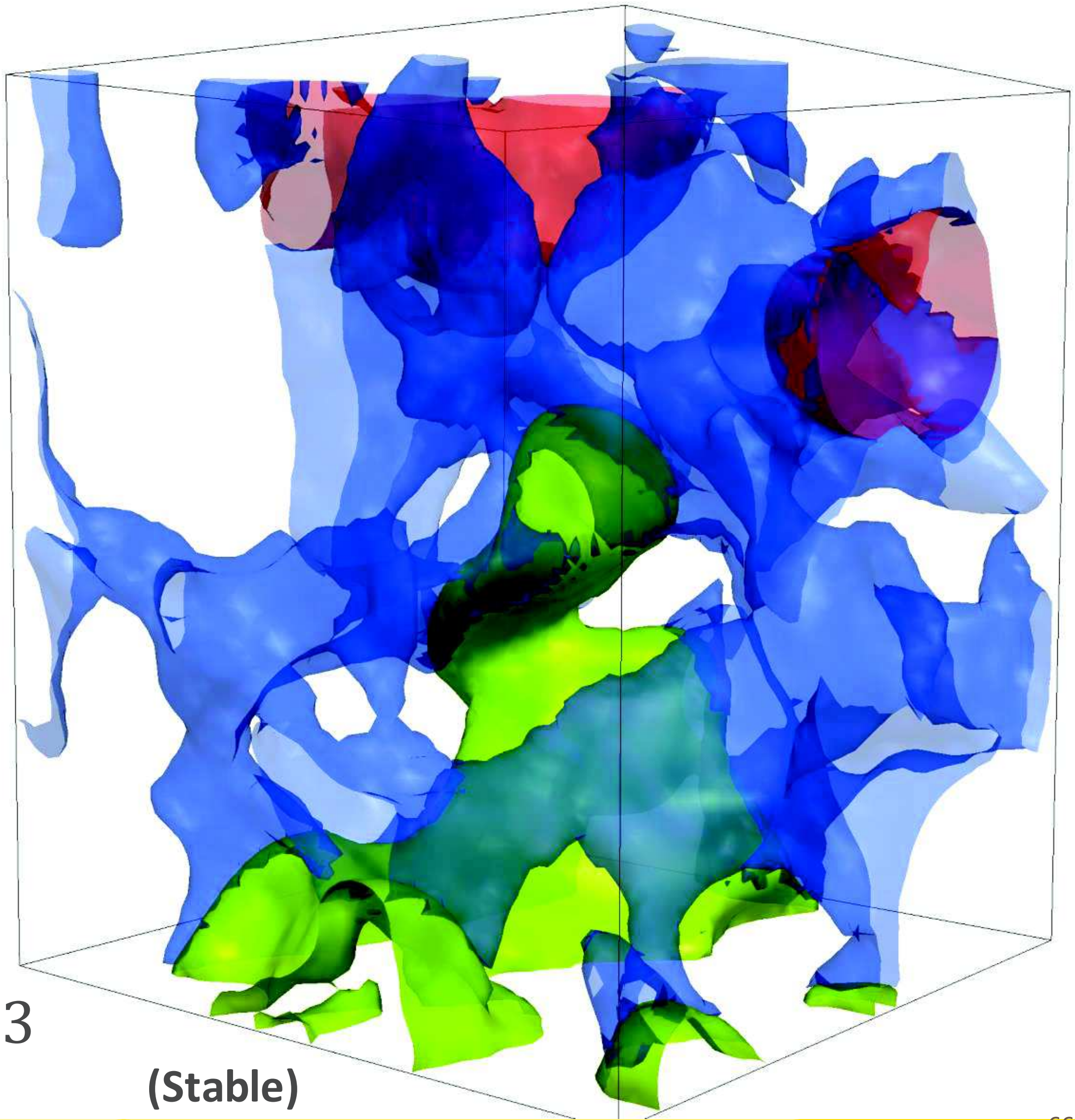

(Stable)

2-Phase Drainage and Imbibition

› Two-phase simulations with $\theta_{ow} = 20°$ (Jettestuen et al., WRR 2013)

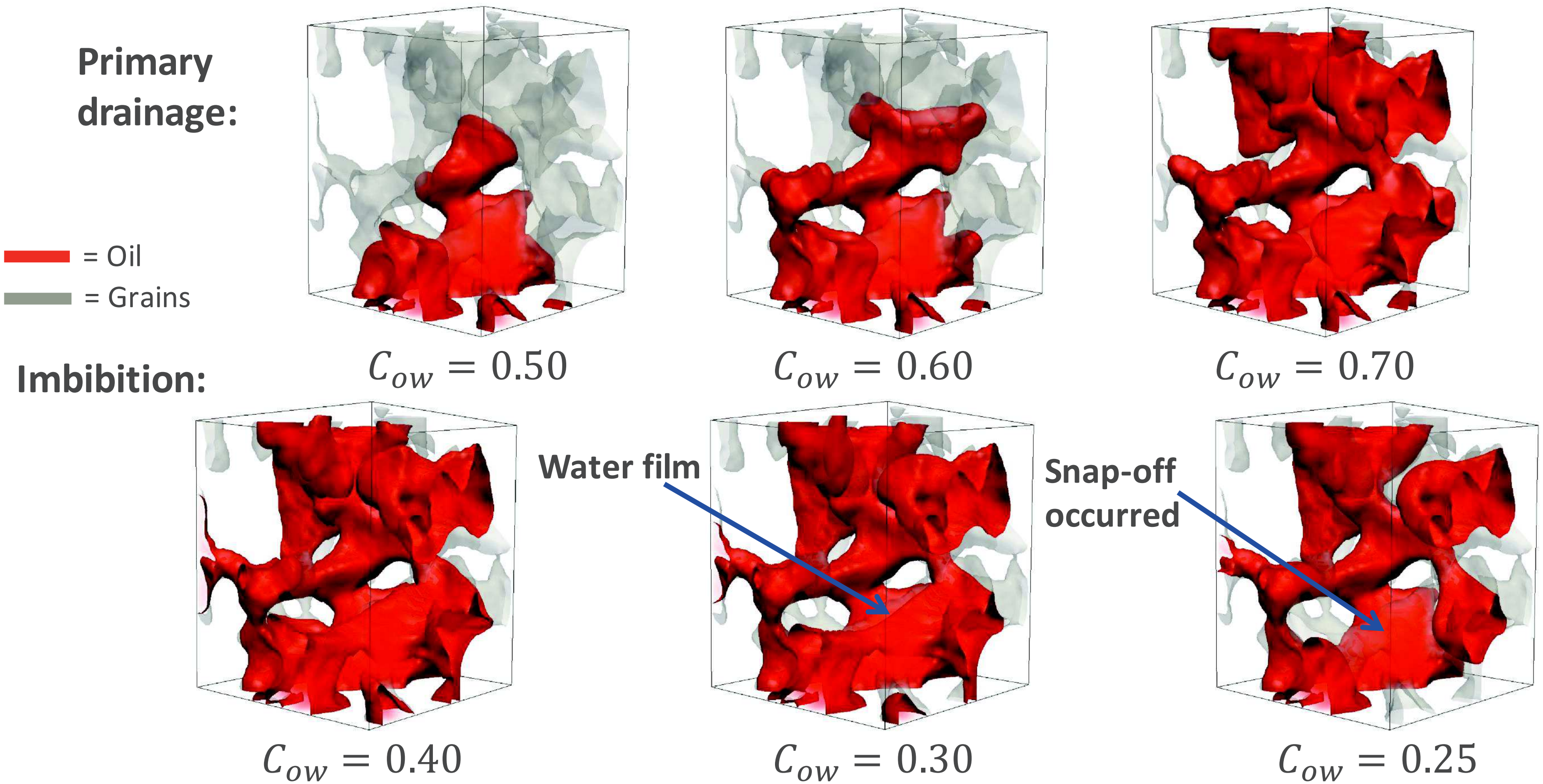

- Non-wetting phase retracts to larger pore openings after growth of wetting-phase films has led to snap-off in pore-throat constrictions

3-Phase Gas and Water Invasion

- **Gas invasion:**

Water
Oil
Gas

Trapped water

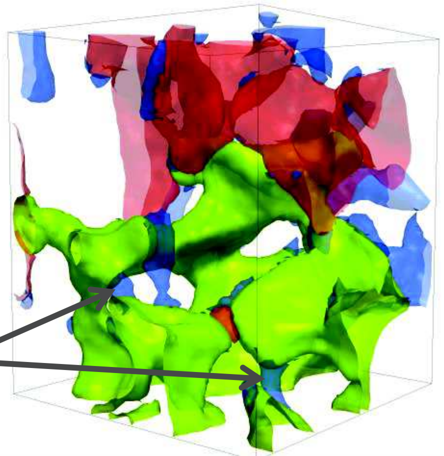

$S_{wi} = 0.13$

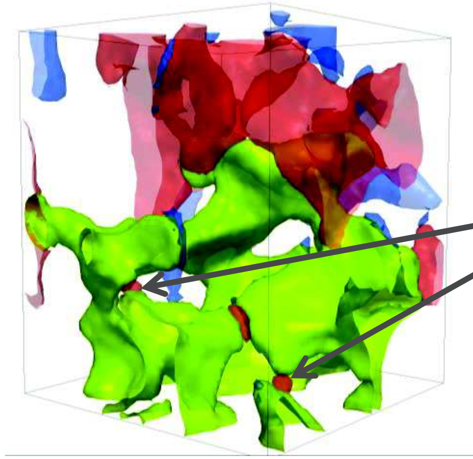

$S_{wi} = 0.06$

Trapped oil

- **Simultaneous Gas & Water (SWAG) invasion:**

$S_{wi} = 0.13$

Water cusp growth at gas/oil interface

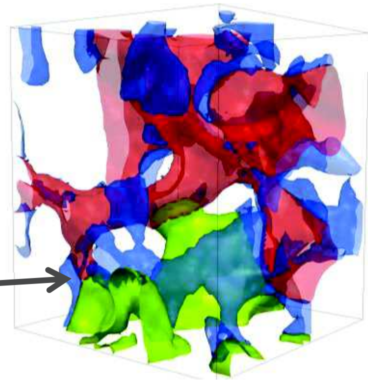

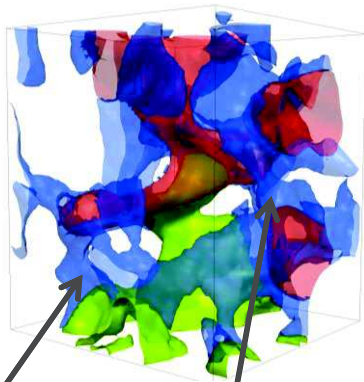

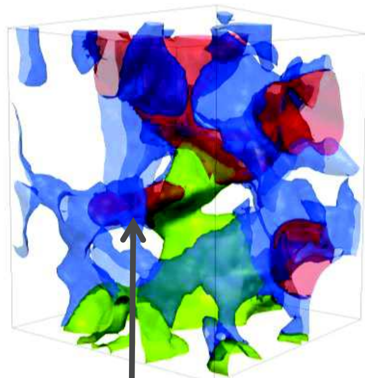

Water snap-off on gas/oil interface

2-phase snap-off

Disconnected oil

3-Phase vs. 2-phase Capillary Pressure Curves

(Water-wet case)

Gas/Oil capillary pressure:

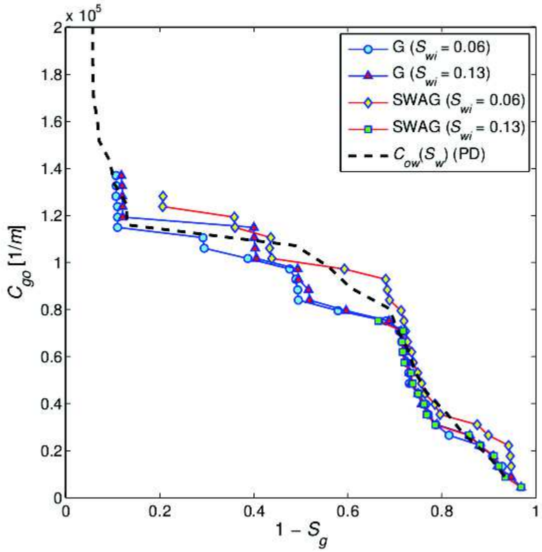

Oil/water capillary pressure:

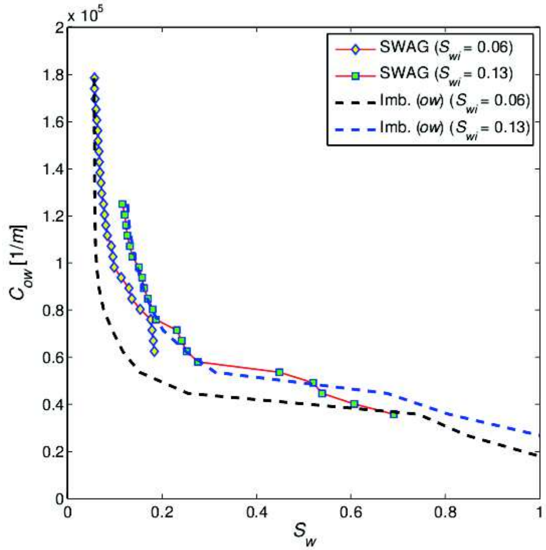

Saturation paths:

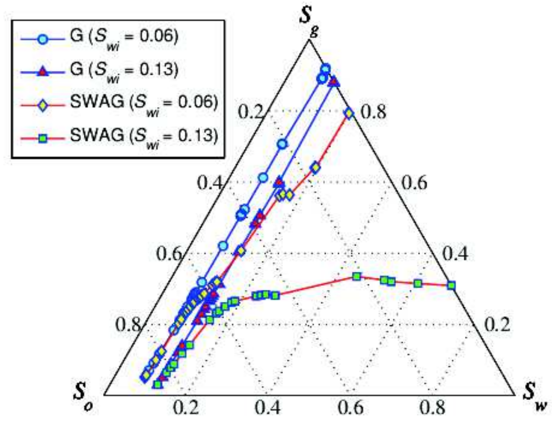

P_{cgo} increases with S_{wi}:

› Gas prefer to displace oil

› Water blocks pathways for gas/oil displacement

P_{cow} can be higher in presence of gas:

› Water snap-off on gas/oil interfaces occurs at higher P_{cow} than water snap-off of oil (2-phase).

Mixed Wettability

› **2-phase water invasion:**

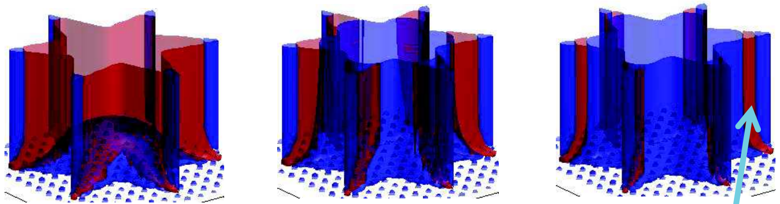

Water-filled, water-wet «porous plate» at water inlet (blue dots).

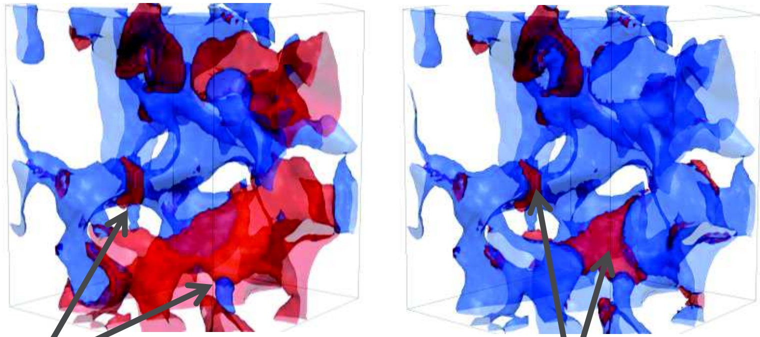

› **3-phase SWAG invasion:**

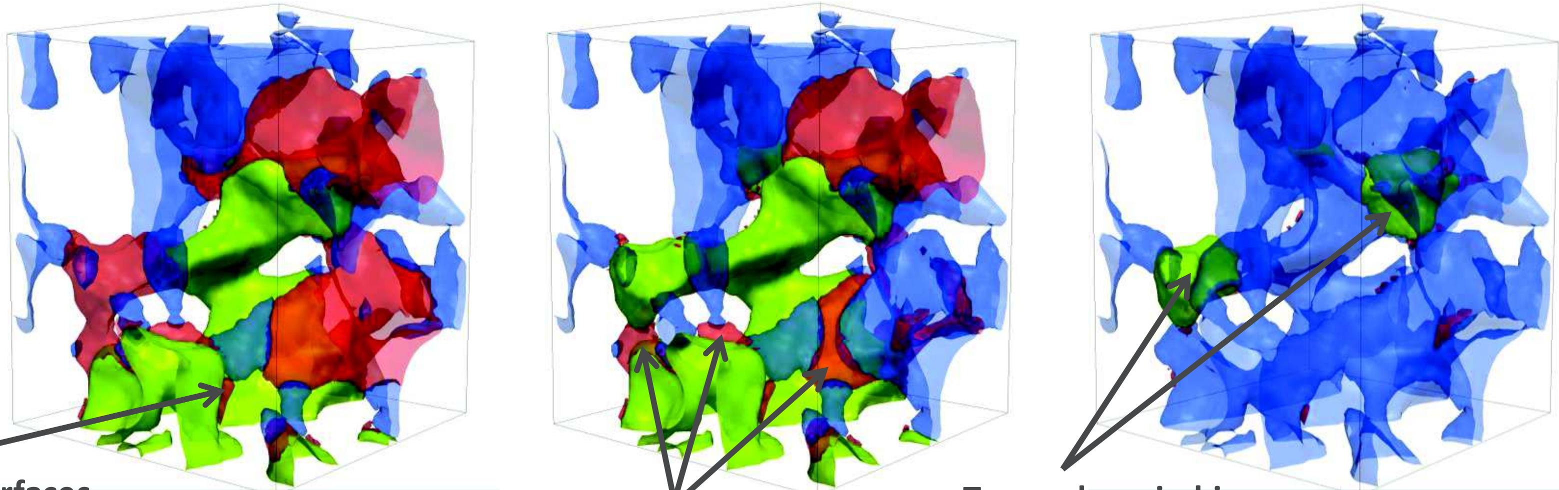

3-Phase vs. 2-phase Capillary Pressure Curves

(«Mixed- to Oil-wet» case)

P_{cgo}-curves:

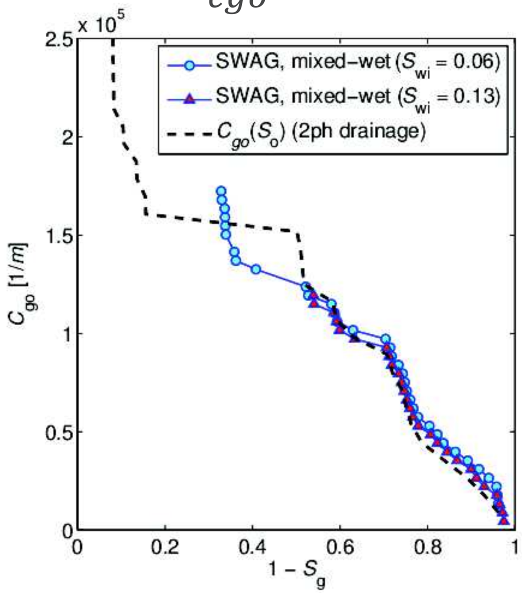

2- and 3-phase curves are similar for high oil saturations.

P_{cow}-curves:

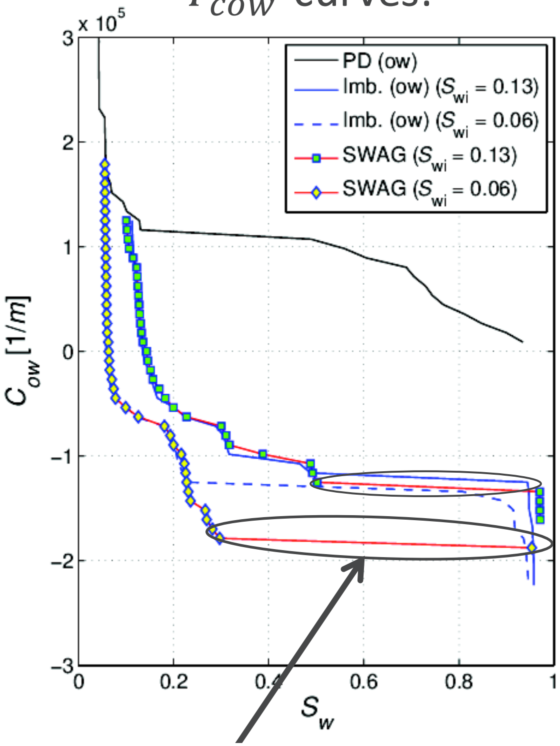

Water displaces gas, with oil cusps/films present.

P_{cgw}-curves:

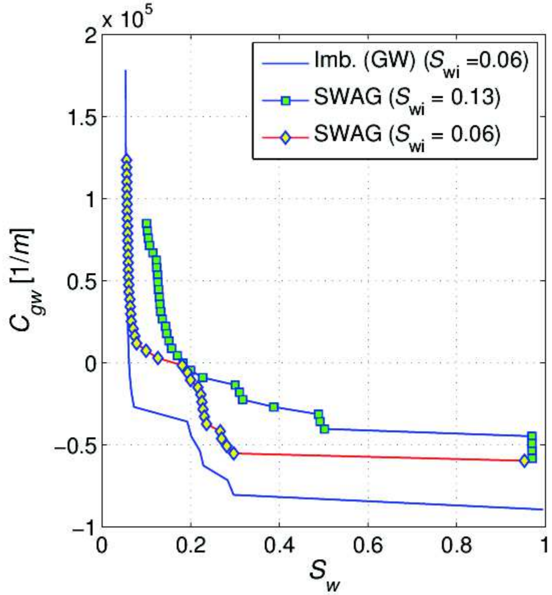

P_{cgw}(3-phase) → P_{cgw}(2-phase) as P_{cgo} increases and P_{cow} decreases (oil saturation decreases)

Validation on idealized geometries

IRIS

› Gas invasion into a water-wet sphere-pack pore throat
› Simulated entry pressure agree with analytic solution (MS-P/Purcell)
› Need for **Adaptive Grid Refinement**

Coarse grid:

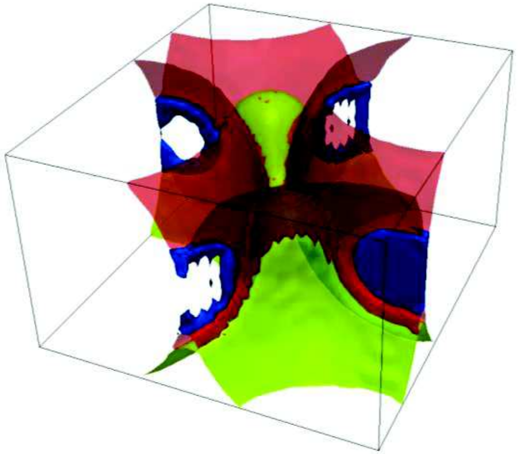

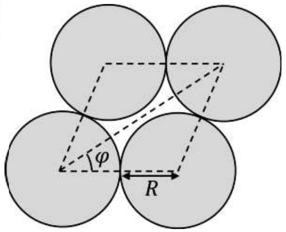

$\varphi = 32°, R = 30\ \Delta x$

Fine grid:

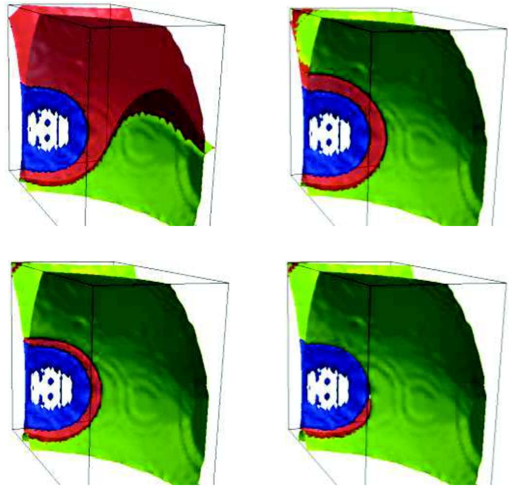

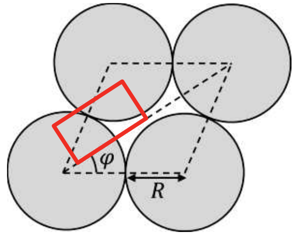

$\varphi = 32°, R = 60\ \Delta x$

- Oil layers vanish and triple lines form during gas invasion.
- Error (MS-P/Purcell) < 2 %.

- Oil layers exist after gas invasion
- Error (MS-P/Purcell) < 3.9 %.
- Thickness of water ring depends on which fluid it contacts.

Volume-preserving motion of isolated ganglia

› Capillary trapping (2- and 3-phase flow)

› Double and multiple displacement events (3-phase flow)

- Example: Gas → disconnected oil → water

› The pressure of the preserved phase volume is calculated as

$$p_i = \frac{V_i^{target} - V_i^n}{\Delta t A_i^n}$$

where:

V_i^{target} = Initial or desired volume of phase i

V_i^n = Volume of phase i in time iteration n

A_i^n = Surface area of phase i in time iteration n

Δt = Time step

› The p_i-term grows or shrinks phase i equally around its boundary

(Saye & Sethian, PNAS, 2011)

Volume-preserving motion - Validation

› Tests of «oil-volume targeting» in right-angled triangle

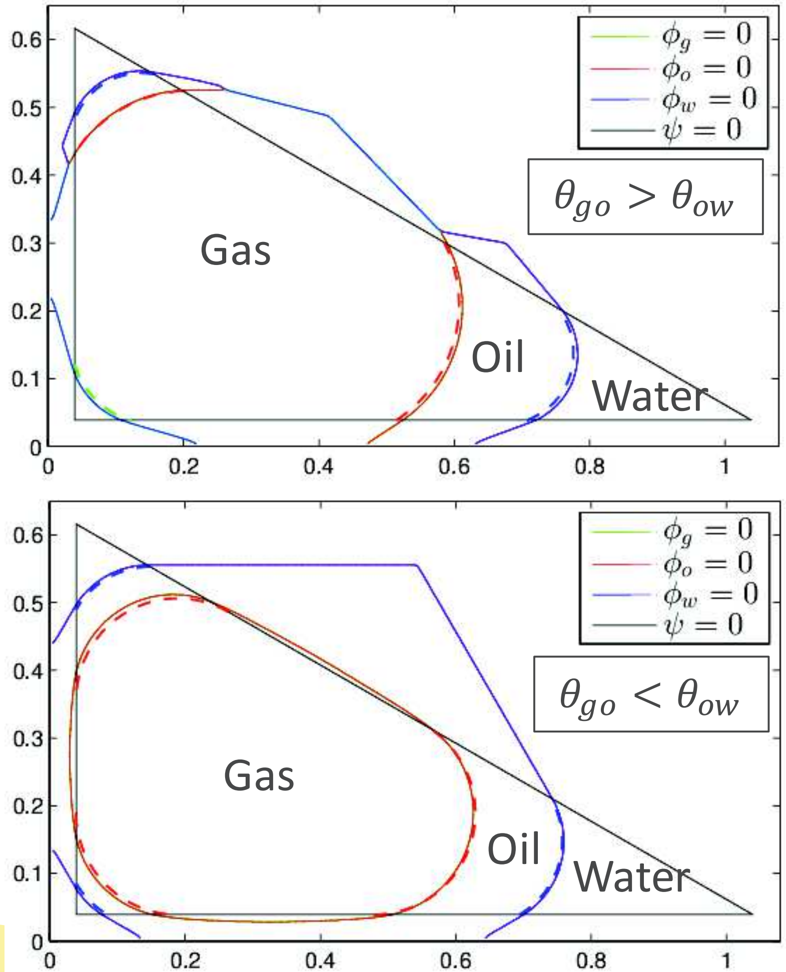

- Analytic solutions (dashed curves)
- Error scales linearly with grid spacing, $\delta A \sim \Delta x$:

$$\delta A = \frac{1}{2} \sum_{i=g,o,w} \int_{\Omega} \frac{H(\psi)\left|H(\phi_{i,true}) - H(\phi_i)\right|}{L_i} dV$$

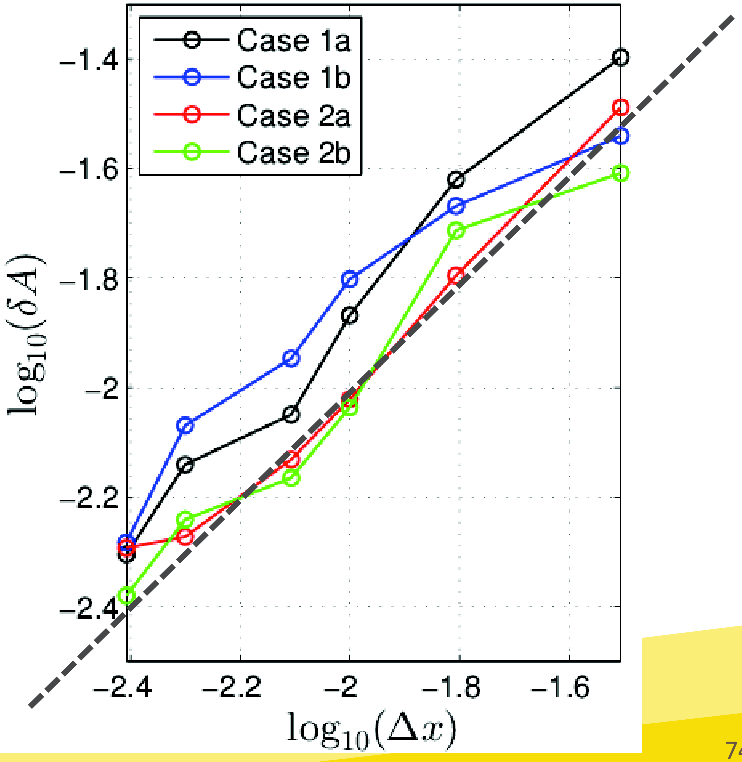

Volume-preserving motion – Sinusoidal Pore

- Double displacement (Gas → isolated oil → water):
- Oil-wet condition
- Behavior between 2 stable configurations

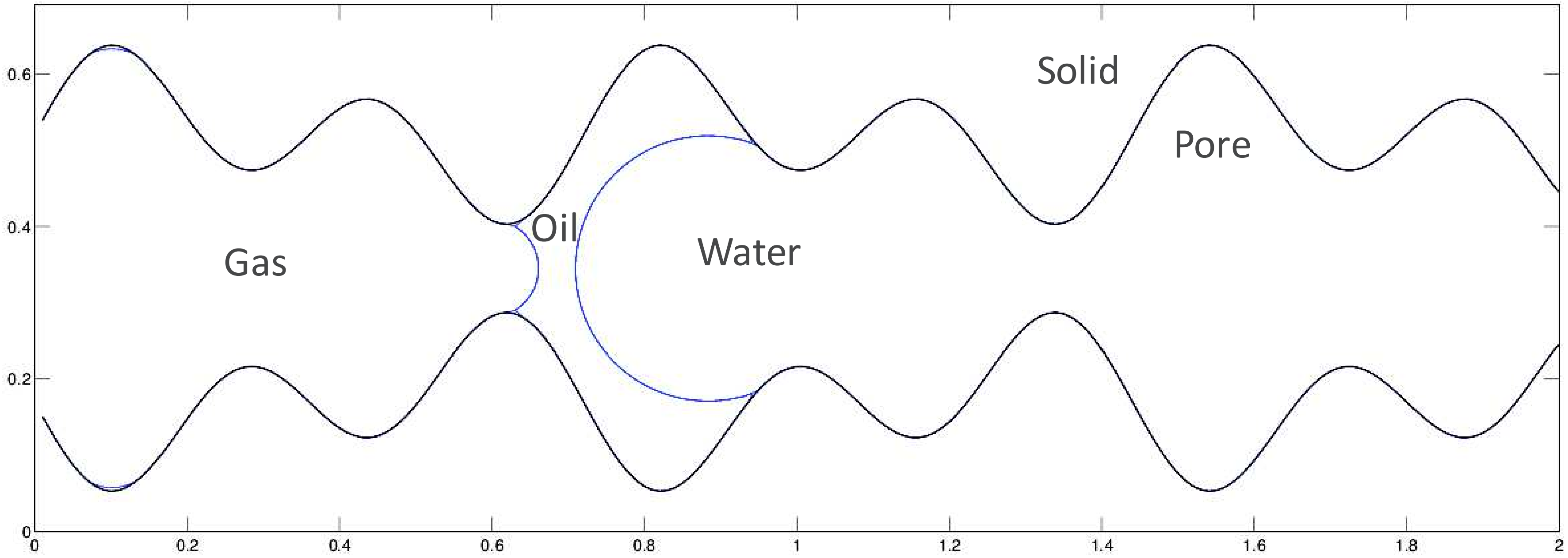

Stable configuration

Volume-preserving motion – Sinusoidal Pore

Triple lines & gas/water interface form

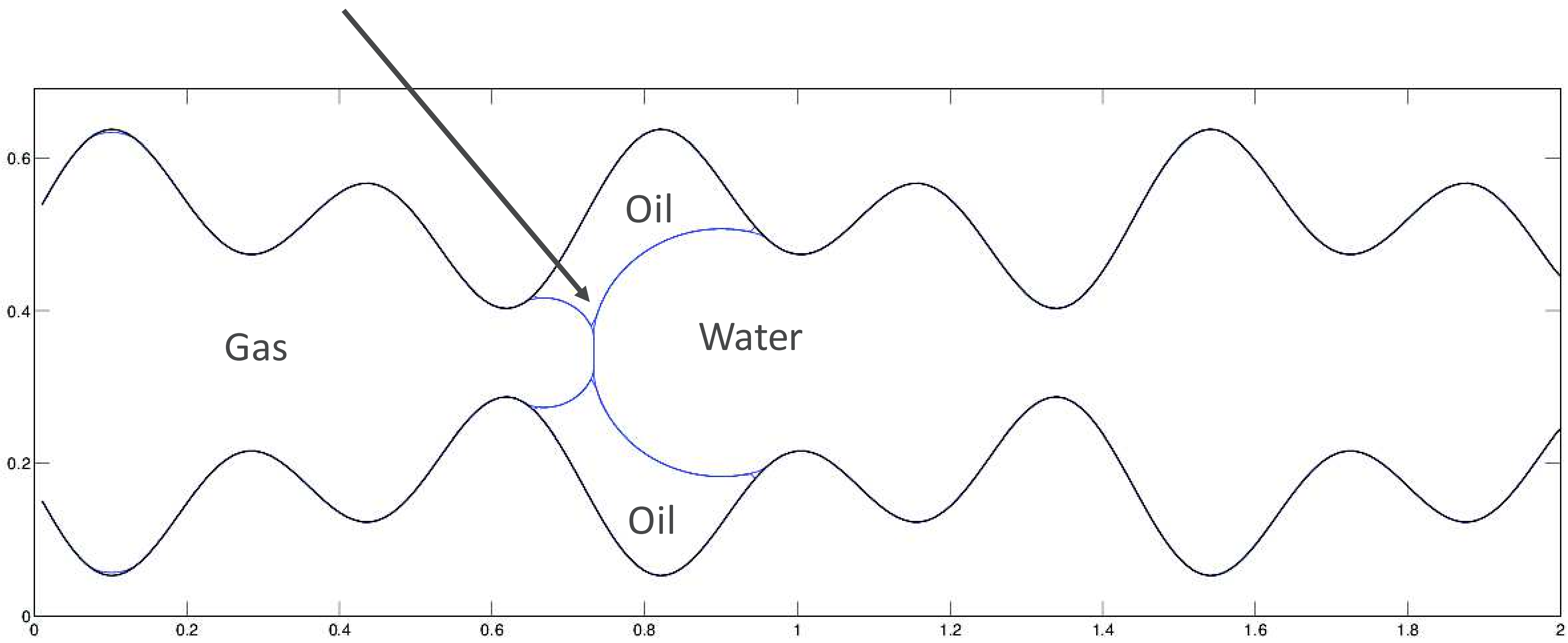

Volume-preserving motion – Sinusoidal Pore

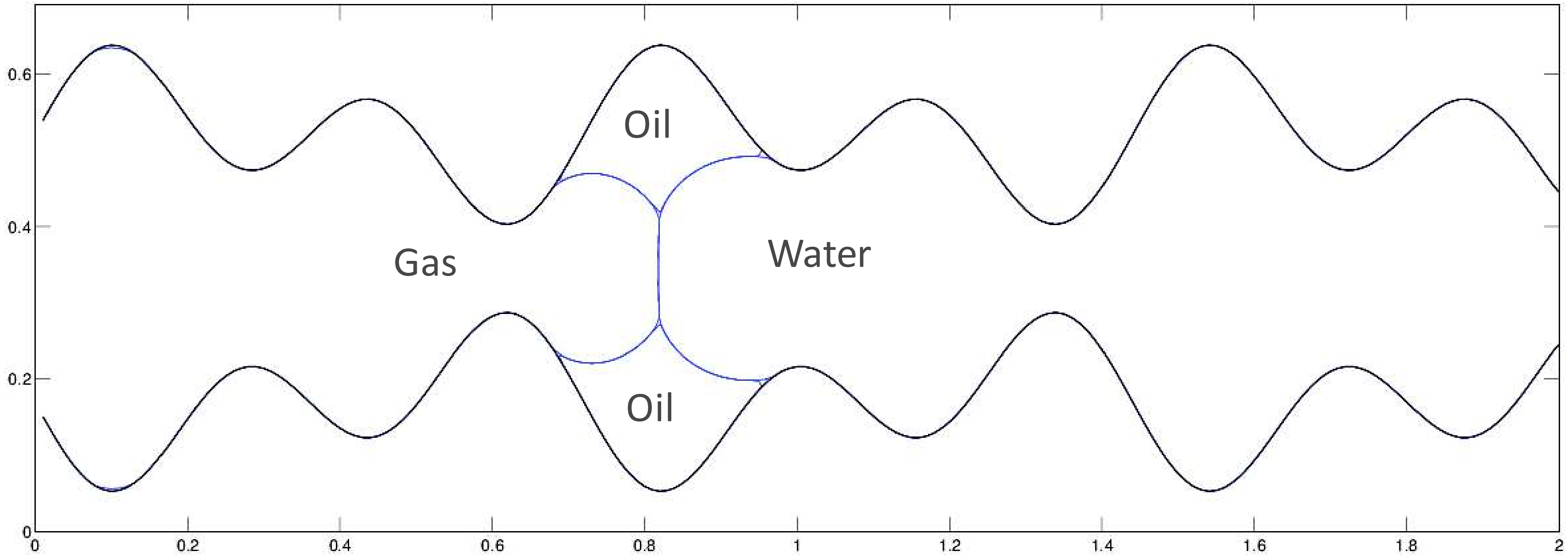

Volume-preserving motion – Sinusoidal Pore

Gas retracts in corners behind the front.

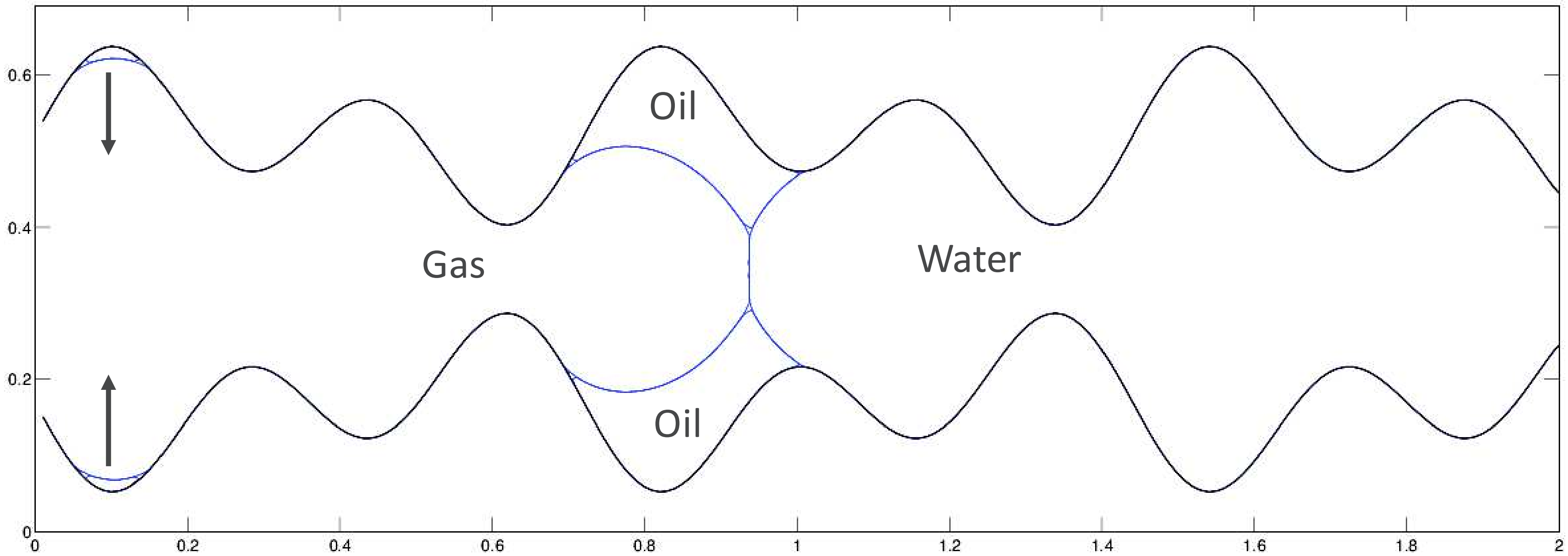

Volume-preserving motion – Sinusoidal Pore

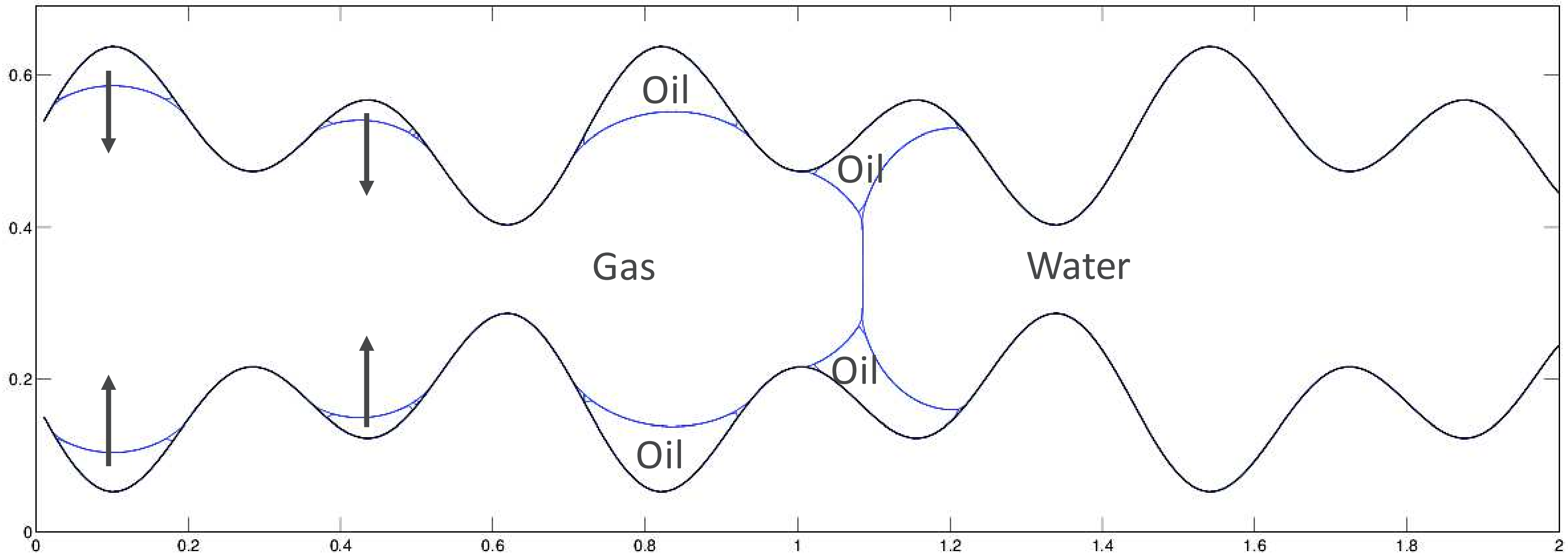

Volume-preserving motion – Sinusoidal Pore

Gas invades corners behind the front.

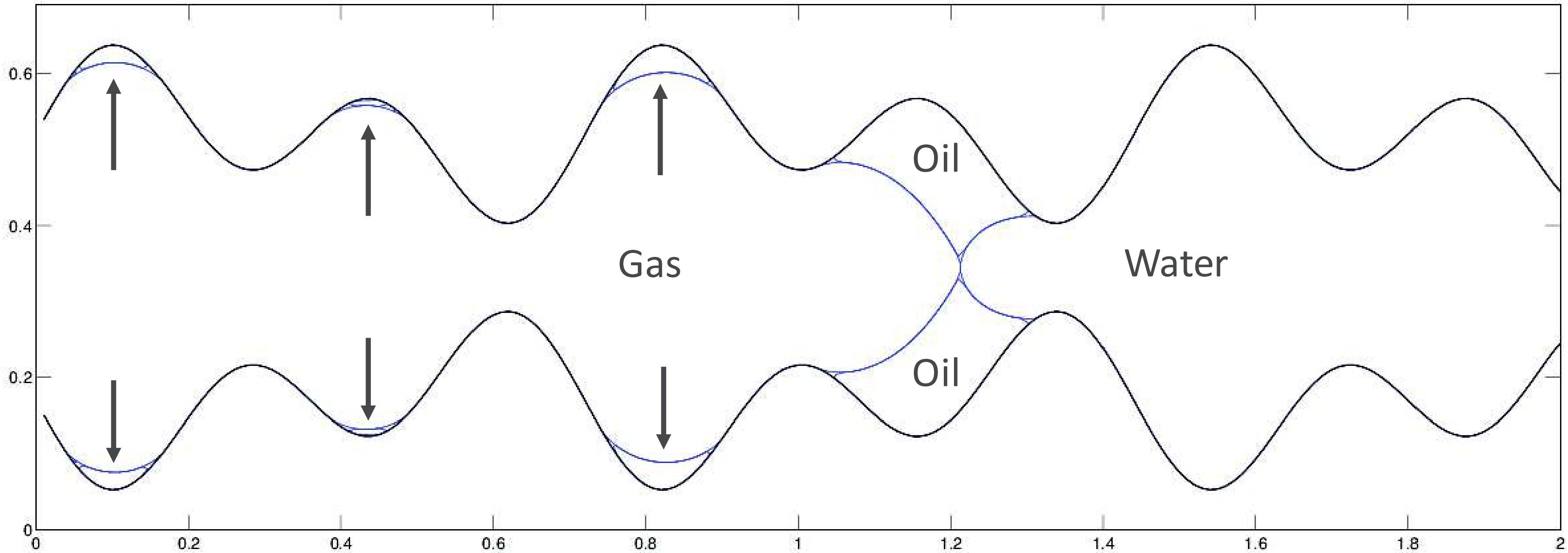

Volume-preserving motion – Sinusoidal Pore

Oil snap-off on gas/water interface

Gas retracts in corners behind the front.

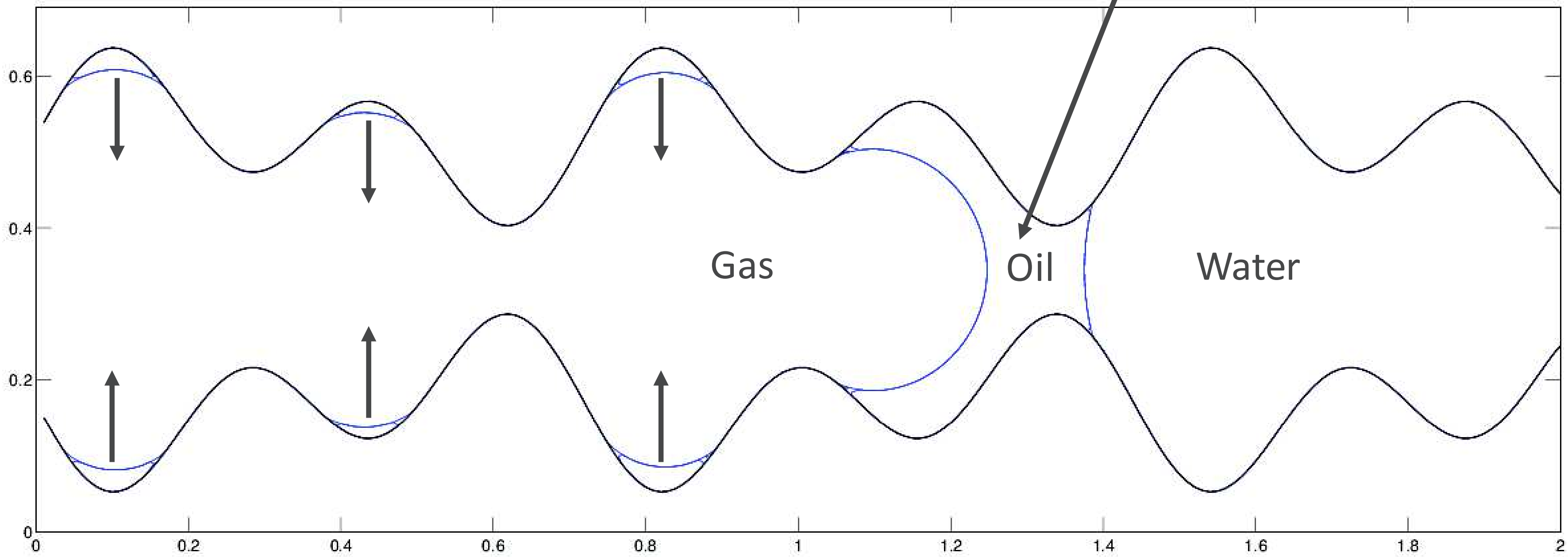

Volume-preserving motion – Sinusoidal Pore

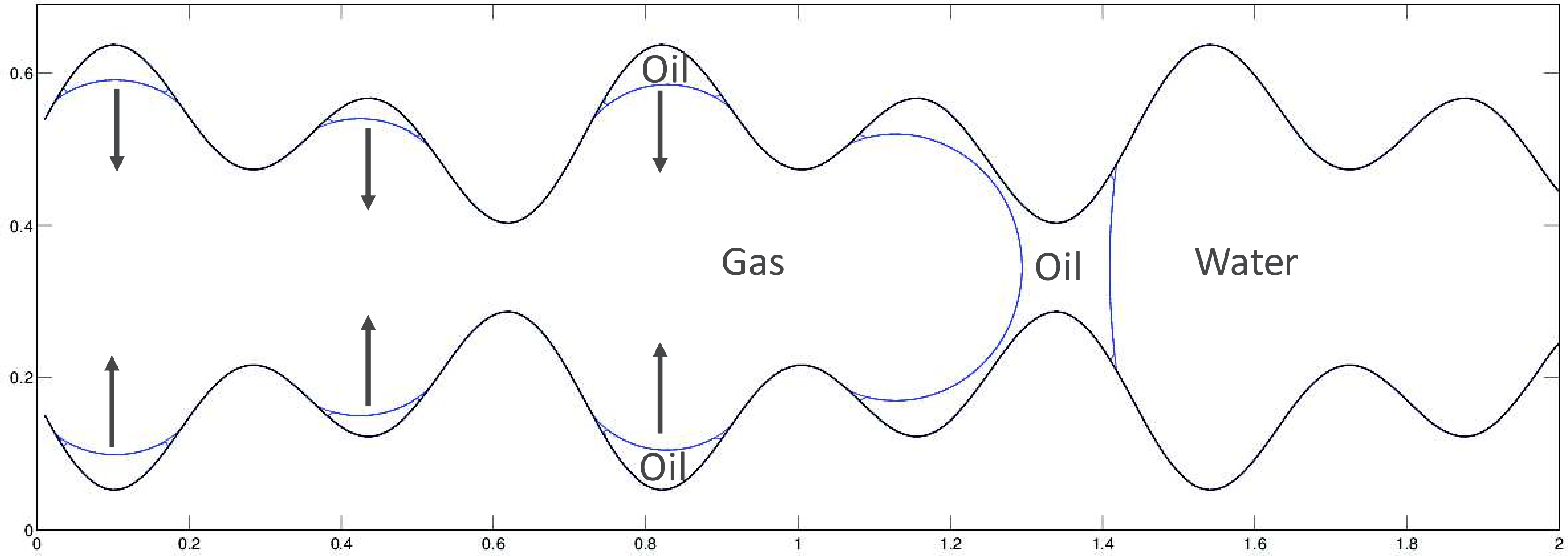

Volume-preserving motion – Sinusoidal Pore

Gas invades the corners when the front is at narrow constriction.

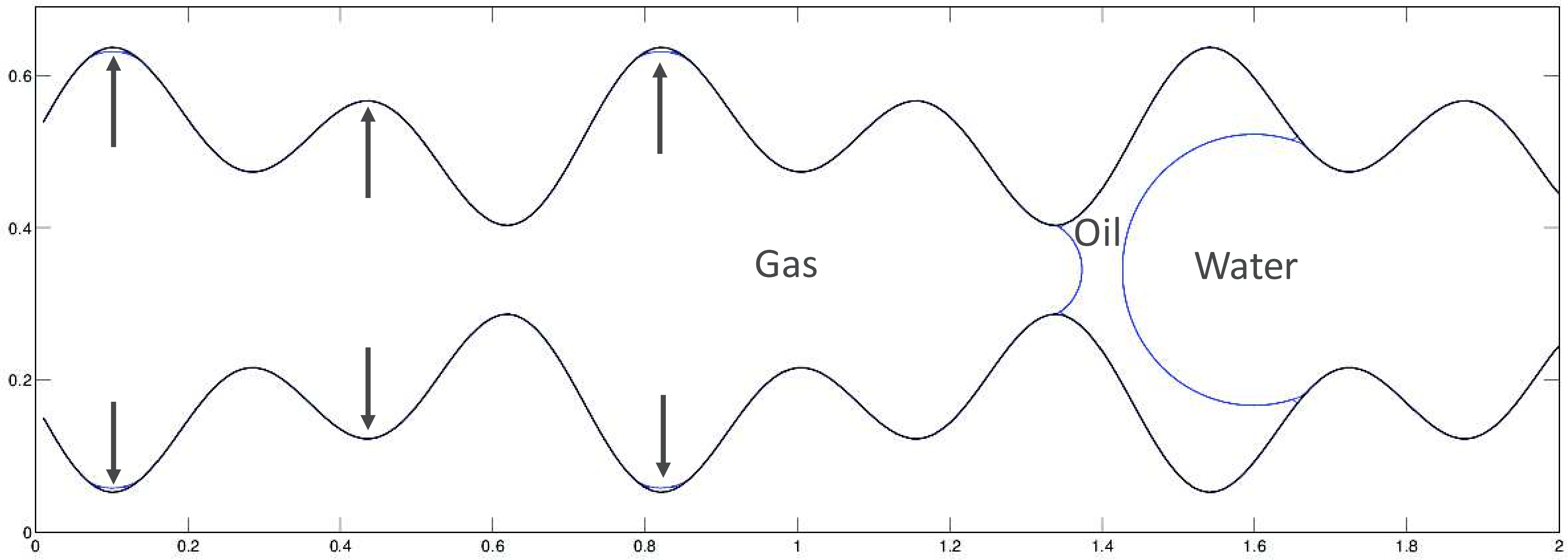

Volume-preserving motion – Sinusoidal Pore

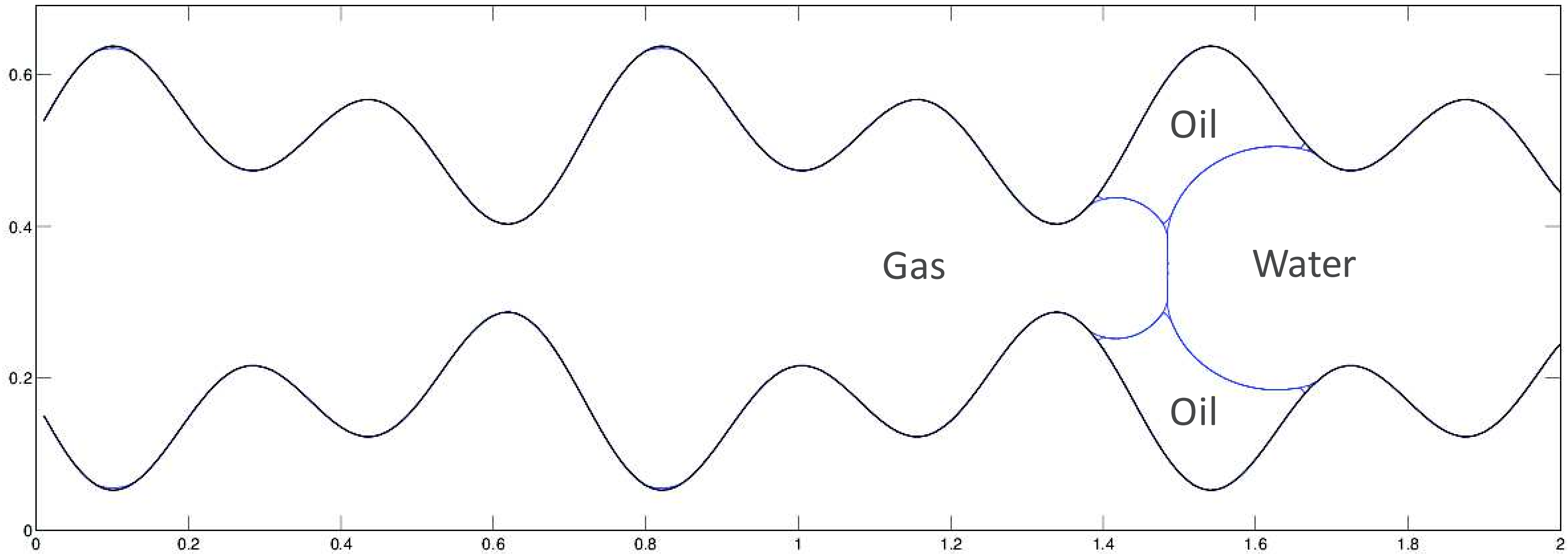

Volume-preserving motion – Sinusoidal Pore

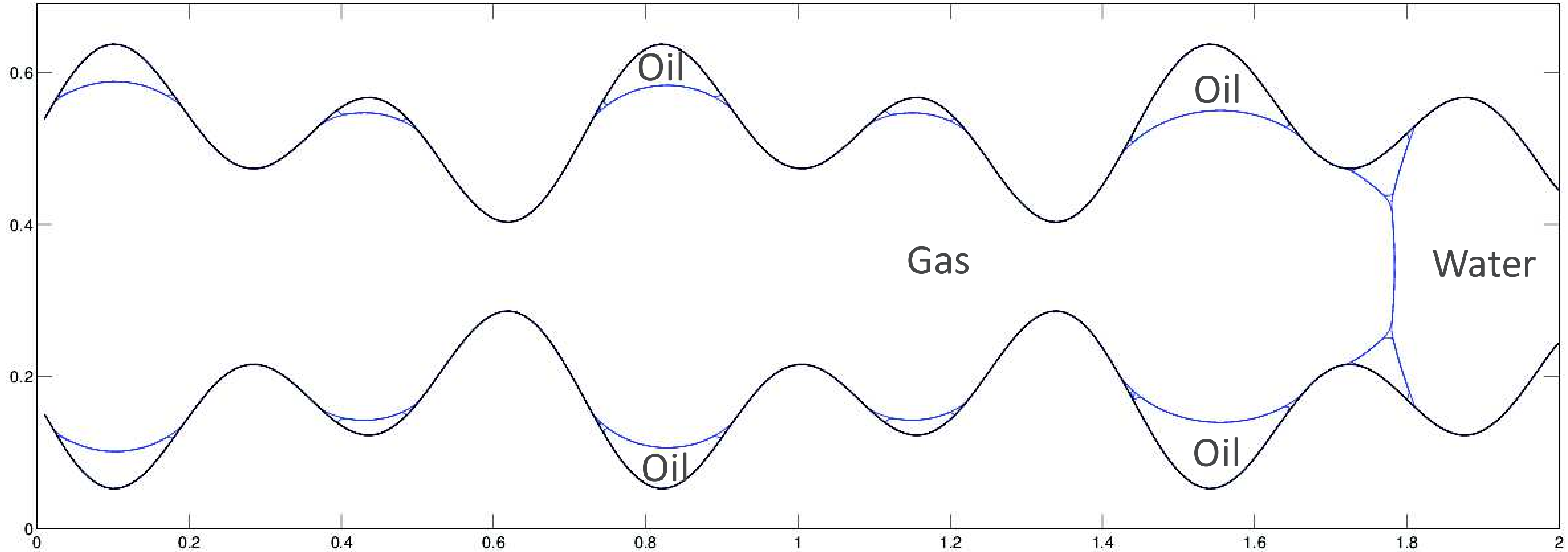

Volume-preserving motion – Sinusoidal Pore

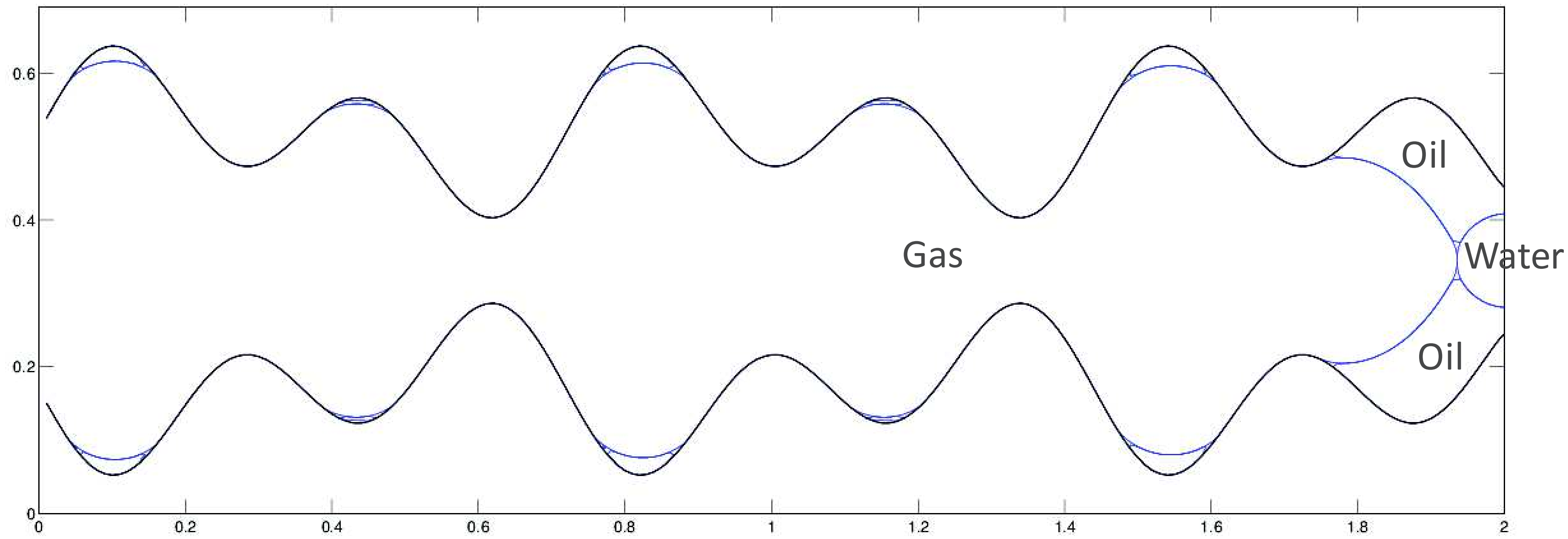

Volume-preserving motion – Sinusoidal Pore

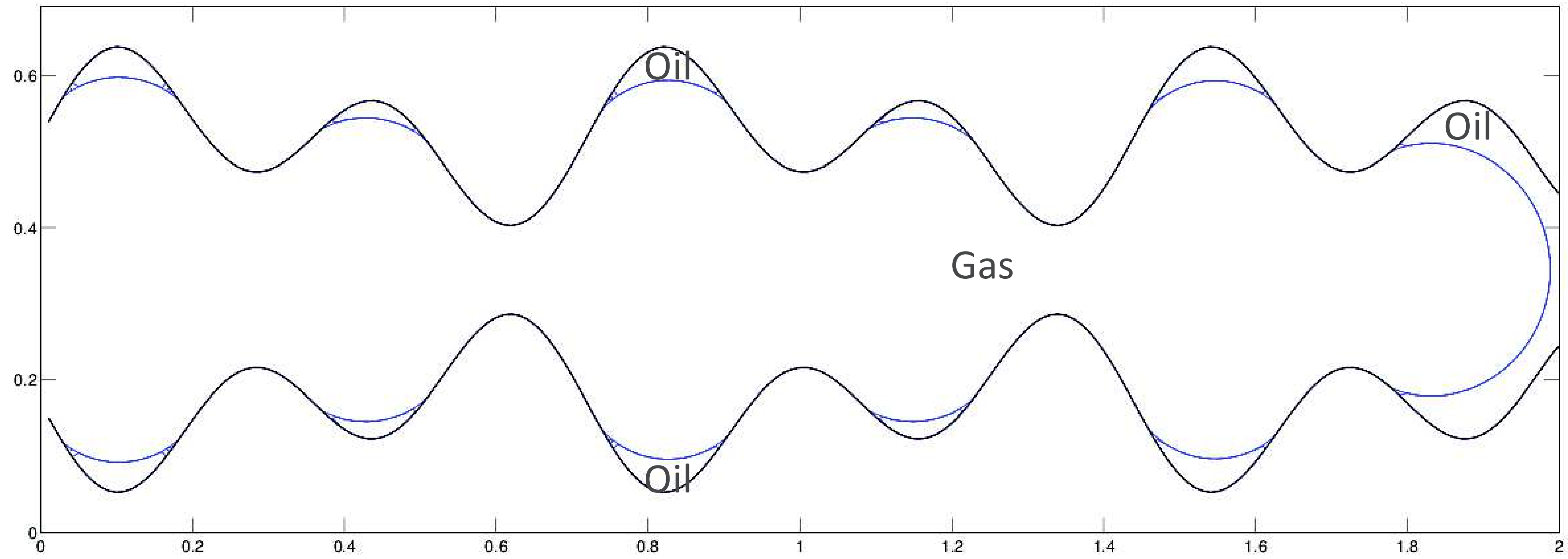

Volume-preserving motion – Sinusoidal Pore

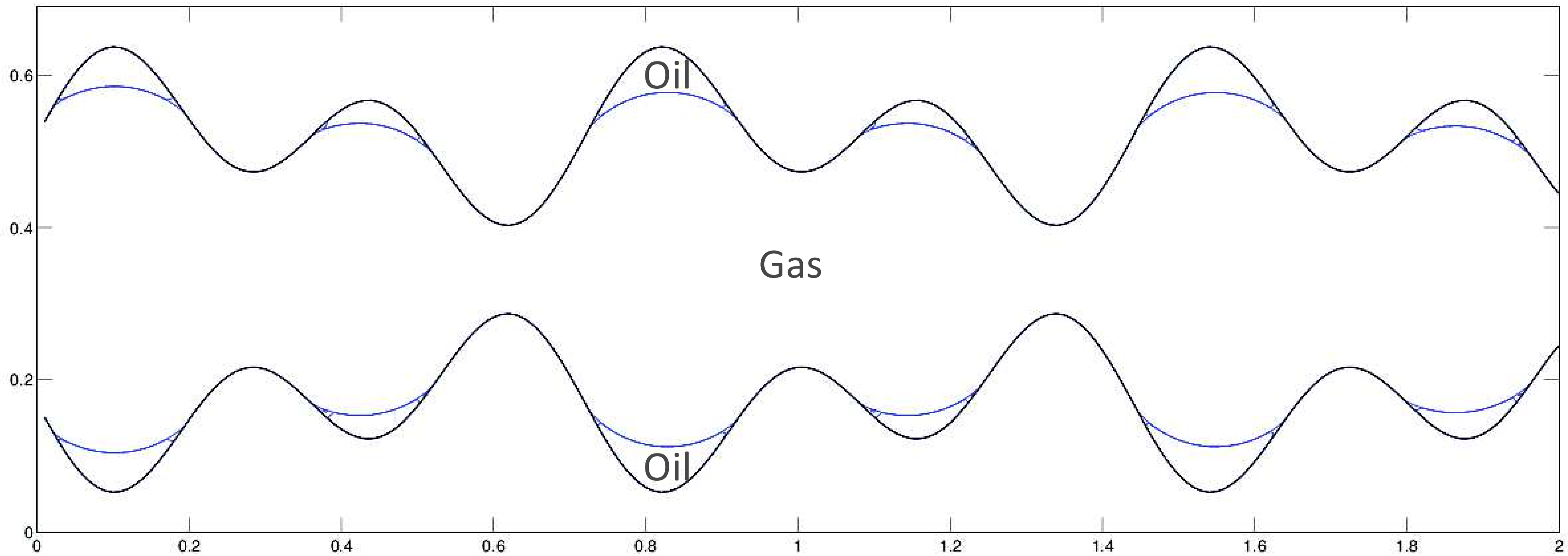

Stable configuration

Volume-preserving motion – Sinusoidal Pore

- 4 simulations (oil-wet and water-wet cases with two different oil volumes)
- Relative volume error is less than 0.2% during the processes

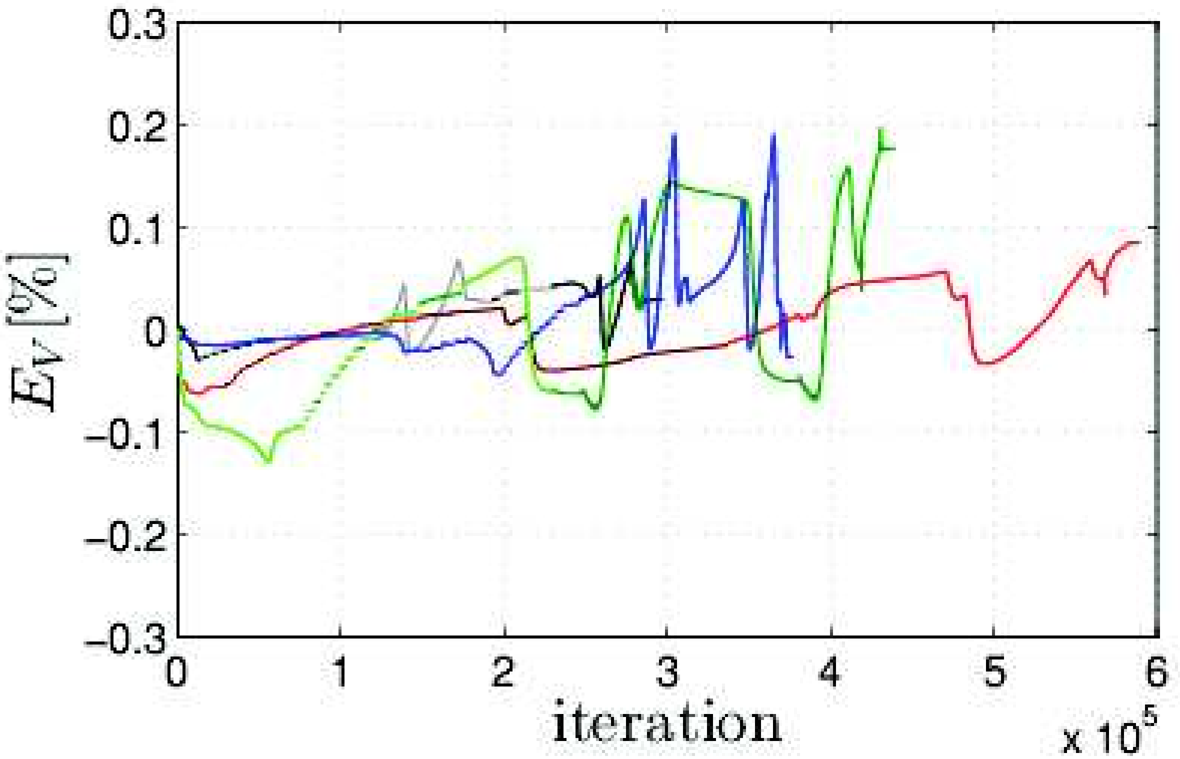

Volume-preserving motion – Sinusoidal Pore

- Significant oil pressure fluctuations as oil moves through narrow and wide regions
- Assuming $\Delta x = 1\mu\text{m}$, P_{cgo} and P_{cow} varies with up to 2 kPa during displacement for water-wet case, and a little bit less for the oil-wet case.

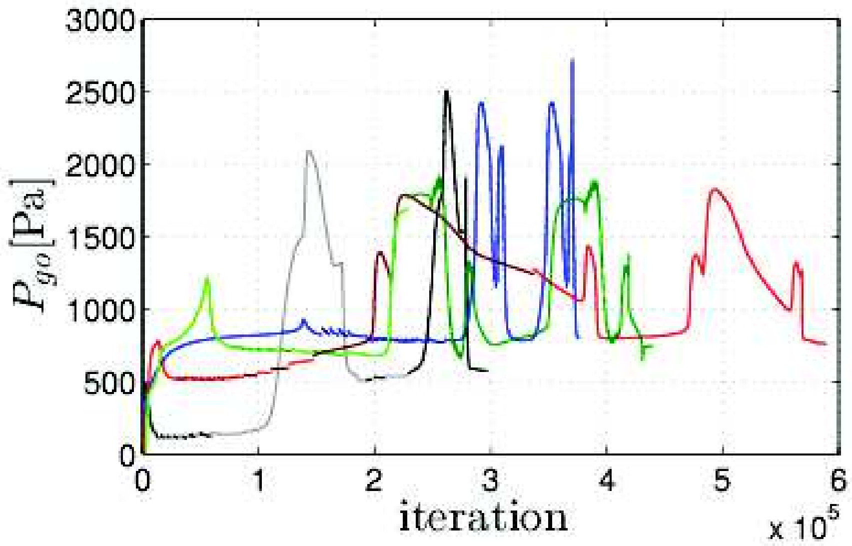

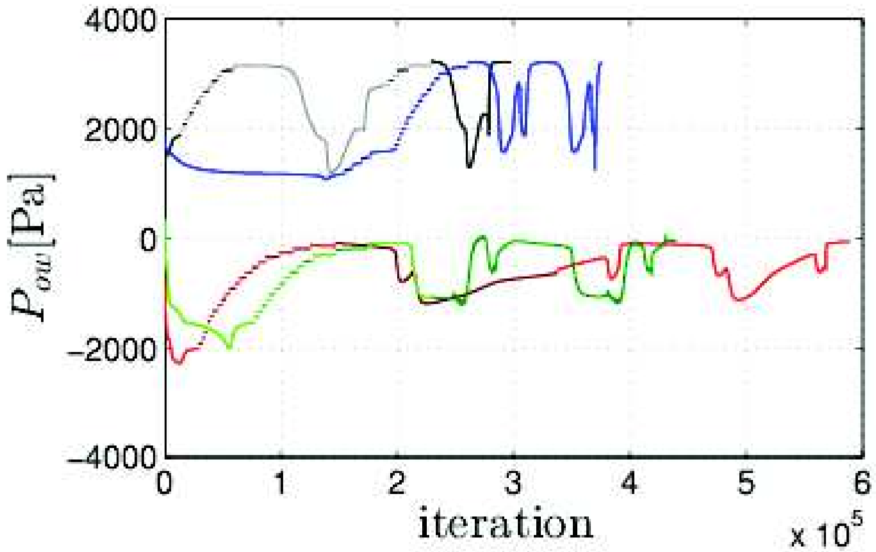

Volume-preserving motion – Sinusoidal Pore

› Gas/water capillary pressure is smaller with disconnected oil present between gas and water:

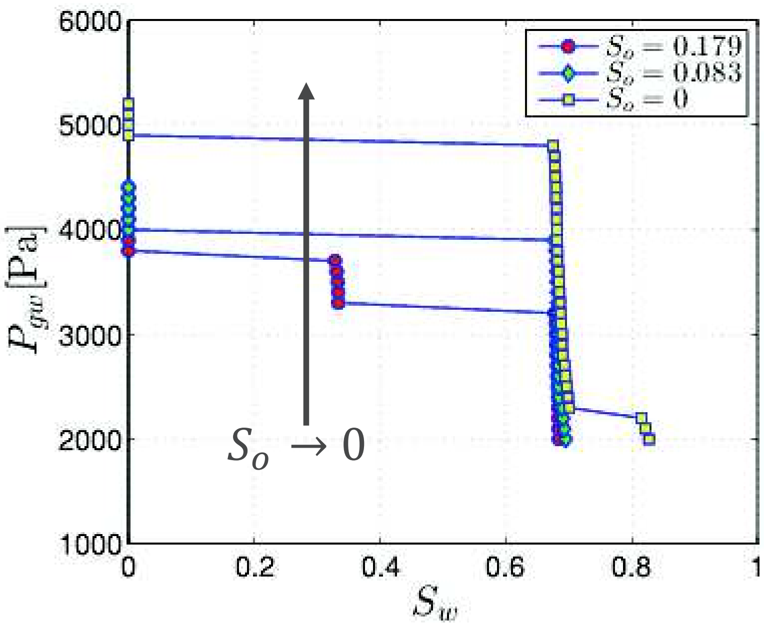

Water-wet case

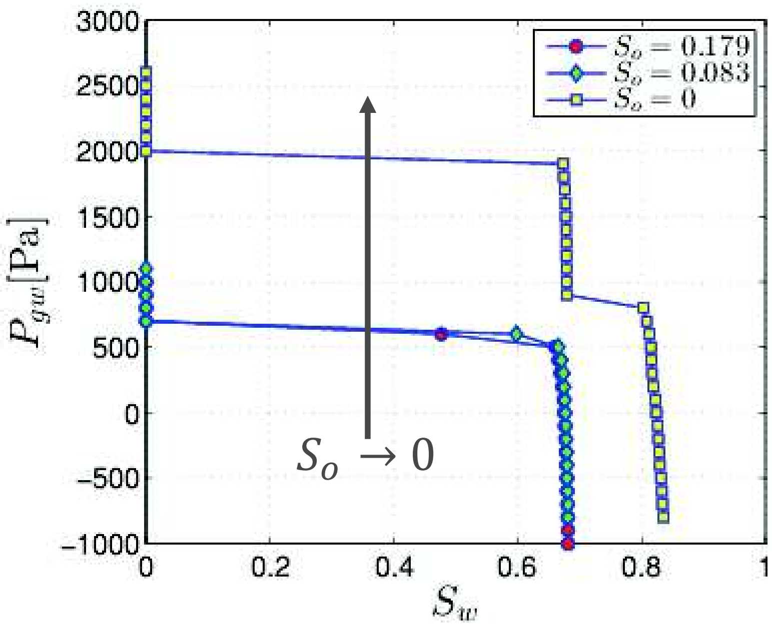

Oil-wet case

Volume-preserving motion in 3D rocks

- Mechanism for mobilizing isolated oil in water-wet rock
- Onset of double displacement (water → isolated oil → gas) by water snap-off at gas/oil interface. Oil volume error < 2%.

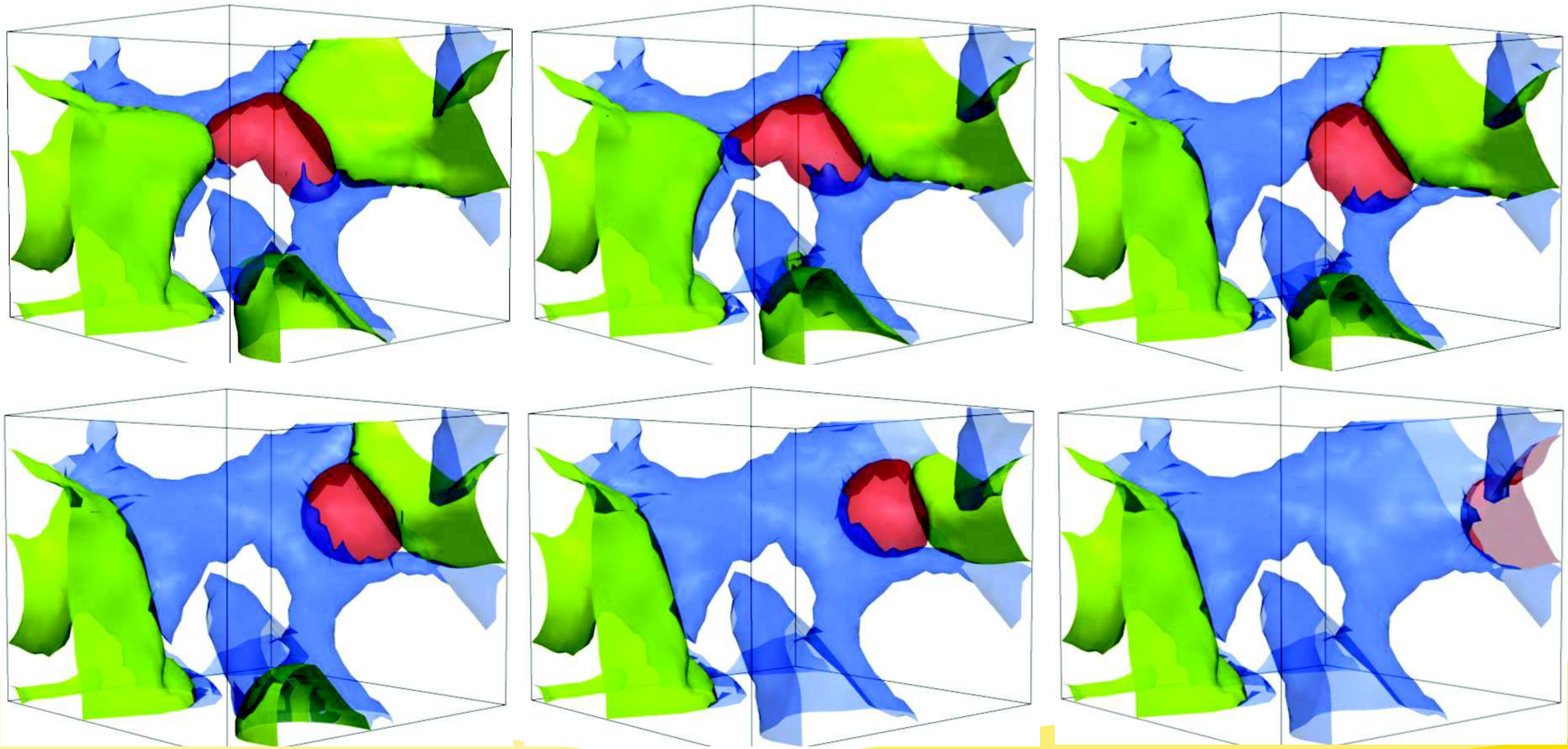

Volume-preserving motion in 3D rocks

- Oil invasion in oil-wet rock and preservation of the gas phase
- Oil surrounds gas due to oil snap-off on gas/water interfaces and gas becomes capillary trapped. Gas volume error < 1.5%.

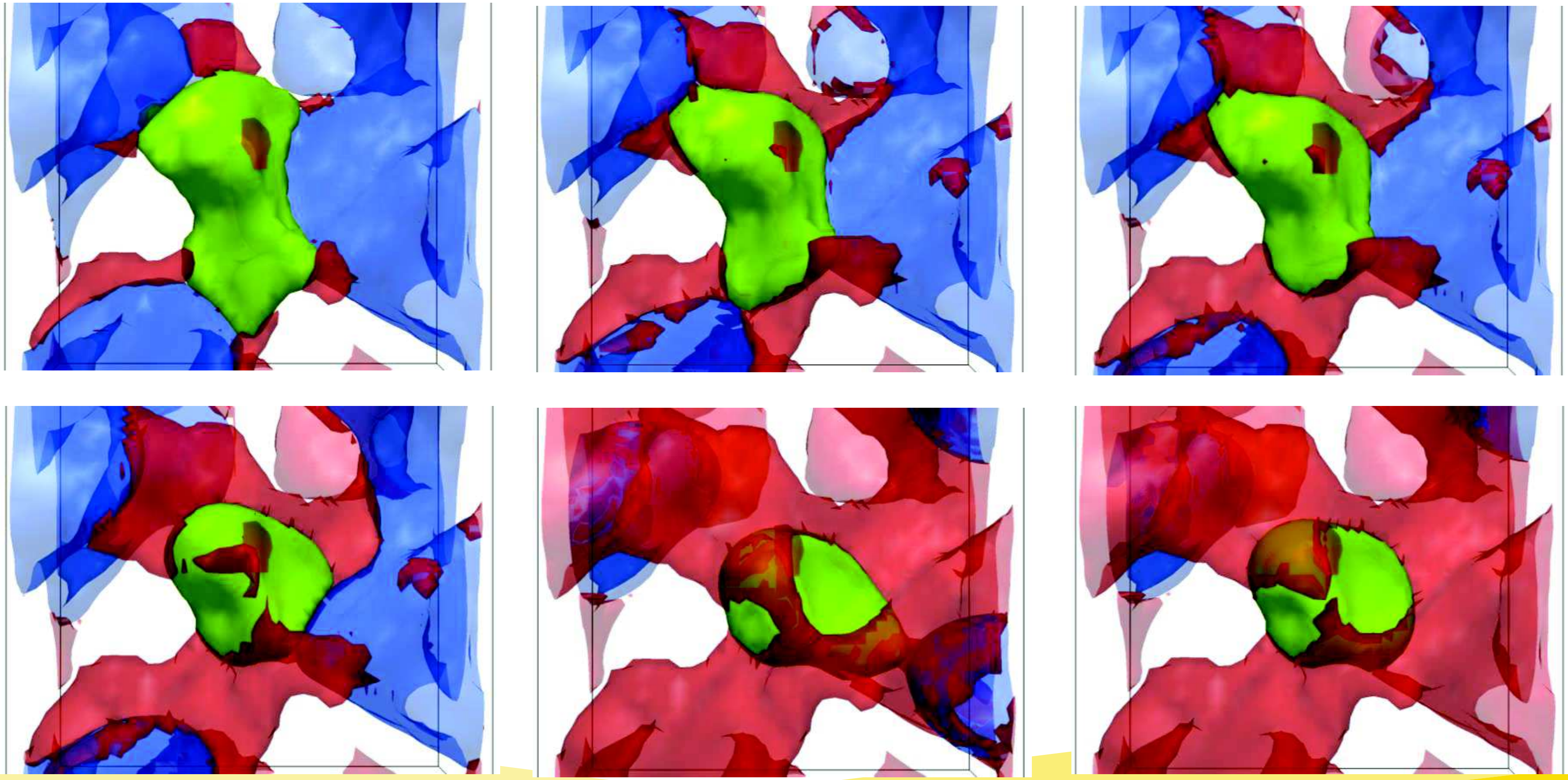

2-phase pore-scale experiments in literature

(Andrew, Blunt et al., TIPM 2015)

- Drainage in Limestone at reservoir conditions (50°C & 10MPa), imaged by x-ray μ-CT
- Water withdrawn at low, constant rate
- Capillary number~10^{-11}

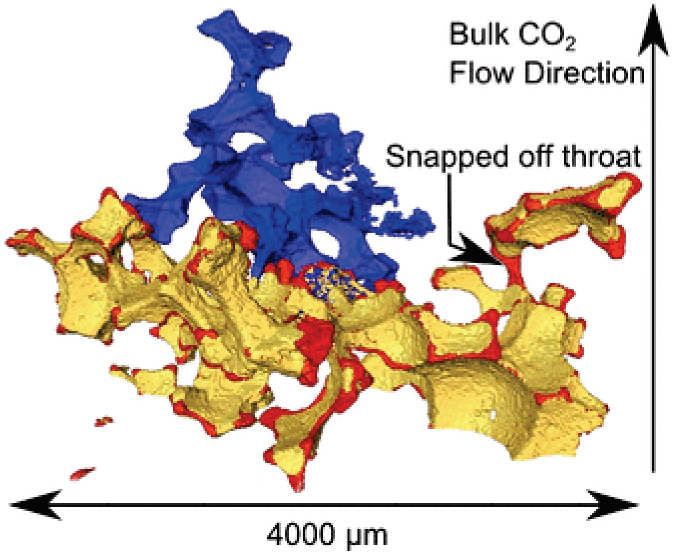

NWP at time t_1

NWP at time $t_2 = t_1 + \Delta t$

- Observations in drainage:
  - Haines jumps with co-operative behavior
  - Capillary pressure before Haines jump (time t_1) is higher than after (time t_2)
  - Snap-off events can lead to temporarily isolated NWP droplets
  - Interfaces vibrate when they are close to critical events
- Imbibition:
  - Ganglion dynamics, etc…
- Do we need to include viscous forces to describe this multiphase behavior at the pore scale?
- Are these observations just a consequence of constant rate?

Can «Volume-Targeting» simulation describe this multiphase behaviour? Yes (at least qualitatively)!

› Approach: Take saturations as input and calculate phase pressures (instead of specifying pressure and calculate saturation)

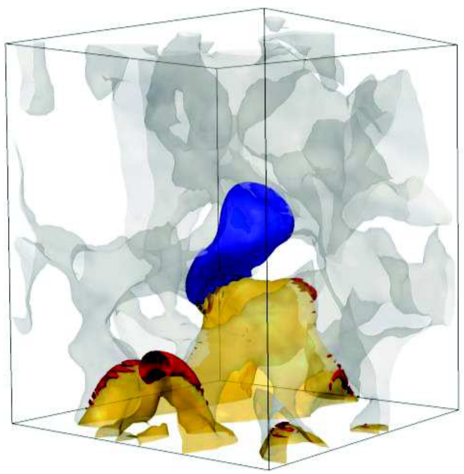

(A)

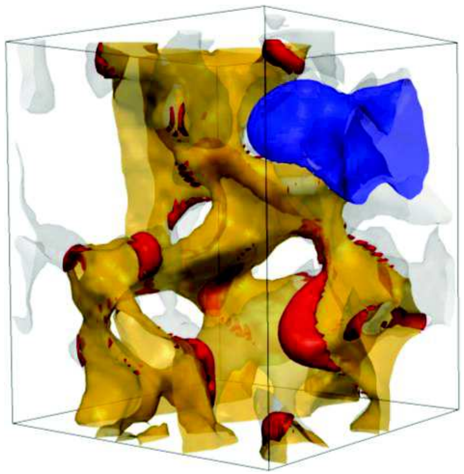

(B)

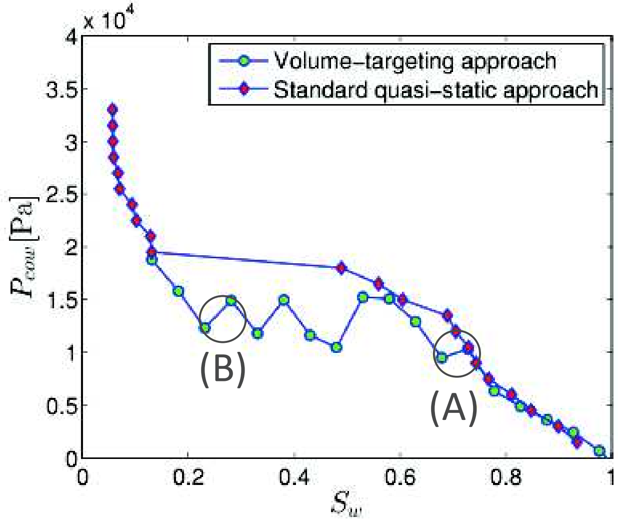

We assume $\Delta S_o = 0.05$

NWP at S_o

NWP at $S_o + \Delta S_o$

For drainage, we observe:

- Haines jumps with co-operative behavior (local imbibition) that results in temporarily smaller capillary pressure
- Interfaces vibrate until target volume is reached accurately

Adaptive Mesh Refinement (AMR) & Parallelization

- Needed for accurate calculations on big domains (heterogeneous chalk)

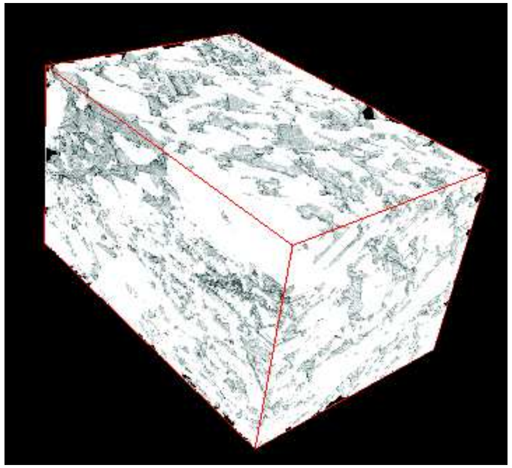

- We will implement AMR & parallelism by coupling our codes to R&D AMR library SAMRAI (developed at LLNL)
- Parallel computations on Notur HPC facilities

Status and Capabilities Multiphase LS Method IRIS

- Quasi-static capillary-dominated displacement at uniform or mixed wettability (for 2 and 3 phases)
- Drainage & imbibition processes (invasion of gas, water or oil)
- Transition from 3- to 2-phase flow
- Motion of wetting-phase cusps and triple lines are captured very well
- Oil layers are modelled accurately if grid resolution is sufficiently fine
- Continuous validation by comparing simulations with analytic solutions on idealized pore geometries.
- Global phase volume preservation

The work plans

First priority:

› Finish AMR & parallelization

› Finish implementation of local volume preservation:

- Volume preservation of individual drops that can merge or break

Then:

› Start simulations on big domains

- Priority: 1. chalk; 2. bead pack; 3. sandstone
- 2-phase motion first, 3-phase motion afterwards
- Relative permeability

› Add compressibility (gas) to volume preservation approach, using EoS

› Introduce gas by depressurization (model gas bubble nucleation)

› Relate water chemistry to changes in wettability

Conclusions

- Multiphase Level Set simulations give increased insight into the pore-scale mechanisms that explain differences and similarities between 2- and 3-phase capillary pressure curves
- Water-wet conditions:
  - Gas/oil capillary pressure increases with Swi, as water blocks gas/oil displacement paths
  - Imbibition oil/water capillary pressure curves differ because «3-phase water snap-off» on gas/oil interfaces occurs at a higher oil/water capillary pressure than standard 2-phase snap-off events
- «Mixed- to oil-wet» conditions:
  - Similar 2- & 3-phase capillary pressure curves for small gas & water saturations
  - Gas is trapped by oil cusps and water in big pores (not narrow throats), but the amount of trapped gas and its location seems to depend on Swi.

Conclusions

› Multiphase Level Set simulations with volume preservation (3 phases) or «volume targeting» (2 phases) show «dynamic» behavior:

- Haines jumps with co-operative behavior due to limited phase availability
- Non-monotonic capillary pressure changes

› Double displacements must be viewed together with snap-off mechanisms:

- Snap-off can represent the onset of double displacements (for mobilizing oil)
- Snap-off can also trap the disconnected fluid permanently
- Pressure oscillations and temporary snap-off events can occur as the disconnected fluid moves through narrow and wide pore regions
- Presence of disconnected oil decreases the gas/water capillary pressure during gas invasion

Acknowledgements

Financial support was provided by the Research Council of Norway (PETROMAKS 2) through grant

234131 – Three-Phase Capillary Pressure, Hysteresis and Trapping in Mixed-Wet Rock,

and ConocoPhillips and the Ekofisk coventurers, including TOTAL, ENI, Statoil and Petoro, through the research center COREC.